DEVELOPMENT OF CONTINUOUS WAVE AND MODE LOCKED TITANIUM SAPPHIRE LASER

WAN AIZUDDIN BIN WAN RAZALI

A thesis submitted in fulfillment of the
requirements for the award of the degree of
Master of Science (Physics)

Faculty of Science
Universiti Teknologi Malaysia

APRIL 2008

To my beloved Ayahanda and Bonda: Wan Razali bin Wan Ismail and Zainab binti Hassan and my sweet brother and sister: Wan Lukman and Fatimah Zahra.

ACKNOWLEDGEMENT

In the name of Allah, Most Gracious, Most Merciful. Praise be to Allah, the Cherisher and Sustainer of the worlds. For His Mercy has given me the strength and time to complete this project.

I would like to express my appreciation to my respected supervisor, Associate Professor Dr. Mohamad Khairi Saidin and Associate Professor Dr. Noriah Bidin for their supervision, guidance, enjoyable discussion and motivation throughout this study.

Beside them, I have much pleasure to those who have assisted me in various ways in carrying out the experimental works. They are my late technician Mr. Nyan Abu Bakar, my new technician Mr. Ab. Rasid Ithnin and all staff that involve during my research.

My thanks are also due to Government of Malaysia through IRPA grant vote 74533 for giving us financial support. Thanks are also due to Universiti Teknologi Malaysia for giving me the opportunity to pursue my master here.

Last but not least, my appreciations go to my friends and my family for continuing support, patience throughout the present work and who have favored me with correspondence. I have much pleasure in expressing my obligation. May Allah bless those who have involved in this project.

ABSTRACT

A Ti:sapphire laser was developed based on self mode-locking technique using a "Z" folded cavity. Diode pumped solid state laser Verdi 5 was used as a pumping source with fundamental wavelength of 532 nm (suitable for the absorption band in Ti:sapphire crystal). Laser cavity was aligned by a set of mirrors with a high reflectivity of 99.8% to reflect the beam within the range of 720 nm to 820 nm, and an output coupler with a 5% transmission. A pair of prism was employed to control the dispersion for producing femtosecond pulse. The pulse was initiated via an external perturbation. The stability of the laser was sustained by providing a water cooling system. The laser operated in two modes which are continuous wave mode (CW) and pulse mode with mode-locked (ML) mechanism. The maximum output power of the CW Ti:sapphire laser is 1.12 W corresponding to a pumping power of 5.5 W and the efficiency of 26%. The optimum average power of mode-locked Ti:sapphire laser is 577 mW corresponding to the same pumping power of 5.5 W and a lower efficiency of 18%. The frequency of mode-locked laser pulse obtained is 96.43 MHz. The spectrum of laser radiation is centered at 806.74 nm with a bandwidth of 22.37 nm at full width half maximum (FWHM). The pulse duration of the mode-locked Ti:Sapphire laser is 30.53 femtosecond.

ABSTRAK

Pengayun laser Ti:nilam telah dibangunkan berdasarkan teknik mod terkunci sendiri menggunakan rongga lipatan "Z". Diode pam laser keadaan pepejal Verdi 5 telah digunakan sebagai sumber pengepaman dengan panjang gelombang asas 532 nm (sesuai untuk jalur penyerapan bagi hablur Ti:nilam). Rongga laser disusun atur melalui satu set cermin yang terdiri daripada cermin pantulan tinggi (99.8%) untuk memantulkan alur dalam julat 720 nm hingga 820 nm, dan pengganding keluaran dengan penghantaran 5%. Sepasang prisma untuk mengawal sebaran digunakan untuk menghasilkan denyut femtosaat. Denyut dicetuskan melalui gangguan luaran. Kestabilan laser dikekalkan dengan membekalkan sistem air penyejukan. Laser dioperasi dalam dua mod iaitu mod selanjar dan mod denyut dengan mekanisma mod terkunci. Kuasa keluaran maksimum laser selanjar Ti:nilam ialah 1.12 W sepadan dengan kuasa pengepaman 5.5 W dan kecekapan 26%. Kuasa purata optimum bagi laser Ti:nilam mod terkunci ialah 577 nm sepadan dengan kuasa pengepaman yang sama iaitu 5.5 W dengan kecekapan yang lebih rendah 18%. Frekuensi laser denyut mod terkunci ialah 96.43 MHz. Spektrum sinaran laser berpusat pada 806.74 nm dengan lebar jalur 22.37 nm pada lebar penuh separuh maksimum. Tempoh denyut bagi laser Ti:nilam mod terkunci ialah 30.53 femtosaat.

TABLE OF CONTENTS

CHAPTER	TITLE		PAGE
	DECLARATION		ii
	DEDICATION		iii
	ACKNOWLEDGEMENTS		iv
	ABSTRACT		v
	ABSTRAK		vi
	TABLE OF CONTENTS		vii
	LIST OF TABLE		xi
	LIST OF FIGURES		xii
	LIST OF SYMBOLS		xvii
	LIST OF APPENDICES		xix
1	**INTRODUCTION**		
	1.1	Introduction	1
	1.2	Literature Survey	2
	1.3	Problem Statement	5
	1.4	Research Objective	5
	1.5	Research Scope	5
	1.6	Thesis Outline	6

2 THEORY

2.1 Ultrashort laser pulse 8
2.2 Mode Locking 9
2.2.1 Mode locking Technique 10
2.2.1.1 Active mode locking 10
2.2.1.2 Passive mode locking 11
2.2.1.3 Kerr Lens mode locking 12
2.3 Dispersion 14
2.3.1 Source of dispersion 17
2.4 Laser Oscillator 20
2.4.1 Cavity Configuration 21
2.4.2 Cavity Optimization 23
2.4.3 Astigmatism correction 27
2.5 Optical Pumping System 28
2.6 Temperature Control 29

3 RESEARCH METHODOLOGY

3.1 Introduction 31
3.2 Alignment of the cavity 31
3.3 General setup 33
3.3.1 Pumping Source Alignment 33
3.3.2 Focusing DPSS beam 34
3.3.3 Linear cavity alignment 35
3.3.4 The cooling system 37
3.4 Continuous Wave operation 39
3.4.1 “Z” folded cavity 39
3.4.2 Testing the CW output 40
3.4.3 Optimum CW operation 42
3.5 Femtosecond operation 43
3.5.1 Dispersion Control 43

3.5.2 Optimization of femtosecond pulse operation. 45
3.5.3 Starting the femtosecond pulse operation 46
3.6 Output measurement 48
3.7 Laser component and equipment 49
3.7.1 Active Medium – Ti:sapphire 50
3.7.2 Verdi 5 Diode Pumped Solid State Laser 55
3.7.2.1 Verdi 5 operation 58
3.7.2.2 Beam profile of Verdi 5 59
3.7.2.3 Laser spectrum of Verdi 5 61
3.7.3 Optical component of Ti:sapphire laser 62
3.7.3.1 Dielectric Mirrors 62
3.7.3.2 Focusing Lens 62
3.7.3.3 Output coupler 63
3.7.3.4 Prism 64
3.7.4 Detection Devices 64
3.7.4.1 Power meter 64
3.7.4.2 Beam Star CCD profiler 65
3.7.4.3 Spectrometer 65
3.7.4.4 Oscilloscope 66
3.7.4.5 Photodetector 67
3.7.4.6 Fast Photodetector 67
3.7.5 Software 68
3.7.5.1 Matrox Inspector 2.1 68
3.7.5.2 ToptiCalc V25 68

4 CHARACTERIZATION OF TITANIUM SAPPHIRE LASER BEAM

4.1 Introduction 70
4.2 The fluorescence of Ti:sapphire crystal 70
4.2.1 Estimation of pulse duration 74

4.3 Characterization of Continuous Wave (CW) Laser 75
4.3.1 Spectrum of continuous wave beam 75
4.3.2 The power of continuous wave beam 78
4.3.3 Beam profile of continuous wave beam 80
4.4 Characterization of Mode-locked Laser 82
4.4.1 Compensating Effect 83
4.4.2 Cleaning Factors 84
4.4.3 Stability zone 86
4.5 Mode-locked pulse 87
4.6 Femtosecond pulse duration 89

5 CONCLUSION AND SUGGESTIONS
5.1 Conclusion 91
5.2 Problem 92
5.3 Suggestions 94
REFERENCES 96
APPENDIX A 103
APPENDIX B 104
PRESENTATIONS 105

LIST OF TABLES

TABLE NO.	TITLE	PAGE
3.1	Physical properties of Ti:sapphire	50

LIST OF FIGURES

FIGURE NO.	TITLE	PAGE
1.1	The improvement of ultrashort pulse generation	3
2.1	Schematic of a modulator insertion in cavity	10
2.2	Loss modulation for active mode locking	11
2.3	Schematic of insertion a saturable absorber in cavity	12
2.4	Kerr Lens mode locking process.	12
2.5	(a) Physical aperture and (b) gain aperture	13
2.6	The effect of the dispersion to the pulse	15
2.7	Dispersion due to slab geometry	17
2.8	Grating pair operation.	18
2.9	Prism pair operation.	19
2.10	Laser oscillator	21

2.11	Commonly used cavity for Ti:sapphire Oscillator	21
2.12	Typical cavity for Ti:sapphire oscillator	22
2.13	Schematic diagram of Ti:sapphire oscillator	23
2.14	Schematic diagram of the tightly focused four mirror resonator configurations.	24
2.15	Beam diameter as a function of the stability parameter	26
2.16	Optical pumping system	28
2.17	Absorption and emission process	29
2.18	Lifetime of the upper laser level of Ti:sapphire as a function of temperature	30
3.1	Overall experimental setup of Ti:sapphire laser.	32
3.2	Alignment of the pumping source	34
3.3	Alignment for focusing the DPSS beam	35
3.4	Alignment of linear cavity	36
3.5	New focal point formations after passing mirror M1	36
3.6	Crystal holder	37
3.7	The pipe installation at crystal holder	38

3.8	The schematic of cooling system	38
3.9	Alignments of “Z” folded cavity	40
3.10	Beam alignment method	41
3.11	Laser output detected using IR card	42
3.12	Alignment setup of femtosecond operation	44
3.13	Alignment of the prism pair and M4	46
3.14	Femtosecond pulse detect using fast photodetector	47
3.15	Femtosecond pulse spectrum	48
3.16	Setup for the output detection	49
3.17	Absorption and fluorescence spectra of the Ti:Sapphire	51
3.18	Octahedral configuration of $Ti:Al_2O_3$	52
3.19	Crystal structure of sapphire at crystallographic c axis	52
3.20	Energy level diagram for Ti^{3+} in sapphire	53
3.21	Schematic diagram of Brewster angle experiment	54
3.22	Brewster angle determination	55

3.23	The DPSS laser system	56
3.24	The optical components in the laser cavity	56
3.25	Power supply Front panel control	59
3.26	3D (a) and 2D (b) beam profile of Verdi 5 DPSS laser	60
3.27	a) Horizontal cursor profile b) Vertical cursor profile	61
3.28	The spectrum of Verdi 5 DPSS laser output	61
3.29	Ti:sapphire gain cross section	63
4.1	The experimental setup for the fluorescence detection	71
4.2	The fluorescence intensity as a function of wavelength	72
4.3	The fluorescence intensity at different pumped power	73
4.4	The fluorescence intensity as a function of pumping power	74
4.5	The Ti:sapphire laser output spectrum	76
4.6	The spectrum intensity at different pumped power	77
4.7	The spectrum intensity as a function the power	78
4.8	Output power as a function of the pumping power	79

4.9	3D beam profile in near field	80
4.10	2D beam profile in near field	81
4.11	3D beam profile in far field	81
4.12	2D beam profile in far field.	82
4.13	Output power as a function of the pumping power	83
4.14	Output power before and after cleaning	85
4.15	Output power by adjustment of the M1 and M2 spacing	87
4.16	Oscillogram of mode-locked pulses	88
4.17	Spectrogram of mode-locked pulse	90
5.1	DPSS laser during operation	93

LIST OF SYMBOLS

E	-	Energy
h	-	Planck constant
ω	-	Frequency
ΔE	-	Standard deviation in the energy
Δt	-	Pulse's temporal duration
$\Delta\omega$	-	Spectral bandwidth
$\phi(\omega_0)$	-	Absolute phase
$\phi'(\omega_0)$	-	Group velocity
$\phi''(\omega_0)$	-	Group velocity dispersion
$\phi'''(\omega_0)$	-	Third Order Dispersion
ω_0	-	Central frequency
λ	-	Wavelength
l	-	Distance between the apexes of the prism
n	-	Index of refraction of the prisms
λ	-	Free space wavelength of interest
β	-	Propagation angle of a ray
$d^2P/d\lambda^2$	-	Dispersion in cavity
$d^2n_{cry}/d\lambda^2$	-	Product of second order dispersion of crystal
t	-	Thickness of the crystal
δ	-	Stability parameter
f	-	Focal length
d	-	Arm length

R	-	Radius of curvature
θ	-	Optimal fold angle
τ_p	-	Pulse width
$\Delta\nu$	-	Gain bandwidth
c	-	Light speed

LIST OF APPENDICES

APPENDIX	TITLE	PAGE
A	Index refraction for sapphire	103
B	Tools for cleaning optical component	104

CHAPTER 1

INTRODUCTION

1.1 Introduction

Through the improvement of lasers, currently it is possible to observe motion in nature with unprecedented temporal resolution. With the ultrafast (10^{-15}) laser usage, exploring physical phenomena is possible. Ultrafast laser are currently following the path already taken by many physic invention. The continuing development of ultrafast laser technology have led to many new and fascinating application in physics, engineering, chemistry, biology and medicine (Sutter *et al.,* 1998).

Among the ultrafast lasers, Ti:sapphire laser is the most popular laser used. Current areas of activity using Ti:sapphire lasers include nonlinear conversion, high-repetition-rate systems, extended operating range and novel resonators. The widespread applications of Ti:sapphire include LIDAR (Rodriguez *et al.,* 2004), dual-wavelength DIAL systems, fundamental research, spectroscopy, as well as tunable Optical Parametric Oscillators (OPO) pumping and simulating diode pumping in solid-state lasers (McKinnie *et al.,* 1997 and Xu *et al.,* 1998)

The development of ultrafast laser technology has shown the rapidly progress over the past decade. This is due to the great feature of the lasers that give superior performance for many applications. There are four features of the ultrafast laser that makes it so special. The first feature is the ultrashort pulse duration. Through this feature this laser allows very fast temporal resolution. Therefore this kind of laser can 'freeze' the motion of fast moving object including molecules and electrons. Professor Ahmed Zewail has won a Nobel Prize in chemistry by observing the molecule reaction in slow motion using ultrafast laser (Smith, 1999). The second feature of ultrafast laser is high pulse repetition rate. With multi gigahertz repetition rates, this laser was used in high capacity telecommunication systems, photonic switching devices, optical interconnection and for clock distribution. The third feature is, ultrafast laser have broad spectrum which supports good spatial resolution for optical coherence tomography (OCT). OCT is a technique for non-invasive cross-sectional imaging in biological systems. Lastly, the ultrafast laser has high peak intensity. This high intensity source makes 'non-thermal' ablation (without increase temperature) is possible. The ability of intense ultrashort-pulse lasers to fabricate microstructures in solid targets is very promising and the quality of ablated holes and pattern is much better using femtosecond laser.

1.2 Literature survey

Over the last two decades there have been a series of impressive achievements in the technology of short pulse lasers. From tens of picoseconds in the mid 1970's, laser pulse durations have now been reduced to only a few femtosecond pulses of 20 -100 fs are common in many laboratories. The reduction of pulse duration has been accompanied by large increases in the peak pulse intensity, from 10^{14} - 10^{15} W/cm^2 in

the mid 1980's up to 10^{18} - 10^{22} W/cm^2 in 2004 (Tate, 2004). The improvement of the ultrashort pulse laser is shown in Figure 1.1.

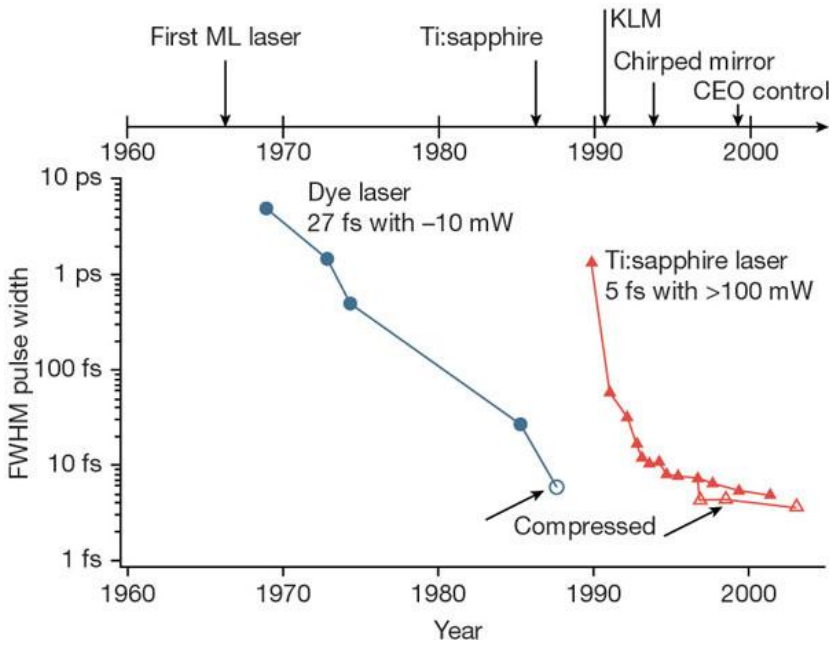

Figure 1.1 The improvement of ultrashort pulse generation (Keller, 2003)

Figure 1.1 illustrated the improvement in pulse generation since the first demonstration of a laser in 1960. Until the end of the 1980s, ultrashort pulse generation was dominated by dye lasers, and pulses as short as 27 fs with an average power of 10 mW was achieved (Valdmanis and Fork, 1986). After external pulse compression a pulses as short as 6 fs was produced. However, this situation changed with the discovery of the Ti:sapphire lasers.

Since the discovery of laser action in Ti:sapphire in 1982, Ti:sapphire become one of the most widely used solid-state laser material (Kuhn, 1998). It combines the excellent thermal, physical and optical properties of sapphire with the broadest tunable range of any known material (Eggleston *et al.,* 1988). It can be lased over the entire band from 660 to 1100 nm. The Ti:sapphire crystal also become as the breakthrough of

ultrafast solid state lasers because it is first solid state laser medium was able to support ultrashort pulses without cryogenic cooling.

Ultrafast laser was first generated in 1965 by passive mode-locking of a ruby laser (Shapiro, 1977). Then one year later Nd:glass laser was successfully produce pulse duration of some picoseconds by using the same technique. In 1981, the first light pulse with duration less than 0.1 picoseconds or 100 femtosecond was generated by improvements of the passively mode-locked dye laser (Rudolf and Wilhelmi, 1989).

This progress of femtosecond pulses generation by solid state laser have followed from the self mode-locking in a Ti:sapphire laser by Sibbett group in 1991 (Keller, 2003) The self mode-locking behavior has known as *Kerr Lens Mode-locking* (KLM). It is the basis for femtosecond pulse generation in a wide variety of solid state laser system. Nevertheless, several mode-locking methods for Ti:sapphire laser were reported, which including active mode-locking with an acoustic optical modulator, additive pulse mode-locking (APM), passive mode-locking using organic dyes or semiconductor doped glass as saturable absorber and resonant passive mode-locking (RPM) (Keller *et al.*, 1991 and Sarukura and Ishida, 1992). Perhaps among all of the various schemes, KLM is most famous and simplest technique used (Huang, 1995). The KLM of Ti:sapphire lasers was discovered in 1991 and capable to produce the shortest pulse which is less than 6 fs duration. However shorter sub-5 fs pulse has been demonstrated with external cavity pulse compression (Fermann *et al.*, 2001 and Xu *et al.*, 1998). The KLM process will be discussed in detail in Chapter 2

1.3 Problem Statement

A Ti:sapphire crystal is the most important solid state medium to generate femtosecond pulse laser. This is because its posses a broad gain bandwidth. However, it is not an easy task to generate femtosecond laser. Only knowledgeable and experience scientist will be able to take the challenge. The difficulties arise due to the precision optical components and procedure alignment. Therefore this work has been carried out in order to study the design of femtosecond laser.

1.4 Research Objective

The objective of this research is to study the construction of femtosecond laser by using Ti:sapphire crystal based on KLM technique. The study includes the identification of optical components, gain medium and pumping source. The crucial part of the work is the alignment of the laser cavity. Finally, the laser output obtained will be characterized.

1.5 Research Scope

In this research Ti:sapphire crystal was employed as gain medium. The crystal was pumped by green laser. In this case Diode Pumped Solid State (DPSS) laser Verdi 5 was employed. The fluorescence of the crystal immediately produced after excited by

DPSS laser was studied. The configuration of the cavity was chosen to be in “Z” folded type. The lasing was tested in two modes. Firstly in continuous wave operation and secondly in mode-locked operation. A prism pair was conducted to compensate the dispersion. High speed photodetector was utilized to detect the mode-locked signal. The spectrum analyzer was used to measure the wavelength of the output beam and estimate the pulse duration.

1.6 Thesis outline

The thesis is divided into seven chapters. The first chapter will discuss about the ultrafast laser advantages and reviewing some improvement regarding ultrafast laser.

Chapter II reviews the theory related to the research. This will explain the detail of the mode-locking technique and theory behind the development of the Ti:sapphire laser such as dispersion compensation and cavity design.

Chapter III describes the methodology of the project. This would include entire materials used to setup the laser cavity such as active medium, pumping source and optical components. The measurement equipments and software for analysis utilize are also will be included.

Chapter IV explains about the pumping source used to excite the Ti:sapphire crystal. In this part all the specifications and procedure to handle the DPSS laser are provided. Lastly the operation of the laser system and the characterization of the laser output will be discussed.

Chapter V discusses the procedures to align the Ti:sapphire laser. This includes the alignment of the lens, mirrors, output coupler and prism pair for Continuous Wave and mode-locked cavity. In addition, this part also discuss about the optimization of femtosecond operation. Since the alignment of the cavity is very critical, therefore this chapter is the most important part in this work.

The characterization of the Ti:sapphire laser is explained in Chapter VI that have been constructed. This includes the spectrum of the beam, the output power, the beam profile and the estimation of the pulse duration.

Finally the conclusion of the project is made in Chapter VII. The summarization contains the synopsis of the project, the problem involved during the performance of the project. Last but not least, further works to be carried out in the future are suggested.

CHAPTER 2

THEORY

2.1 Ultrashort laser pulse

Ultrafast pulse occur on femtosecond (10^{-15} s) or shorter time. Because the energy in the amplifying material is released in such short pulse, each pulse has a very high power output. Peak powers of up to one terawatt (10^{12} W) have been achieved. In order to generate ultrafast pulse, medium with large number of frequency modes allow it to produce on a very short time scale.

According to Heisenberg uncertainty principle (Donnelly and Grossman, 1998)

$$\Delta E \Delta t \geq \frac{\hbar}{2} \tag{2.1}$$

where ΔE is the standard deviation in the energy and Δt represents the amount of time it takes the expectation value of some operator to change by one standard deviation. Since for photon, $E = \hbar \omega$, Equation (2.1) can be written as:

$$\Delta\omega\Delta t \geq \frac{1}{2} \tag{2.2}$$

In the context of laser pulse $\Delta\omega$ refers to the spectral bandwidth of the pulse and Δt describes the pulse's temporal duration. Therefore smaller Δt demands a larger $\Delta\omega$, or frequency range. Heisenberg uncertainty is fundamental to understand the generation of ultrashort light pulses. The more precise a photon can be placed in time, the more uncertain the photon energy is. In other word, the pulsed laser light must be broadband and contain a spectrum of colors (Wang, 1999).

2.2 Mode-Locking

There are many uses of very short duration laser pulses in the fields of digital communications, diagnostics of ultrafast processes, and ablation of materials without causing significant heating of the material. Much effort has been made to develop the techniques for generating short pulses. Q-switched process can produce pulses that are limited to minimum pulse durations of a few nanoseconds. Another technique that has allowed the generation of the optical pulses as short as 5 fs (5×10^{-15} s) is known as mode-locking (Silfvast, 2004).

The technique of laser mode-locking has been around for more than 35 years. The first mode-locking was demonstrated in 1964 and has since then developed into a very active research area (Koumans, 2001). Ultrashort pulses with pulsewidth in picosecond or femtosecond regime are obtained from solid state laser by mode-locking. Mode-locking also has been proven can produce a train of the time domain requires a broad spectrum in the frequency domain.

2.2.1 Mode-locking Technique

There are several techniques to achieve mode-locking. Practically, there are three main techniques to produce mode-locking namely active mode-locking, passive mode-locking and Kerr lens mode-locking.

2.2.1.1 Active mode-locking

Active mode-locked involves placing a very fast shutter in the laser cavity. The mode-locking take place if the shutter opens only for a very short period of time at every time the light pulse make a complete round trip in the cavity. It can be explained by considering a laser with many modes oscillating simultaneously.

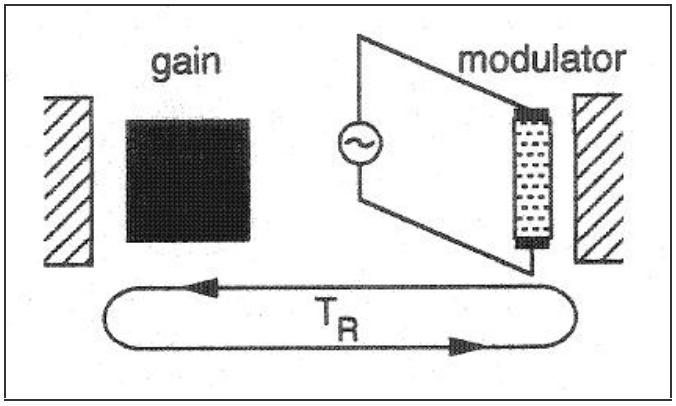

Figure 2.1 Schematic of a modulator insertion in cavity

Consider a loss modulator such as acousto optics modulator inserted in the cavity as shown in Figure 2.1 (Kowalevicz, 2004). In this system, locking of the modes will be made by modulating the loss at a period equal to cavity round trip time $T_R=2L/c$ (Figure 2.2). If the loss is higher than gain, the pulse cannot be produced. Means, no single mode can oscillate. When the loss modulates in laser cavity, the superposition of the modes

will occur. Then construct a pulse that would arrive at the modulator just before it opened and pass through just before it closed.

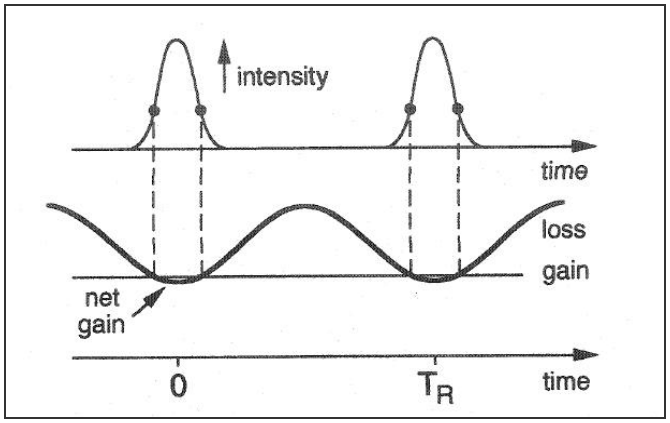

Figure 2.2 Loss modulation for active mode-locking

2.2.1.2 Passive mode-locking

Passive mode-locking is the most common method to generate ultrashort pulse. Since it uses the pulse to modulate itself therefore it has some advantage. Firstly it required no external synchronization. Secondly the response of the modulator can be extremely fast. Passive mode-locking is acquired by inserting a saturable absorber into the laser cavity, preferably close to one of the mirrors as shown in Figure 2.3. A saturable absorber is a medium whose absorption coefficient decrease as the intensity of light passing through it increase. Thus it transmits intense pulse with relatively little absorption and absorb weak one. When a saturable absorber is used to mode-lock a laser, the laser is simultaneously Q-switched.

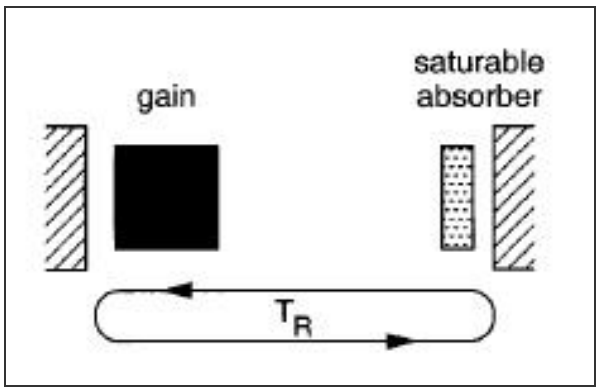

Figure 2.3 Schematic of insertion a saturable absorber in cavity (Haus, 2000)

2.2.1.3 Kerr Lens mode-locking

Kerr lens mode-locking (KLM) is a process based on the nonlinear effect of self focusing. This effect will produce an intensity-dependent change in the refractive index of material. When a Gaussian beam passing through a material with the beam more intense at the center than the edge, the index of refraction of the material will become higher at the center (Aschom, 2003). Therefore creating a lens which is focused the beam within the material such as shown in Figure 2.4. This process will form and effective fast saturable absorber. Compared to the bleachable dyes, the Kerr effect is extremely fast, wavelength independent, and allows the generation of a continuous train of mode-locked pulsed from Continuous Wave (CW) pumped laser.

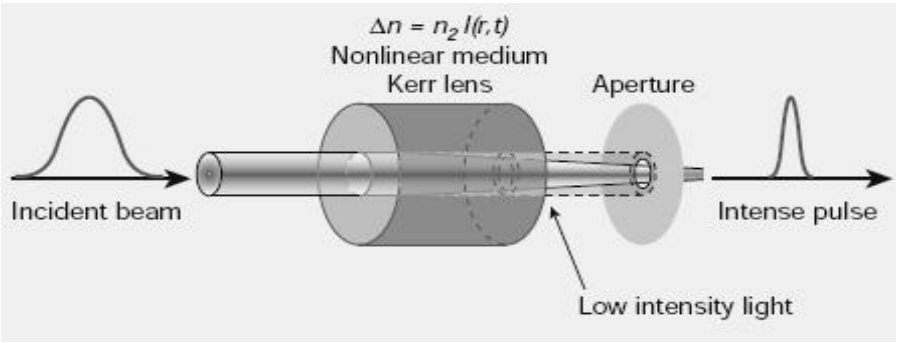

Figure 2.4 Kerr Lens mode-locking process (Keller, 2003)

The self focusing effect will create pulse mode-locked set of mode that generates short pulses regime and CW mode regime. Two techniques can be used to achieve KLM which is hard aperture and soft aperture technique. Figure 2.5(a) shows KLM on physical aperture also known as *physical aperture* or *hard aperture*. The aperture placed between the laser gain medium and the mirror, is small enough in diameter to provide a relatively high loss for the CW mode. However, if a light pulse with higher intensity than the CW beam is generated within the gain medium, thereby providing a more favorable environment for a pulsed laser than for a CW laser. The same aperturing effect can be achieved by making a smaller-diameter pump beam than the CW mode size, as shown in Figure 2.5 (b) call as *gain aperture* or *soft aperture*.

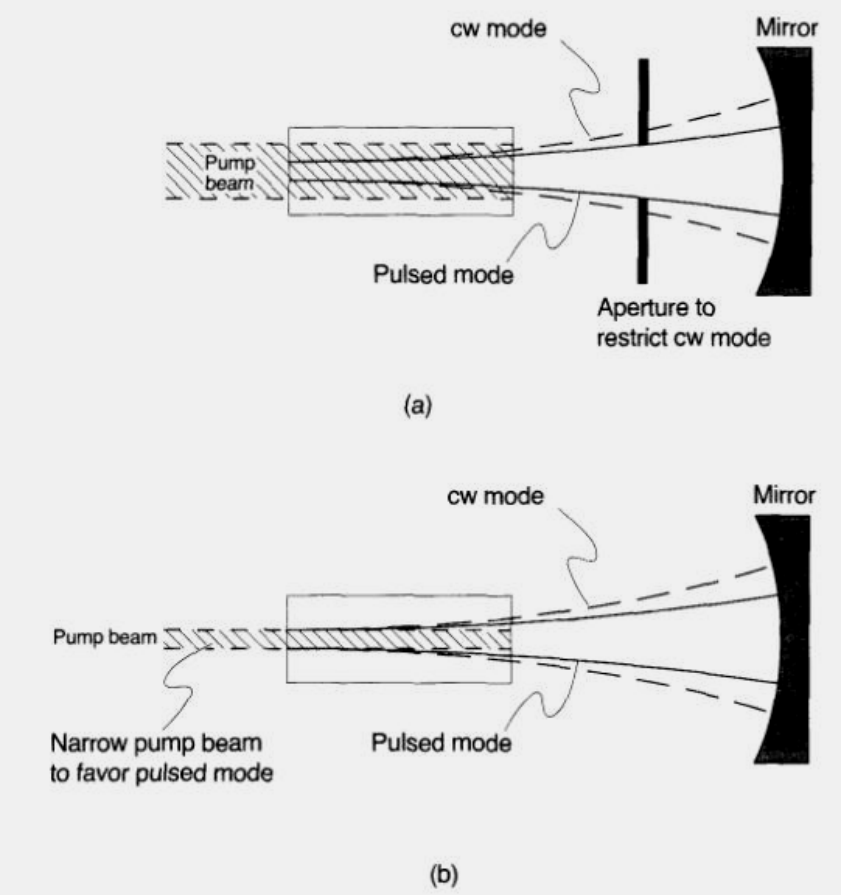

Figure 2.5 (a) Physical aperture and (b) gain aperture

The *self focusing* also describes as *self phase modulation* (SPM) and often termed the *Kerr effect* (Kuhn, 1998). As discussed before, as the intensity of the pulse increases, the index of refraction of the material will increase and the pulse focused. Temporal SPM is time dependent phase shift that occurs as the pulse sweep through the dispersive material. The rising intensity on the front edge of the pulse increases the index of refraction. This will delay the individual oscillation and thus red shift the rising edge. The reverse effect occurs on the trailing edge. Thus, temporal SPM chirp the pulse.

For ultrashort pulse generation, the round trip time in the resonator for all frequency component of the light must be the same. Otherwise, frequency components with different phase shift will longer add coherently and the mode-locking will break down. In the normal laser operation, temporal SPM will cause a red shift of the pulse and the Group velocity dispersion (GVD) will also cause a red shift on the pulse. Thus, in order to achieve transform-limited pulse width, it is necessary to incorporate some type of dispersion compensation that blue shifts the pulse. Prism pair commonly used to introduce the GVD compensation.

2.3 Dispersion

Dispersion is the phenomenon that happens to the light wave and also sound wave. Through this phenomenon the wave become separated into spectral component with different frequencies. In the ultrashort pulse generation the dispersion control is very vital because it can lead to temporal broadening of pulse, limiting the generation of ultrashort pulse and also disable the mode-locking. Figure 2.6 shows the effect of the dispersion to the pulse.

We can see the differences between pulse without dispersion (top) and the pulse after dispersion. According to Figure 2.6, there are two aspects need to be considered. First, the center of the pulse is delayed with respect to a pulse traveling in air. This is usually called the *group delay*, which is not a broadening effect. Second, normally dispersive media such as glass impose a positive frequency sweep or ‘‘chirp’’ on the pulse, meaning that the blue component is delayed with respect to the red and the pulse becomes broadened one. This is due to presence of the positive *Group Velocity Dispersion* (GVD) or by other terms *Group Delay Dispersion* (GDD),

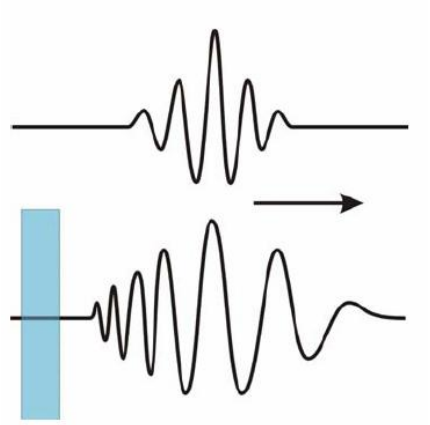

Figure 2.6 The effect of the dispersion to the pulse (Carey, 2002)

The dispersion will cause shorter wavelength to lag behind the longer wavelength. This type of dispersion known as “*positive dispersion*” and the resulting broadened pulse is said to be “*positively chirped*”. When dispersion broadens the bandwidth, ultrashort pulses will have large group delay difference between the two ends of the spectrum. Then limit the mode-locked bandwidth. Since the wavelength on either end of the spectrum will have different group delays, they cannot oscillate synchronously with the pulse in the cavity. Eventually, those wavelengths will experience more loss or less gain due to the Kerr lens mode-locking mechanism and will die out. Therefore, without any dispersion control, it is impossible to get the ultrashort

laser pulses (Huang, 1995). Equation (2.3) illustrates the theoretical effect of dispersion in the cavity (Salin and Brun, 1987).

$$\phi(\omega) = \phi(\omega_0) + \phi'(\omega_0)(\omega - \omega_0) + \frac{1}{2}\phi''(\omega_0)(\omega - \omega_0)^2 + \frac{1}{6}\phi'''(\omega_0)(\omega - \omega_0)^3 + \ldots \qquad (2.3)$$

In Equation (2.3), $\phi(\omega_0)$ is known as the *absolute phase* and describes the exact phase of the central frequency. When considering dispersion $\phi'(\omega_0)$ is known as the *group velocity* and is the first derivative of the spectral phase with respect to frequency evaluated at the central frequency ω_0. Non zero value of the Group Velocity describes a linear translation of the pulse in time. The GVD is represented by $\phi''(\omega_0)$ and is the second derivative of the phase with respect to frequency evaluated at the central frequency. Nonzero GVD values give a parabolic phase profile and are responsible for most of the temporal widening experienced by pulses. Higher order dispersion is labeled as Third Order Dispersion (TOD) $\phi'''(\omega_0)$ (Walker, 2006). As the higher order derivatives usually give very small contribution, the third- and fourth-order dispersion (TOD and FOD) regularly are neglected. Therefore the GVD need to be controlled to obtain ultrashort pulse.

In fact, there are two main dispersive properties applied in femtosecond pulse laser. The first property is GVD which is the tendency of various frequencies of light to propagate at different speed in certain material. In material with positive GVD, the longer wavelength travel faster than the shorter one, thus red wavelength shifting the pulse. The second dispersive property which also plays important role is the *self phase modulation* (SPM).

2.3.1 Source of dispersion

There are several types of the dispersion source. First is dispersion from the material itself. In the solid state laser the material dispersion is unavoidable. This is because the presence of the lenses, mirrors and crystals will introduce material dispersion. Values for the dispersion can be calculated from the refractive index.

The second source of the dispersion is due to slab geometry as shown in Figure 2.7. With the same non zero incident angle, light of different wavelength will travel in different optical paths after entering a dispersive material. This effect happens in addition to the material dispersion. For the broad bandwidth material, this effect will be most severe for ultrashort laser pulse. The Brewster cut of the Ti:sapphire crystal which are commonly used in Ti:sapphire laser will introduce such effect. Longer length of the crystal will give more dispersion effect.

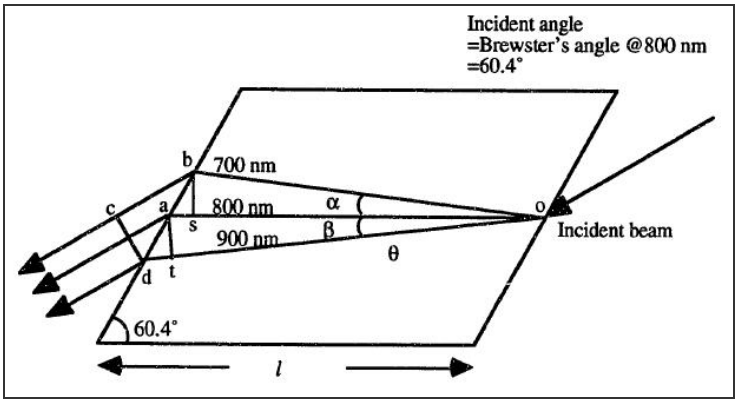

Figure 2.7 Dispersion due to slab geometry

Another source of dispersion is grating and prism pair which can produce negative dispersion. For the grating pair operation as shown in Figure 2.8, the first grating diffract the beam, as a result different wavelength travel in different direction. Since the angle of diffraction for shorter wavelength is smaller than longer wavelength

therefore the transit time for longer wavelength is more than shorter wavelength. After that, the second grating the wavelength will merge together again.

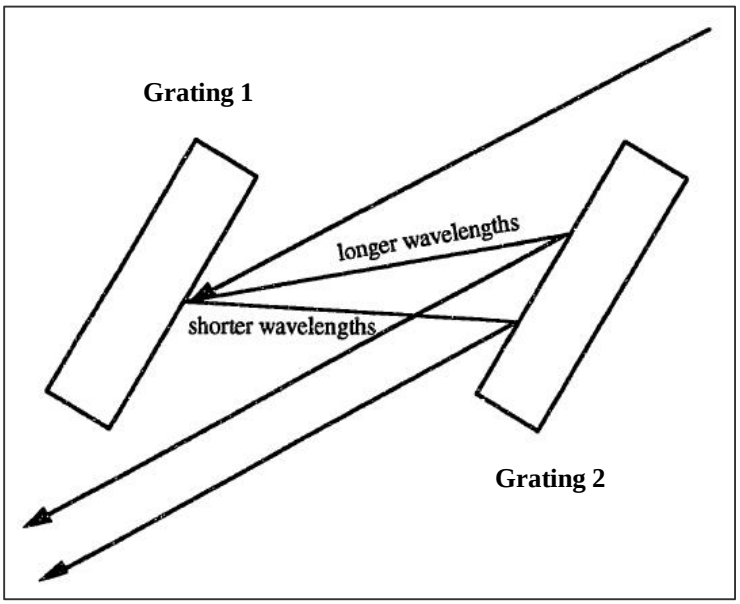

Figure 2.8 Grating pair operation

A prism pair also works similar to the grating pair. In this case the dispersion also introduce by the geometry of the setup which illustrated in Figure 2.9 whereby the shorter wavelength goes through less prism material therefore have shorter optical path. Beside, longer wavelength goes through more prism material therefore have longer optical path. Through this setup the dispersion can be compensated. However the mode-locked operation cannot self stating by using only prism pair in the cavity. Self starting can be achieved by using broadband Semiconductor Saturable Absorber Mirror (SESAM). The SESAM is produced from new development arising from the need for a reliable starting mechanism for ultrashort pulses (Jung *et al.*, 1997).

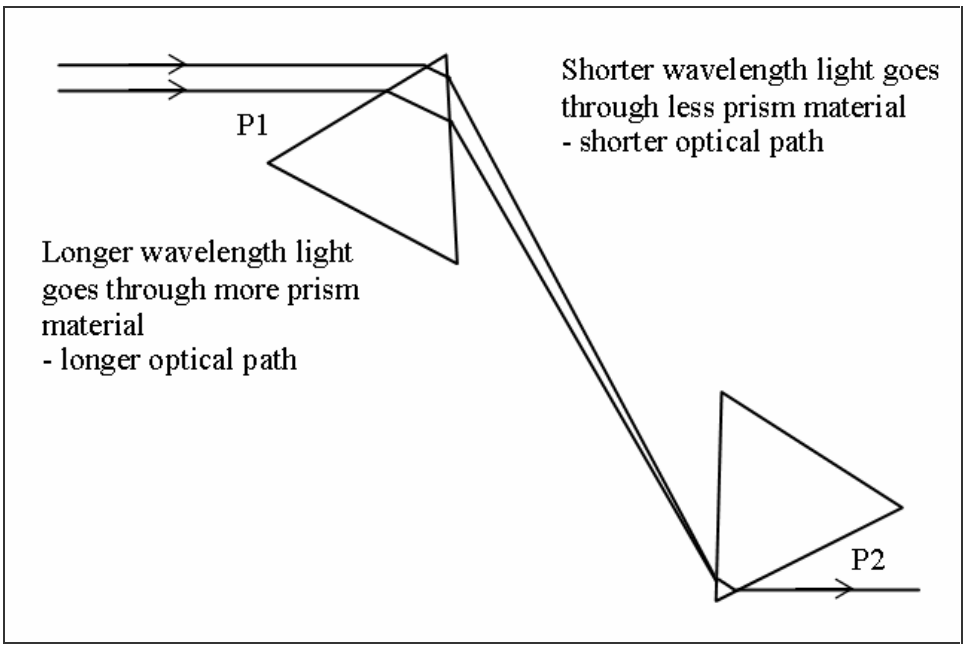
Shorter wavelength light goes through less prism material - shorter optical path
P1
Longer wavelength light goes through more prism material - longer optical path
P2

Figure 2.9 Prism pair operation

In this project prism pair was used as a correction for Group velocity Dispersion (GVD) to reduce the effect of first order dispersion in the Ti:sapphire laser. The method was based upon the earlier work of Fork *et al.* (Pearson and Whiton, 1993). The dispersion of the cavity $d^2P/d\lambda^2$ is given in Equation (2.4).

$$\frac{d^2P}{d\lambda^2} = 4l\left\{\left[\frac{d^2n}{d\lambda^2} + \left(2n - \frac{1}{n^3}\right)\left(\frac{dn}{d\lambda}\right)\sin\beta - 2\left(\frac{dn}{d\lambda}\right)^2\cos\beta\right]\right\} \tag{2.4}$$

Where l is the distance between the apexes of the prism, n is the refractive index of the prisms, λ is the free space wavelength of interest and β is the propagation angle of a ray with respect to a reference line drawn between the apexes of the two prisms.

Distance l, required for correction GVD passing through the length of material, in this case Ti:sapphire crystal. Distance l is calculated by dividing dispersion in cavity

$d^2P/d\lambda^2$ by the product of second order dispersion of the Ti:sapphire crystal $d^2n_{cry}/d\lambda^2$ and the thickness of the crystal, *t*. Then Equation (2.5) was produced.

$$-\frac{d^2 n_{cry}}{d\lambda^2} t = \frac{d^2 P}{d\lambda^2} \tag{2.5}$$

By solving the Equation (2.4) and (2.5) with n = 1.71125, $dn/d\lambda$ = -0.04958 μm^{-1}, $d^2n/d\lambda^2$ = 0.1755 μm^{-2} (for prism made of SF10 glass at wavelength of 800 nm), t = 13 mm and $d^2n_{cry}/d\lambda^2$ = 0.1745 μm^{-2}. The index refraction and properties for sapphire were shown in Appendix A. From this calculation the prism pair separation l is determined as 19 cm.

2.4 Laser oscillator

Basically, a laser consists of a pumped amplifying medium positioned between two mirrors as illustrated in Figure 2.10. The purpose of the mirrors is to provide what is described as 'positive feedback'. This means simply that some of the lights that emerge from the amplifying medium are reflected back into it for further amplification. Laser mirrors usually do not reflect all wavelengths but the reflectivity is matched to the wavelength at which the laser operates. An amplifier with positive feedback is known as an oscillator.

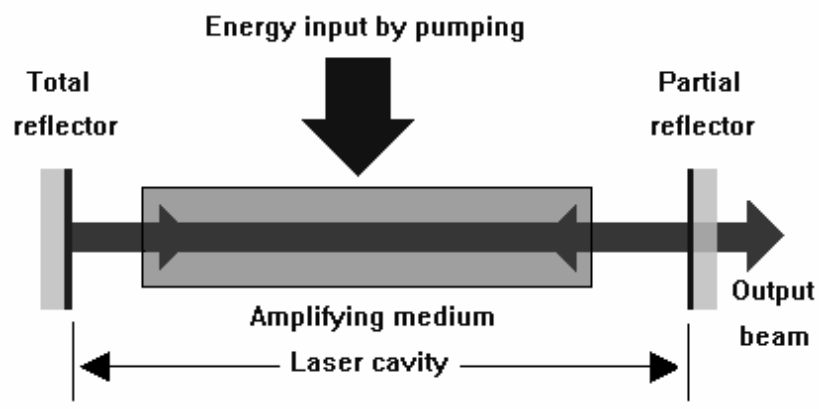

Figure 2.10 Laser oscillator

2.4.1 Cavity configuration

In the construction of the Ti:sapphire laser, it is different than the regular setup as common laser design which is in straight line. Basically, there are two commonly used cavities for Ti:sapphire laser as depicted in Figure 2.11.

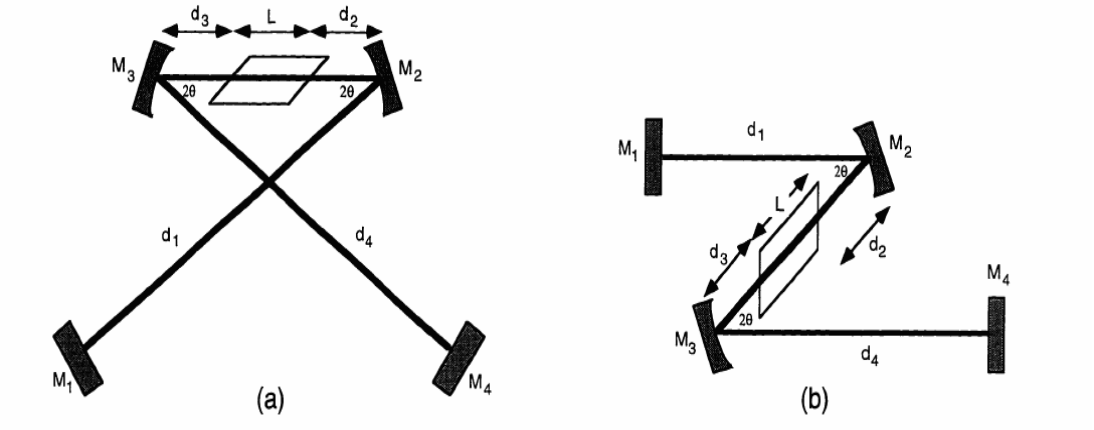

Figure 2.11 Commonly used cavity for Ti:sapphire laser (Koumans, 2001)

The Ti:sapphire laser design can be in an "*X*" or "*Z*" configuration. The folded cavity suitable to obtain good mode matching with pump and to provide tight focusing in the mirror (Mukhopadhyay *et al*., 2003). Beside it can control the astigmatism produce from laser cavity by adjusting the angle of the arm. Both types work equally well and usually selected based on considerations of available space in setting up the cavity (Silfvast, 2004). Nevertheless, "Z" configuration is commonly used for Ti:sapphire laser as well as for Cr:LiSAF and Cr:LiAF (Kalashnikov *et al.*, 1997).

The schematic layout for typical cavity is illustrated in Figure 2.12. It is consists of output coupler (M1), end mirror (M2), two curve mirrors (M3, M4) with 10 cm radius of curvature (ROC) focusing into a Ti:sapphire crystal, and a pair of intracavity prisms for dispersion compensation**.**

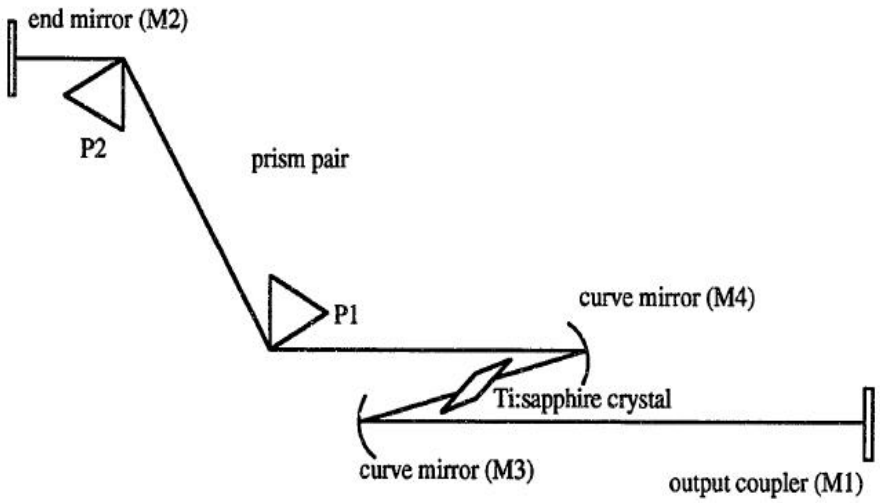

Figure 2.12 Typical cavity for Ti:sapphire laser (Huang, 1995)

However, recent research had successful to replace the prism usage (Sutter, *et al*. 1998 and Bartels, *et al* 1999) with the negative dispersion mirrors that reflect light with longer wavelength from deeper region in the coating than light with shorter wavelength.

This technique found to be more compact, reliable, and user friendly than any previous femtosecond laser. Beside it is more easier to compensate the dispersion especially produce by the Ti:sapphire crystal.

2.4.2 Cavity Optimization

In this part, the calculation of the cavity is included to determine d_1, d_2 and d_f (see Figure 2.13). The calculation for all parameters is referred to Xu *et al.*, (1998). The entire setup for such cavity is shown in Figure 2.13.

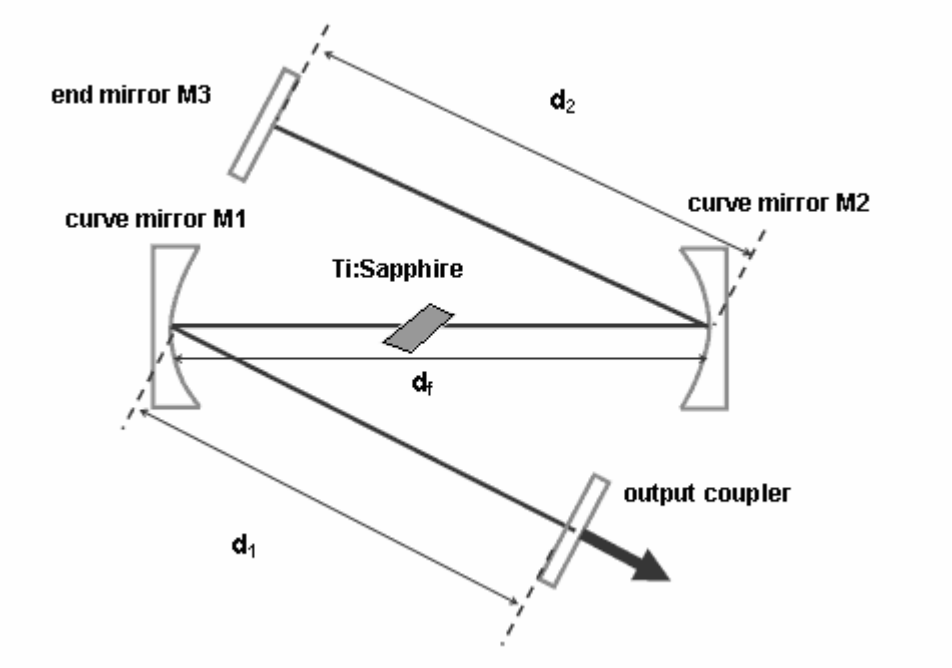

Figure 2.13 Schematic diagram of Ti:sapphire laser

The simple schematic for the folded cavity is shown in Figure 2.14 which is equivalent with lens system for the matrix analysis. However this diagram is not considering the astigmatism produce by the cavity.

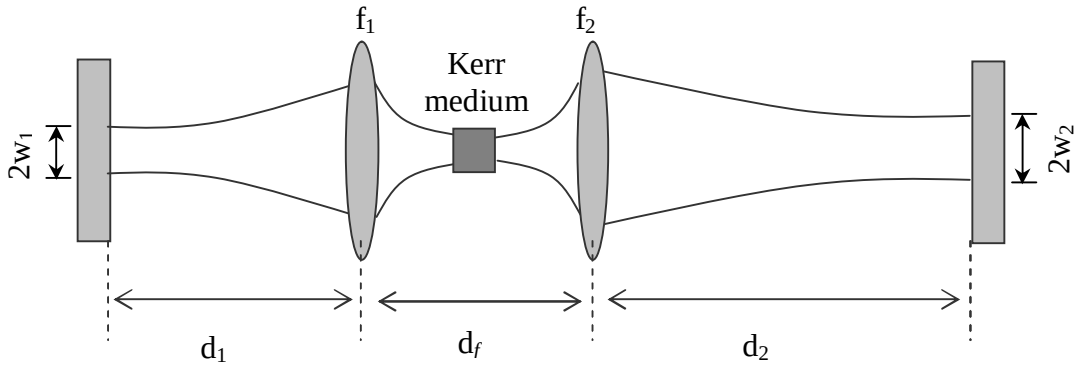

Figure 2.14 Schematic diagram of the tightly focused four mirror resonator configurations.

The spherical mirror will act as a focusing element which is provide a tightly focused resonator mode in the gain medium if the condition of $d_1/f_1>>1$ and $d_2/f_2>>1$. Therefore in this setup d_1 and d_2 are chosen to equal with 60 cm and 80 cm respectively to satisfy the tightly focused condition.

The range value for stable resonator given by:

$$0 < \delta < \delta_1 \text{ and } \delta_2 < \delta < \delta_{\max}, \tag{2.6}$$

where,

$$\delta_1 = \frac{f_2^2}{d_2 - f_2}, \delta_2 = \frac{f_1^2}{d_1 - f_1} \quad \text{and} \quad \delta_{\max} = \delta_1 + \delta_2 \tag{2.7}$$

Therefore

$$d_f = f_1 + f_2 + \delta \tag{2.8}$$

Where δ is stability parameter and f is focal length. By substituting the Equation (2.8) with f = 5 cm, d_1 = 60 cm and d_2 = 80 cm the δ_1, δ_2 and δ_{max} is equal to 0.33, 0.45 and 0.79 respectively. The position of δ_1, δ_2 and δ_{max} are shown in Figure 2.15. The stability region is separated by forbidden zone. For symmetric design whereby d_1 equal to d_2, forbidden zone will be removed, in other word there is just a single stability region. In this design unequal arm was used which is known as *asymmetric design*. Therefore the stability region is split into two as shown in Figure 2.15. When d_1 is shorter than d_2, the position of the outer stability region will shift away from the forbidden zone, but maintain the beam diameter. This shifting also occurs when d_2 is shorter than d_1.

The Kerr lens mode-locking can be optimized by the adjustment of the arm length ratio. For the symmetric cavity the maximum Kerr lens sensitivity occur when the laser operate at the center of stability with the crystal put at the center between two curve mirrors. However the stability of the symmetric cavity is easy to effect by the environment. Therefore asymmetric cavity is typically used for KLM laser. For the best KLM performance, the arm length ratio should in the range between 4:3 and 2:1 (Kowalevicz, 2004).

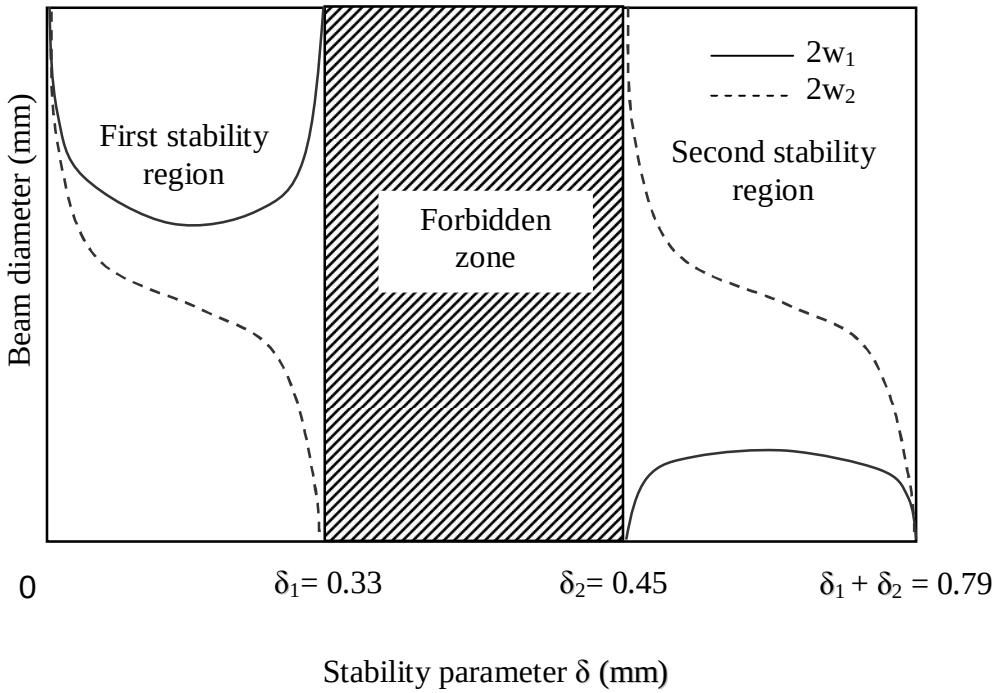

Figure 2.15 Beam diameter as a function of the stability parameter δ

In order to get the KLM the hard aperture and soft aperture KLM can be used. As discussed before, hard aperture mode-locking uses a physical slit within the cavity to block the CW components of light. Beside soft aperture mode-locking uses the gain medium as the aperture (see Figure 2.5). For soft aperture Kerr Lens Mode-locking an asymmetric cavity configuration is predicted to be most favorable for strong SAM (Self Amplitude Modulation) and δ adjusted to δ_2 in second stability zone. For hard aperture mode-locking uses a physical slit within the cavity to block the CW components of light. Beside soft aperture mode-locking uses the gain medium as the aperture (Xu, *et al.*, 1998). In general, the cavity becomes a stable resonator when the curve mirrors separation $d_f \geq f_1 + f_2$ with f_1 and f_2 is the focal length of the curve mirror (Kowalevics, 2004). As a result of using the Equation (2.6), (2.7) and (2.8) the value of d_1, d_2 and d_f can be determined as d_1 = 60 cm, d_2 = 80 cm and d_f = 10.5 cm, respectively.

2.4.3 Astigmatism correction

As a result of the presence of Brewster angle in the Ti:sapphire crystal, some astigmatism is introduced in the cavity which can lead a beam waist size difference between sagittal (perpendicular to the plane of incident) and tangential (parallel to the plane of incident) plane (Kowalevicz, 2004). Astigmatism needs to be reduced because it can cause unstable mode-locking (Lytle *et al.*, 2004) and also reduced output power. Although, the astigmatism correction calculated using the theoretical equation, in contrast to real "Z" folded cavity, astigmatism cannot be completely compensated. The astigmatism just can be minimized by titling the folding mirrors M1 and M2 to a certain angle extension. The optimal fold angle for the cavity to reduce astigmatism can be calculated using the following equation (Kolgenik *et al.*, 1972)

$$2Nt = 2f \sin\theta \tan\theta \equiv R \sin\theta \tan\theta \tag{2.9}$$

where

$$N = (n^2 - 1)\sqrt{n^2 + 1/n^4} \tag{2.10}$$

By solving the Equation (2.9) and (2.10) we can get the angle is:

$$\theta = \arccos\left[-C + \sqrt{C^2 + 1}\right] \tag{2.11}$$

where

$$C = \frac{t\left(n^2 - 1\right)\sqrt{n^2 + 1}}{n^4 R} \tag{2.12}$$

Where t and n are the thickness and the refractive index of the Brewster angled medium, R is the radius of curvature of the folding mirrors. With refractive index of n = 1.76, a

thickness of t = 13 mm and curvature radius of R=100 mm. From the calculation θ is obtained as 19.24^{o}.

2.5 Optical Pumping

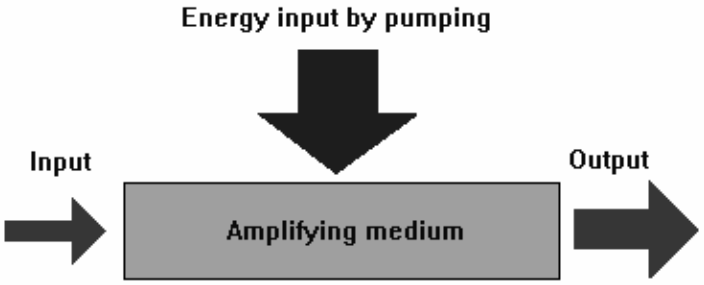

Figure 2.16 Optical pumping

In laser terminology, the process of energizing the amplifying medium is known as "*pumping*". Pumping an amplifying medium by irradiating it with intense light is referred to as *optical pumping* (Figure 2.16). The source of pumping can be flashlamp or other laser. In this project Diode Pumped Solid State (DPSS) laser was used as a pumping source, using *End Pumping Method*. When the laser material is pumped by certain pumping source, the light will be absorbed by the active medium. This process will lead to the emission in the laser material such as shown in Figure 2.17.

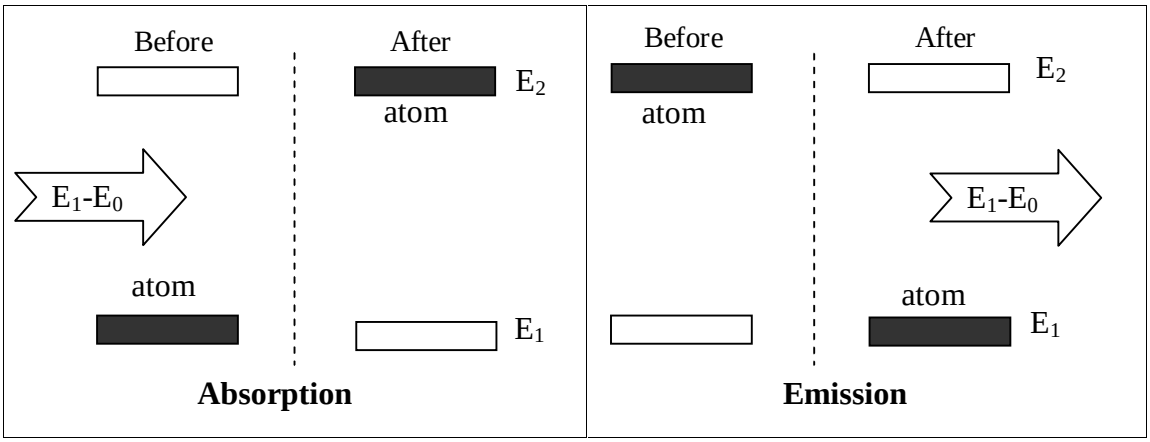

Figure 2.17 Absorption and emission process

There are two types of the emissions which are spontaneous emission and stimulate emission. For the spontaneous emission, the direction and phase of the emitted photons are random. This type emission can't produce laser. The laser will be produced only after the stimulate emission occur.

2.6 Temperature Control

Another aspect to consider on discussing Ti:sapphire laser is temperature control. It is very vital factor for the Ti:sapphire laser system because it can effect the output of the laser such as the power and stability. Moreover, without proper temperature control, Ti:sapphire crystal possibly will be ruined. The upper state lifetime of the Ti:sapphire laser crystal is sensitive to temperature as shown in Figure 2.18. This lifetime has a constant value up to 200 K, and then there is a clear reduction in the lifetime with increasing temperature. At room temperature the upper state laser lifetime is 3.2 μs. To have efficient laser performance, it is important to keep the temperature of the laser crystal near room temperature.

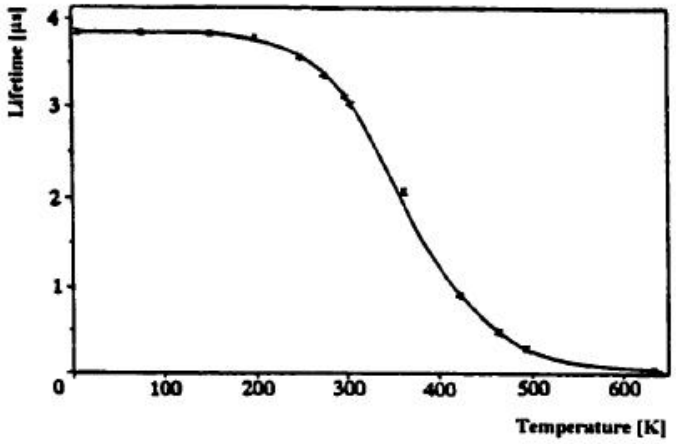

Figure 2.18 Lifetime of the upper laser level of Ti:sapphire as a function of temperature (Elsayed, 2002)

Due to excessive temperature, will result in a reduction of the upper-state lifetime and thereby will increase the laser threshold at the same time will reduce the output power. To improve the situation, cooling system need to be provided. In this project water cooling system was utilized to control the crystal's temperature. Alternatively, Termoelectric cooler (cooled by a Peltier cooler) also can be used.

CHAPTER 3

RESEARCH METHODOLOGY

3.1 Introduction

In this chapter, the experimental techniques used in this study will be described. These comprised the alignment of the cavity and laser components used in this project. The equipments used in the experiment and software conducted in the analysis also included.

3.2 Alignment of the cavity

The alignment of the cavity is a very challenging task in the construction of the Ti:sapphire laser. Moreover for the mode-locked laser operation requires extremely precise alignment compare to the CW operation. It also needs to have careful design of the laser cavity (Kowalevicz, 2004). As discussed previously in chapter 2, the “Z” or

"X" folded is the best cavity for the standard KLM lasers. In this chapter the technique to align Ti:sapphire laser will be discussed. Figure 3.1 shows the overall setup for Ti:sapphire laser. The step by step procedure of alignment for the Ti:sapphire laser will be described in detail. The optical components employed in each of alignment also will be included. Prior to operate the laser either in continuous or pulse mode, the general setup which will be utilized in both operations will be described.

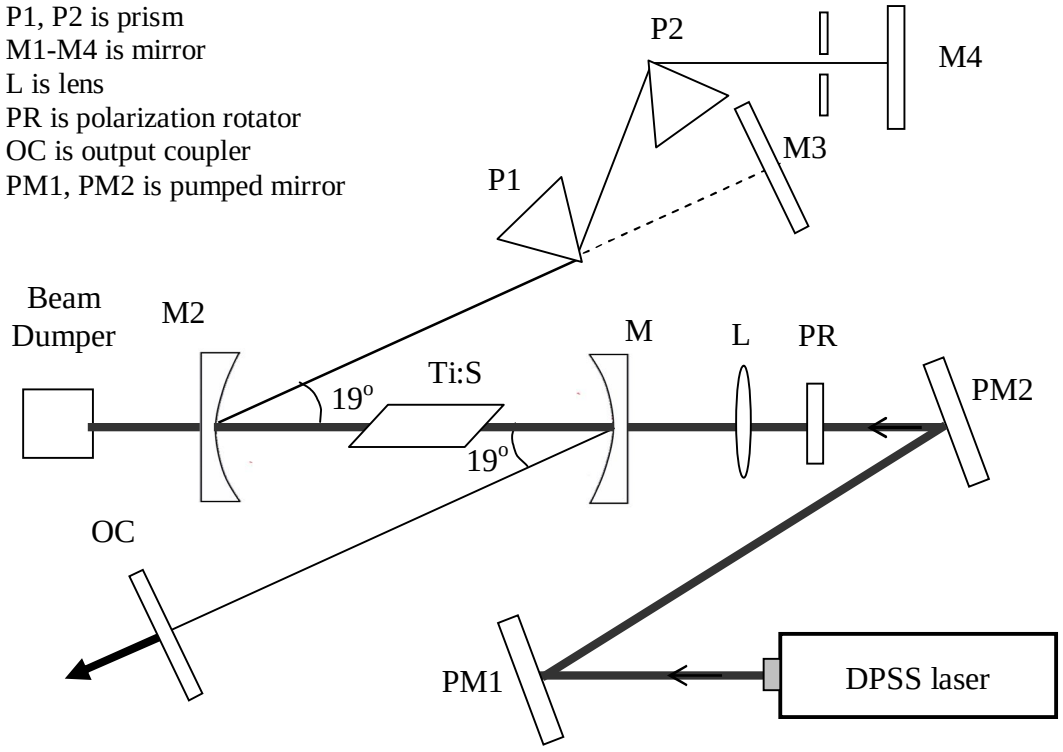

Figure 3.1 Overall experimental setup of Ti:sapphire laser.

3.3 General Setup

Prior to operate the laser either in continuous mode or pulse mode, several major alignments need to be discussed. This including the alignment of pumping source, focusing beam, linear cavity and cooling system.

3.3.1 Pumping Source Alignment

The first step to develop Ti:sapphire laser is to aligned a diode pumped solid state laser as a pumping source. In this alignment two high reflective mirrors at 532 nm known as pumped mirrors (PM1 and PM2) were used to locate the pumping beam. The beam can be positioned easier by using two mirrors rather than just one mirror. Only small power of DPSS laser was operated during this alignment that is about 2 W. The mirror PM1 was placed at an angle upon DPSS laser beam such as shown in Figure 3.2. The beam was reflected to the second mirror of PM2. The output of the DPSS laser is in vertical plane of polarization. The polarization beam was rotated to the horizontal plane in order to prepare a Brewster angle condition of the Ti:sapphire crystal. Thus, a polarization rotator (PR) was employed and placing into the beam path after PM2. The best condition for the beam to become horizontal is identified when only a small portion of the reflected beam from PR was detected near the DPSS laser window.

It is better to note that the beam from the PM2 must always at horizontal or having the same level. This condition can be achieved by using two apertures (A1 and A2). Firstly the DPSS beam needs to enter the first aperture A1. Another aperture A2 was placed about 1 meter away. Second mirror PM2 needs to be adjusted until the beam enters the second aperture A2. Both apertures were aligned in axis by drawing a line on the optical breadboard using pencil. If the beam able to enter both apertures, this indicates that the beam is properly aligned.

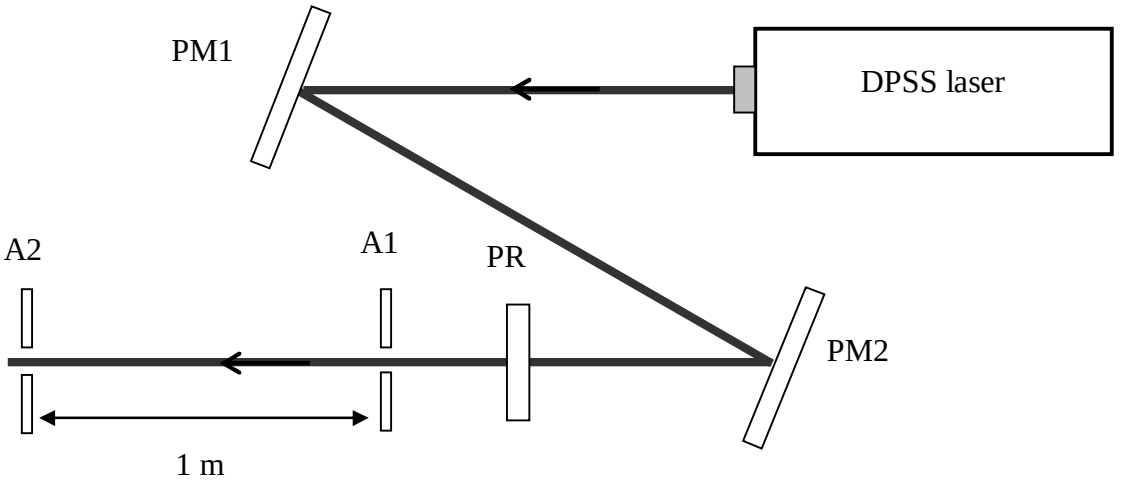

Figure 3.2 Alignment of the pumping source

3.3.2 Focusing DPSS beam

A focusing lens of focal length 100 mm was employed to focus DPSS laser beam such as shown in Figure 3.3. The beam from PM2 needs to be in the center of the lens L. The lens's mounting should be tightened at the base properly to avoid misalignment. Proper alignment of the lens is ensured by placing a screen. In this case a white paper is introduced. Placing at a distance away to see the beam shape after going through L as illustrated in Figure 3.3. The best position is noticed by moving the lens to pro and back, but the beam spot does not move. The aperture A2 is removed in order to observe beam spot. In case the spot moving to the left side, the lens mount was tilted clockwise slightly. If after adjustment the spot not at the center, the lens holder need to be adjusted perpendicular to the beam direction. The beam from L is desired to be reflected back into aperture A1. The same procedure was repeated several times until the spot will not move.

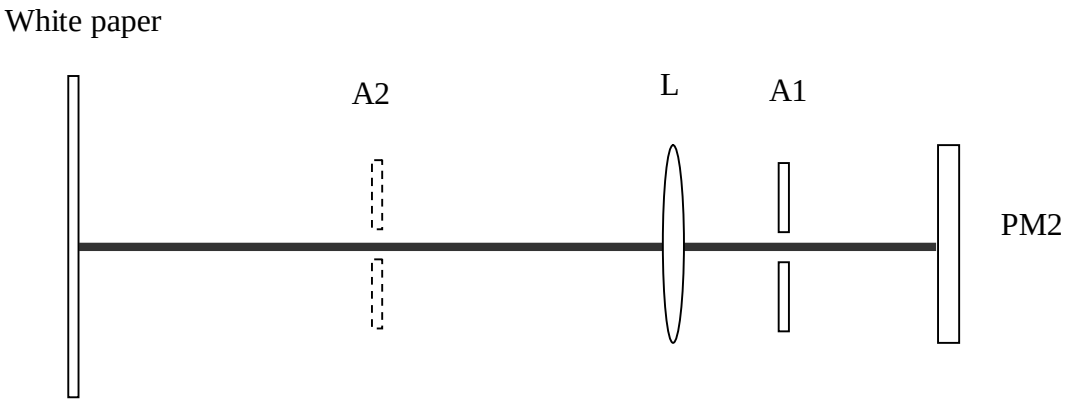

Figure 3.3 Alignment for focusing the DPSS beam

3.3.3 Linear cavity alignment

The focused beam of DPSS laser was used to excite active medium in this case Ti:sapphire crystal. The stimulated emission from the crystal is then amplified in a linear cavity. The linear cavity was developed by using two concave mirrors M1 and M2. The configuration of cavity is shown in Figure 3.4. The procedure of the alignment was started by inserting concave mirror M1 in front of the lens L. Introducing M1 in the path of focused beam, subject to increase the focal length such as illustrated in Figure 3.5. The beam was focused about 110 mm away from the original focal point.

A Ti:sapphire crystal was placed at a new position of focal point. The crystal was adjusted until the focused beam passing through at the center. The angle of the crystal was also adjusted to minimize the reflection. The other crucial parameter desire to be considered in the performance of alignment is its crystallographic axis. This was implemented by introducing a polarization cube PC.

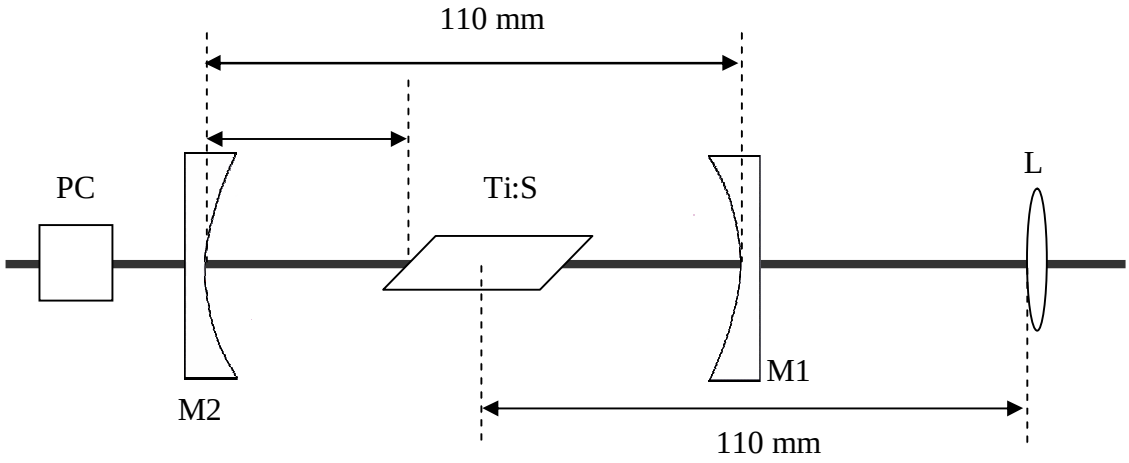

Figure 3.4 Alignment of linear cavity

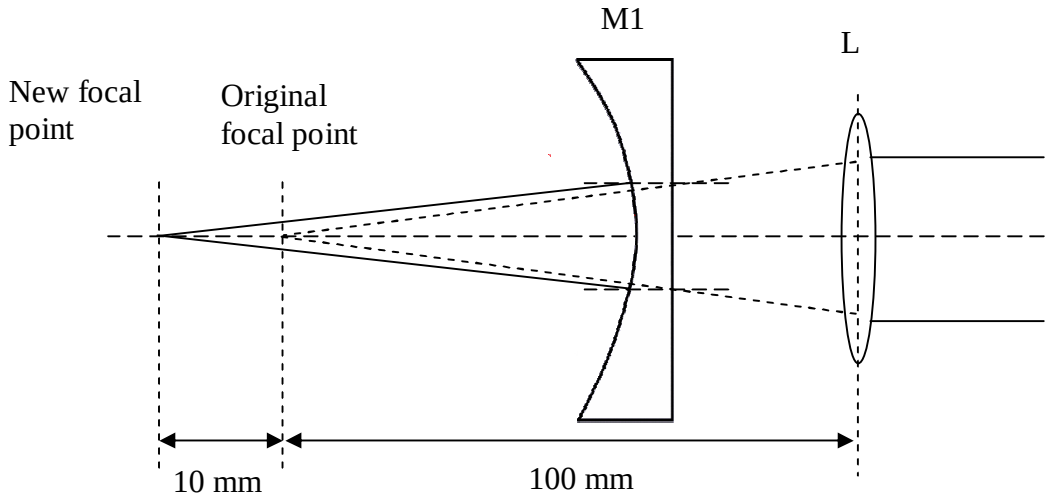

Figure 3.5 New focal point formations after passing mirror M1

In order to find the suitable crystallographic axis a screw 1 on the crystal holder was manipulated such as depicted in Figure 3.6. The adjustment was continued until a minimum reflected power from polarization cube PC was detected. This point is referring as a *dark field*. When the *dark field* condition was achieved, the holder of the crystal was tightens. Mirror M2 was then inserted into the system. The distance between

mirror M1 and M2 surface was chosen approximately at 110 mm. This distance will be optimized during the laser operation. The beam dumper was put beyond the mirror M2 to block the beam.

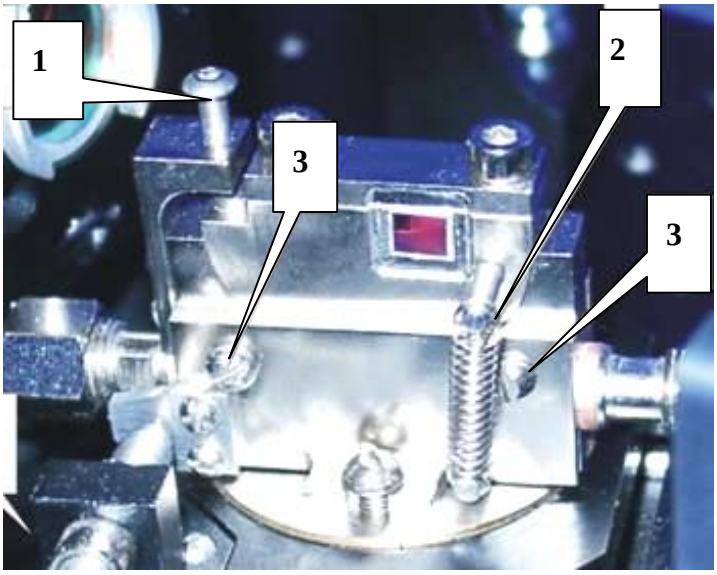

Figure 3.6 Crystal holder (1) Screw for aligning crystallographic axis orientation, (2) Spring, (3) Fixing screw

3.3.4 The cooling system

Gain medium Ti:sapphire crystal will be pumped by high power diode laser. The crystal was pumped using end pumping technique. To avoid temperature gradient during pumping process, the crystal was desired to be cooled. In fact cooling the crystal will also give an advantage to stable the output laser.

The cooling was installed by providing the chilled water such as illustrated in Figure 3.7. The inlet and outlet of the pipe were connected to the crystal holder. The temperature was maintained as ambient temperature. However, the water was pumped so

that it was circulated during the pumping process. The schematic of cooling system is shown in Figure 3.8.

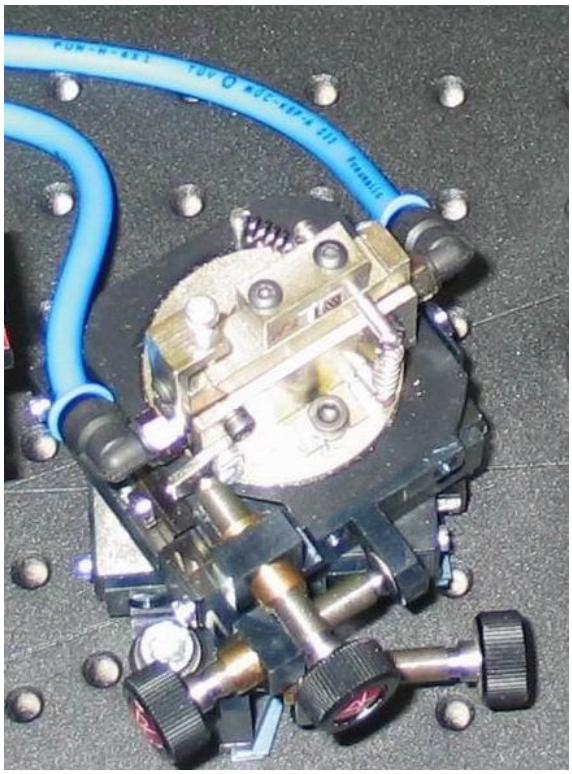

Figure 3.7 The pipe installation at crystal holder

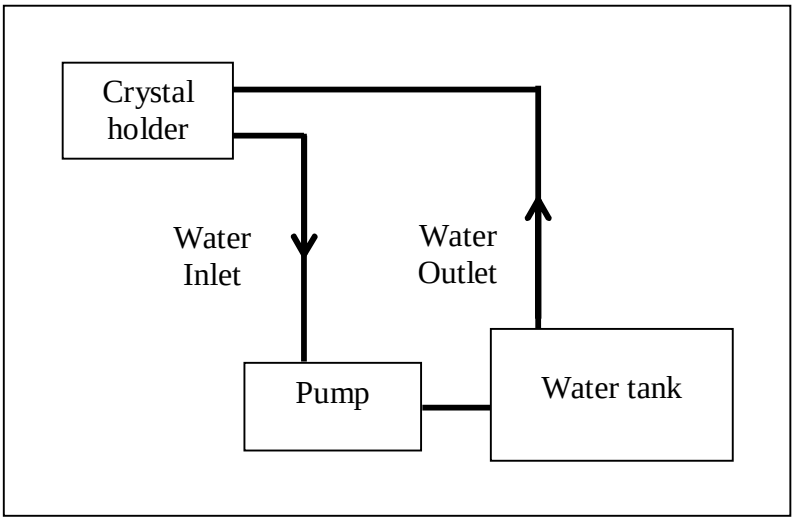

Figure 3.8 The schematic of cooling system

3.4 Continuous Wave operation

Finally to complete the task and operated the laser in continuous awe, two final mirrors were inserted into the linear cavity. The last two mirrors are consisted of output coupler OC and rear mirror M3. The insertion of these two mirrors changed the linear cavity to become "Z" folded cavity configuration.

3.4.1 "Z" folded cavity

The procedure to complete the development is describe. First the focusing lens L was determined to be at the best position. This was performed by introducing a white paper behind mirror M2. The beam spot was ensured to be existed at the center of the mirror M2. This is similar procedure as implemented in Figure 3.3.

After optimizing the best position of the focusing lens L, an output coupler OC was inserted into the system. Similarly, the OC also need to be aligned at the best location. The procedure for this alignment is entirely different with the focusing lens. In this case, luminescence of the Ti:sapphire crystal was utilized. The luminescence was illuminated at the center of the output coupler (OC). The presence of the beam can be detected using infrared card. An aperture was employed to enhance the alignment. The luminescence beam was incident on the aperture. The beam from the output coupler was ensured to be reflected back on the aperture.

Finally, the configuration of "Z" folded cavity was completed by inserting the last mirror of M3. The position of M3 is shown in Figure 3.9. In order to avoid astigmatism phenomenon, the mirror M3 and OC have to be aligned at an angle of 19^{o}

with respect to the optical axis of the pair spherical mirror. The portion pumped beam was ensured to be located at the center of mirror M3.

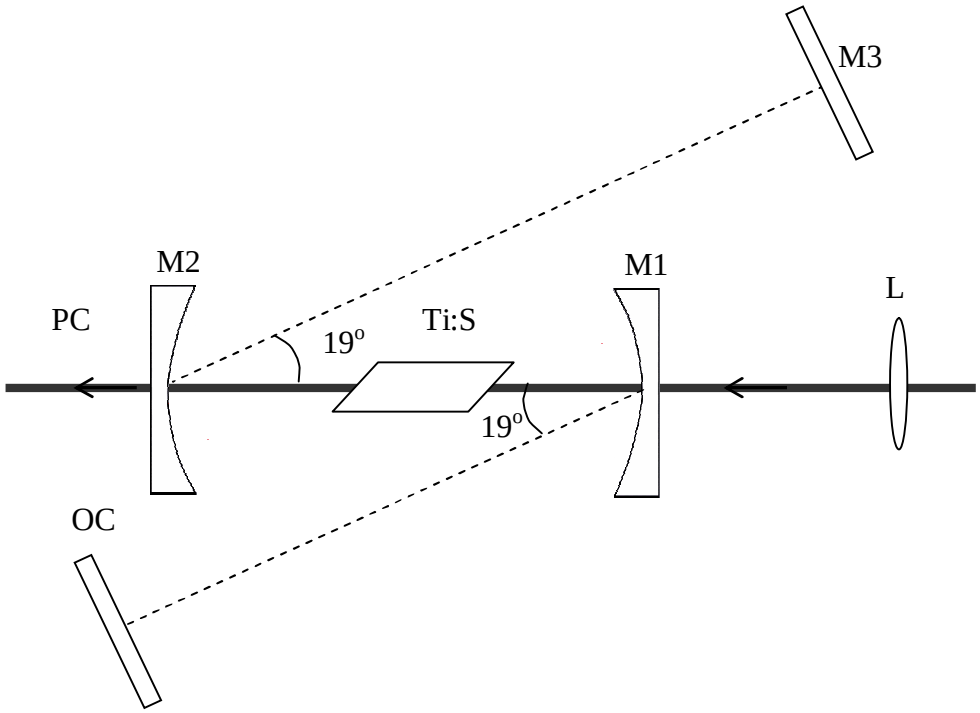

Figure 3.9 Alignments of "Z" folded cavity

3.4.2 Testing the CW output

Now let we considered the propagation of the beam in the laser. Ensure that the OC are reflected to M1, M2 and M3. Overlapping beam between OC and M3 was determined either by using IR viewer or IR card. IR viewer is better to used but not available in our lab. Therefore the testing was carried out using IR card. The IR card needs to be placed in front of the M3 followed by a red filter which was used to block the green beam as shown in Figure 3.10.

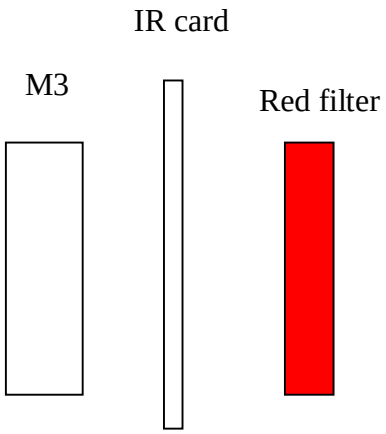

Figure 3.10 Beam alignment method.

The IR beam shows on the IR card should be overlapped. The first IR at the M3 is came from the fluorescence of the Ti:sapphire crystal at initial stage and the second IR beam was reflected by the output coupler OC. The first IR beam need to be adjusted until illuminated beam fall at the center of mirror M3. After that the output coupler OC was adjusted until the second IR beam overlap with the first one. This step was repeated at the output coupler OC without using red filter. When the entire IR beams are overlapping, this indicates that the mirrors were properly aligned. If a correct alignment has been done, the laser generation should be produced. The laser output detected using IR card such as shown in Figure 3.11. If no lasing appeared, a photodetector could be used to detect the beam. The photodetector is more sensitive compared to the power meter and gives faster response to the power changing. The photodetector was coupled to an oscilloscope. The output coupler OC and mirror M3 need slightly adjustment, to achieve optimum power as manifested in the oscilloscope.

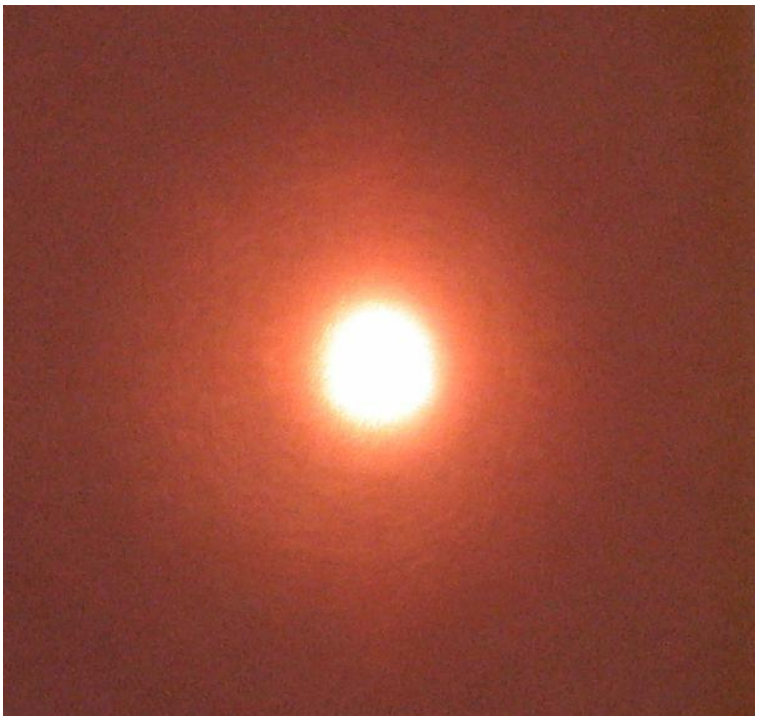

Figure 3.11 Laser output detected using IR card

3.4.3 Optimum CW operation

There are several steps to achieve the maximum power. First, small change is made upon the upper adjustment knob of M3. When the power decrease, upper adjustment knob of output coupler OC need to optimize and see if the new optimum is higher or lower. If it is higher continue move the upper adjustment knob of output coupler OC at the same direction. If the power turn lower, move the upper adjustment knob of output coupler OC in the opposite direction. These steps are repeated, if neither direction makes it go up, it is at the maximum condition. After that, upper adjustment knob of M3 and output coupler OC was adjusted by using the same step as explained before. This adjustment need to repeat several times until the optimum power achieved.

3.5 Femtosecond operation

In the alignment of femtosecond operation, the discussion is divided into three sections. The first part involves the dispersion control. The second part, explains the optimization of femtosecond pulse. In third part describes the starting of femtosecond pulse.

3.5.1 Dispersion Control

The same "Z" folded cavity of CW Ti:sapphire laser was employed to generate femtosecond pulse. However to convert from CW to become pulse laser, another components are required. A pair of prism needs to be added in the cavity as shown in Figure 3.12. The usage of the prism is to control the dispersion in the cavity. By controlling the dispersion in the cavity a femtosecond pulse laser could be achieved.

The procedure of alignment was started by inserting a prism P1. Firstly we need to insert a prism (P1) near the deviation angle. After the desired place is obtained, the prism's holder was tightened to fix it on the optical table. Adjustment knob of prism P1 was adjusted slowly, in this manner prism was slightly moved into the beam path. Just a few fraction of the beam was required to be inside the prism. A stop point for correcting the alignment of the prism was then needs to be found. Stop point is the condition whereby the beam starts to change direction as the prism rotated. The prism was tightened after getting the stop point.

A second prism P2 was then aligned into the cavity using the same procedure of prism P1. The distance between the prisms is set around 19 cm as calculated using

Equation (2.4) and (2.5). The separation of the prisms will introduce negative dispersion in the cavity which is to compensate the dispersion in cavity. The best position is determined using the same procedure of prism P1. The prism P1 was adjusted until the beam from P1 strikes P2. Both prisms are ensured to be at the same level. After that mirror M4 was aligned such as shown in Figure 3.12. The arm length between the M2 to M4 was set to be in the ratio of 4:3 of the M1-OC length. With the alignment of mirror M4 the basic alignment of femtosecond operation was completed. The mirror M3 was used only during alignment procedure but not included during femtosecond operation this illustrates by the dotted line in Figure 3.12.

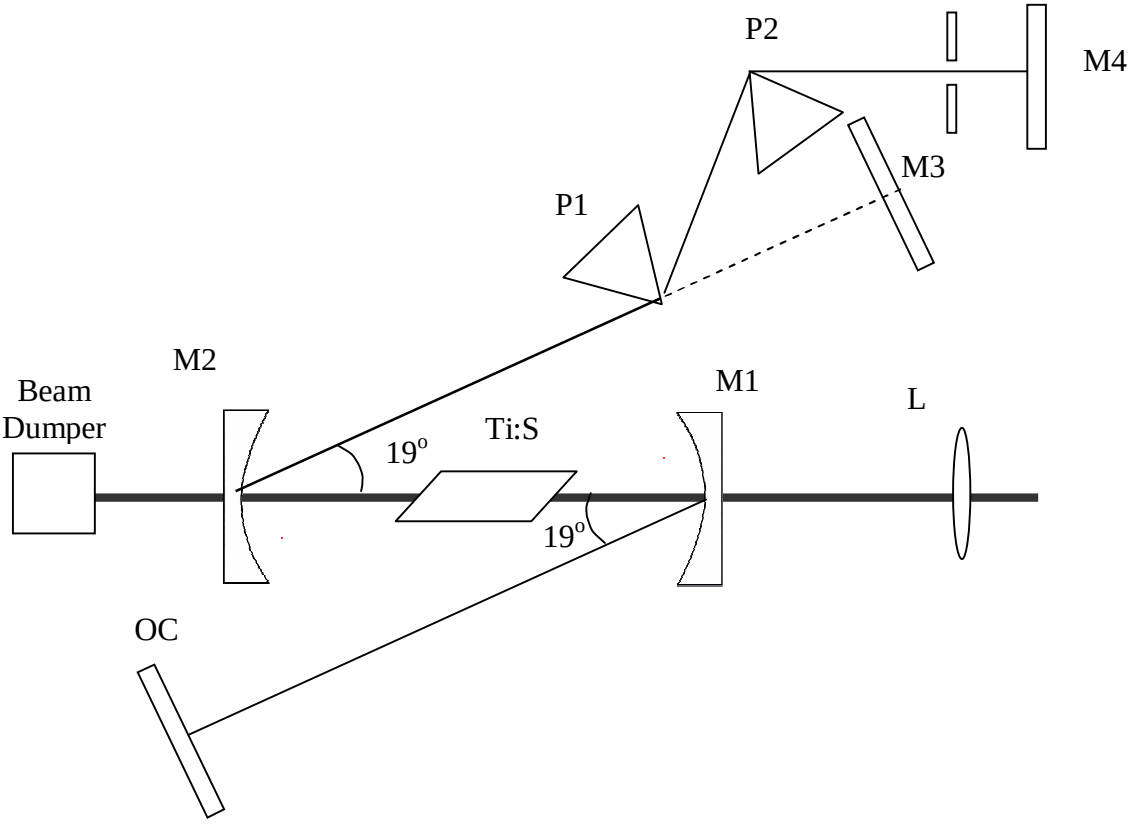

Figure 3.12 Alignment setup of femtosecond operation.

3.5.2 Optimization of femtosecond pulse operation

Firstly prism P1 was inserted in the beam path. All the beams need to strike on the prism P1. By a slight adjustment of mirror M4, the laser pulse generation through the prism would be produced. The mirror M3 can be blocked because there is still green laser will be reflected back in the cavity. After lasing generation achievable, OC and M4 were aligned until a maximum output power was produced. The power should at least 40 % of output power without prism to ensure enough power was produced during the femtosecond operation. Otherwise the first alignment setup of CW operation should be repeated. When the maximum output power was obtained by a proper adjustment of the mirrors, the reflected beam from the prism apex was aligned.

By using IR card two spots were appeared. Ensure that the spots are parallel to each other by aligning the prisms. The distance between two spots for P1 needs to pass through the apex of prism. This can be ensured by setting the distance between two spots reflected by the prism approximately 1-2 mm (Figure 3.13). The distance between two spots represented the beam insertion in the prism. The lower beam inserted in the prism mean the higher positive dispersion produced. Hence the beam insertion should be minimized. However, ensure that not loosing laser generation. The same procedure was used to align the P2. The slit is used to remove the CW beam element in the femtosecond pulse.

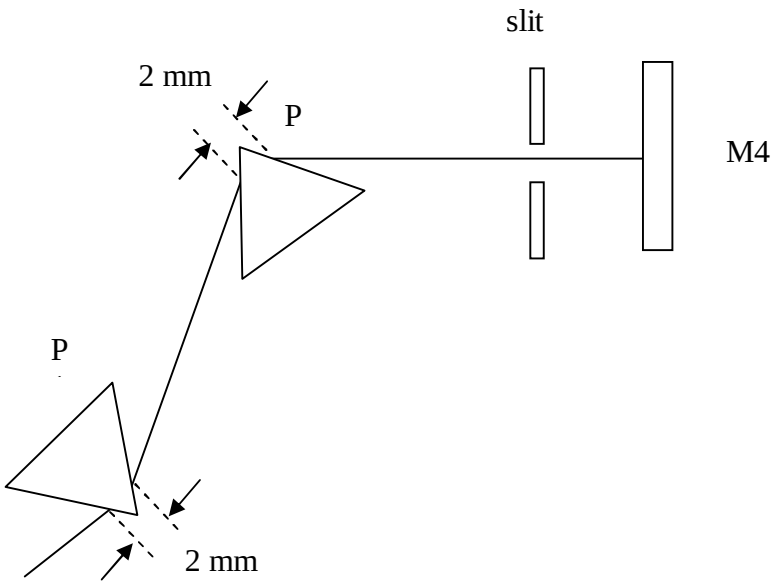

Figure 3.13 Alignment of the prism pair and M4

3.5.3 Starting the femtosecond pulse operation

In this laser design, the femtosecond regime does not self starting. Initiating self starting femtosecond regime can be performed by using a Semiconductor Saturable Absorber Mirror (SESAM). Starting the femtosecond operation was carried out by disturbing the prism P2 using finger to give external perturbation (Spence *et al.*, 1991). This disturbance would change the depth of insertion of the prism. As a result, an initial perturbation to generate an intracavity power fluctuation that builds up to a stable circulating femtosecond pulse was produced (Ye and Cundiff, 2005).

The femtosecond pulse was detected by using fast photodetector which coupled to the oscilloscope. At the same time mirror M2 was adjusted until the appearance of pulses. The femtosecond pulse should appear near the end of stability region. Sometimes it's very hard to get the femtosecond because of the dust on the optical component and along the beam path. Therefore all the optical components must always clean. The way

to solve the problem is by covering the entire optical components. Typical example of femtosecond pulse obtained is shown in Figure 3.14.

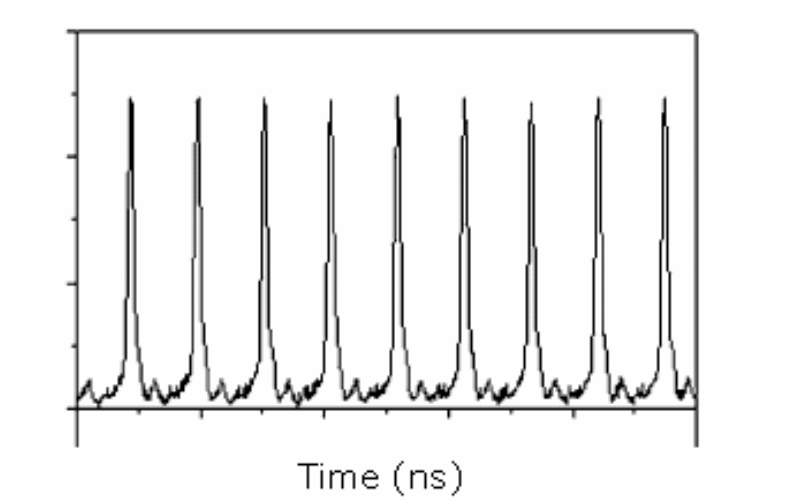

Figure 3.14 Femtosecond pulse detect using fast photodetector (Lin *et al.*, 2002)

Spectrometer was employed to detect the spectrum of femtosecond pulse. The spectral bandwidth of the femto pulse taken at Full Wave Half Maximum (FWHM) should be at least 7 nm and at the center wavelength of around 800 nm. This value is corresponding to pulse duration of 100 femtosecond. Figure 3.15 shows the typical example of the femtosecond pulse spectrum with FWHM of 8 nm.

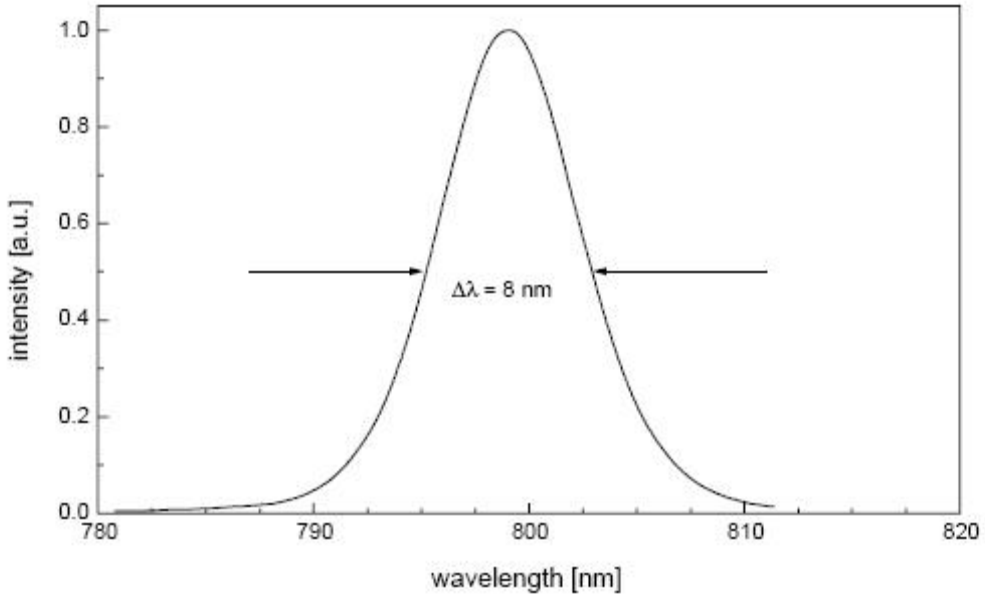

Figure 3.15 Femtosecond pulse spectrum (Schneider *et al*., 2000)

3.6 Output measurement

The output of the femtosecond laser was characterized by using power meter, spectrometer and fast photodetector. It is better to notice that the output coupler is in wedge shape. In this configuration, the output laser could be divided into three major rays namely P_3, P_2 and P_1. The other beam can't be used because the power is too small to detect. The power of the beams produced becomes lower after reflected by output coupler surface. P_3 is lower than P_2 and P_2 is lower than P_1 ($P_3<P_2<P_1$). To be able to synchronize the measurement, two of the beam (P_2 and P_3) are reflected by gold coated mirrors (M_1 and M_2). The reflected beam P_3 was detected by using fast photodetector. Meanwhile beam P2 was observed by using spectrometer and the spectrum was displayed on the monitor. Matrox Inspectror software was utilized to analyze the

spectrum. Beam P1 was directly incident to a power meter to measure the output power of the laser. The setup for output measurements is shown in Figure 3.16.

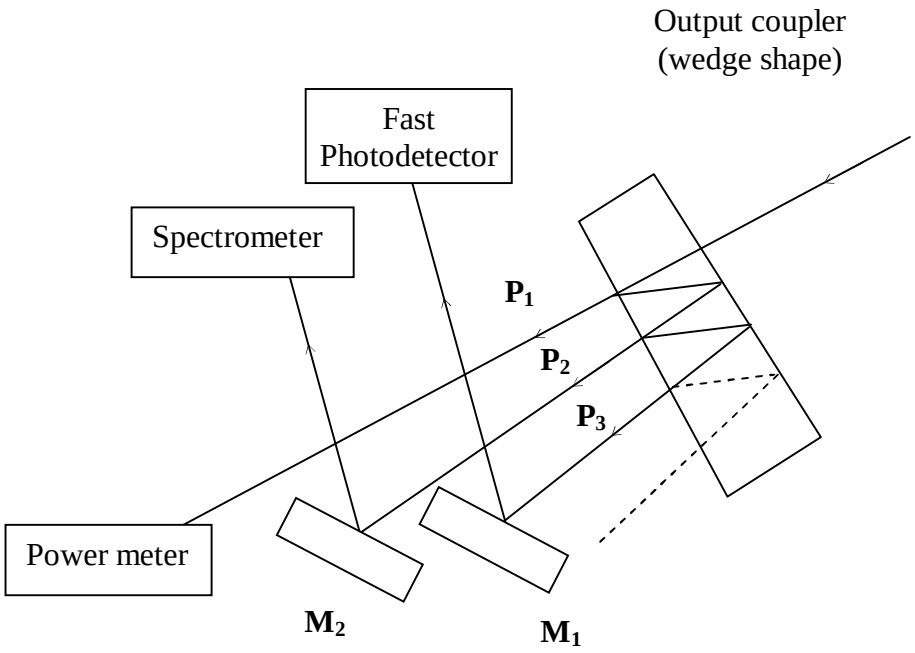

Figure 3.16 Setup for the output detection

3.7 Laser component and equipment

In this section, the material and equipment used in this study will be described. These include the laser material, optical components for resonator development, equipments used in the experiment and software utilized for analysis.

3.7.1 Active medium-Ti:Sapphire

All lasers contain an energized substance that can increase the intensity of light passing through it. This substance is called *amplifying medium* or, sometime, the *gain medium* or *active medium*. The active medium can be a solid, a liquid or a gas.

In this project Ti:sapphire crystal was used as an active medium. Titanium doped sapphire (Ti^{3+}:Al_2O_3) or Ti:sapphire was developed late in laser evolution. Since the discovery of laser action in Ti:sapphire in 1982, it becomes one of the most widely used solid-state laser material (Kuhn, 1998). The very important application of Ti:sapphire lasers is the generation and amplification of femtosecond mode-locked pulse (Koechner and Bass, 2003). It combines the excellent thermal, physical and optical properties of Sapphire with the broadest tunable range of any known material (Eggleston *et al.*, 1998). The physical properties of the crystal are listed listed in Table 3.1.

Table 3.1: Physical properties of Ti:sapphire

Physical properties	**value**
Index of Refraction	$n = 1.76$
Fluorescent lifetime	$\tau = 3.2\ \mu s$
Fluorescent line width (FWHM)	$\Delta\lambda \sim 180$ nm
Peak emission wavelength	$\lambda_p \sim 790$ nm
Peak stimulated cross section • Parallel to c axis • Perpendicular to c axis	 $\sigma_{\parallel} \sim 4.1 \times 10^{-19}\ cm^2$ $\sigma_{\perp} \sim 2.0 \times 10\text{-}^{19}\ cm^2$
Stimulated emission cross section	$\sigma_{\parallel} \sim 2.8 \times 10^{-19}\ cm^2$
Quantum efficiency	$\eta_Q \approx 1$
Nonlinear coefficient	$3.2 \times 10^{-16}\ cm^2/W$
Damage threshold	$10\ J/cm^2$
Thermal conductivity	0.35 W/cm.K

Ti:sapphire crystals has good operation in the pulsed-periodic, quasi-CW and CW modes of operation. Ti:sapphire is a 4-level laser system with fluorescence lifetime of 3.2 μs (Koechner and Bass, 2003). This crystal can be lased over the entire band from 660 to 1100 nm. With broad tunability make it an excellent replacement for several common dye lasing materials. The Ti:sapphire has a wide absorption band (extend about 200 nm) center at near 490 nm (Gan, 1995) as shown in Figure 3.17. Ti:sapphire can be pumped by variety of sources operating in the green-argon ion, copper vapour, frequency-doubled Nd:YAG and dye lasers are routinely used. However, for the commercial Ti:sapphire laser, frequency doubled Nd:YAG or Nd:YLF lasers are used as a pumping source to pump Ti:sapphire crystal (Song *et al.*, 2005).

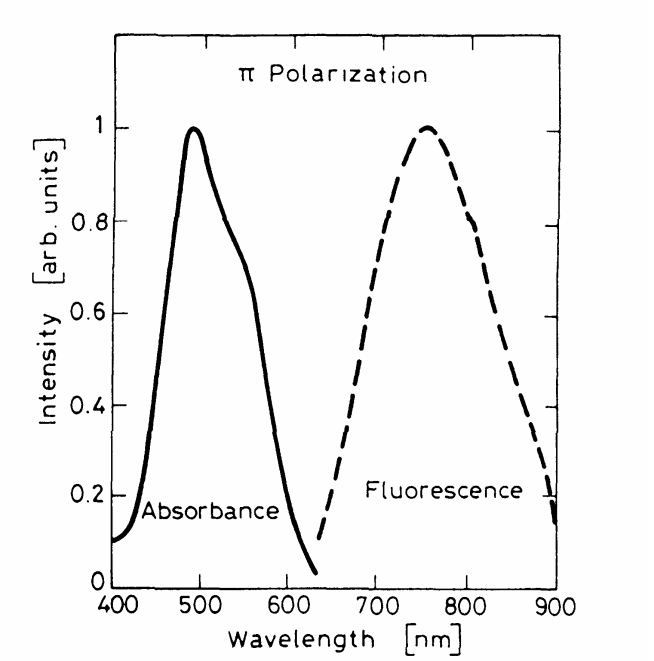

Figure 3.17 Absorption and fluorescence spectra of the Ti:Sapphire

To make Ti:sapphire, Ti_2O_3 is doped into a crystal of $A1_2O_3$ (typical concentrations range between 0.1-0.5% by weight), so that Ti^{3+} ions occupy some of the Al^{3+}ion sites in the lattice. The Ti^{3+} ion possesses the simplest electronic configuration among transition ions, only one electron being left in the 3d shell. The second 3d electron and the two 4s electrons of the Ti atom are in fact used for ionic binding to

oxygen anions. When Ti^{3+} is substituted for an Al^{3+} ion, the Ti ion is situated at the center of an octahedral site whose six apexes are occupied by O^{2-} ions as shown in Figure 3.18. Figure 3.19 shows the crystal structure of sapphire at crystallographic *c axis*. The new technique to growth high quality Ti:sapphire laser crystal is Induction Field Up-Shift method (IFUS) and Temperature Gradient technique (TGT) which differ from Czochralski (CZ) method and Heat Exchange Method (HET) (Fuxi, 1995).

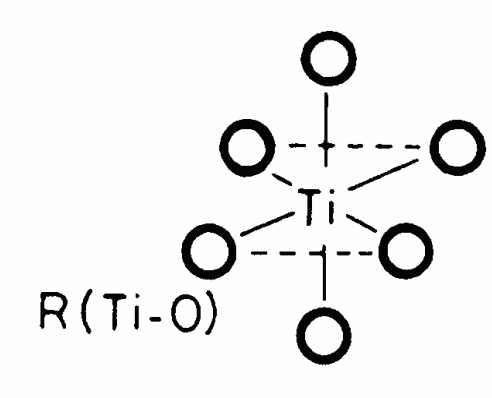

Figure 3.18 Octahedral configuration of Ti:Al_2O_3 (Svelto, 1998).

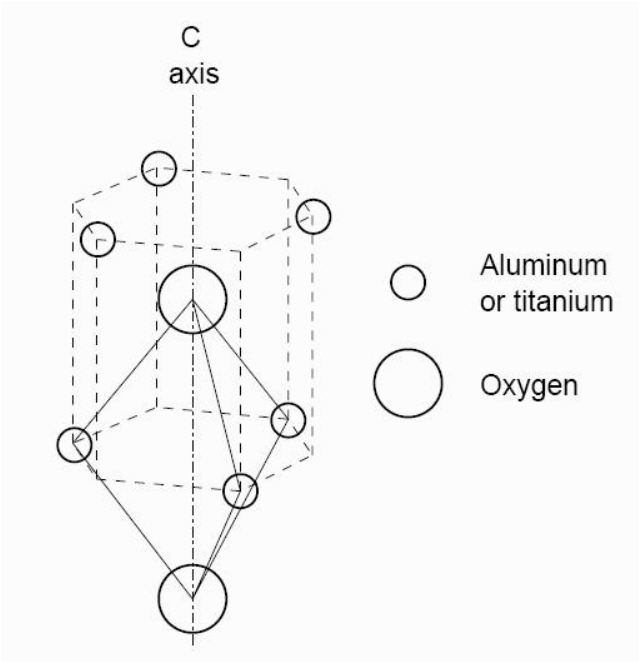

Figure 3.19 Crystal structure of sapphire at crystallographic *c axis*.

When Ti^{3+} ion is introduced into the Ti:sapphire host, the energy level split into two level as shown in Figure 3.20. When the light is absorbed by the titanium atom causing it excite to the highest energy level of ^2E_g. Then through a very fast phonon emission process the atom move to the metastable state of the lowest ^2E_g. The stimulated emission occurs between the ^2E_g excited electronic state and $^2T_{2g}$ ground electronic state. After that follow by multiple phonon emission, which is transfers the ion back to the lowest energy position of the ground electronic state (Elsayed, 2002).

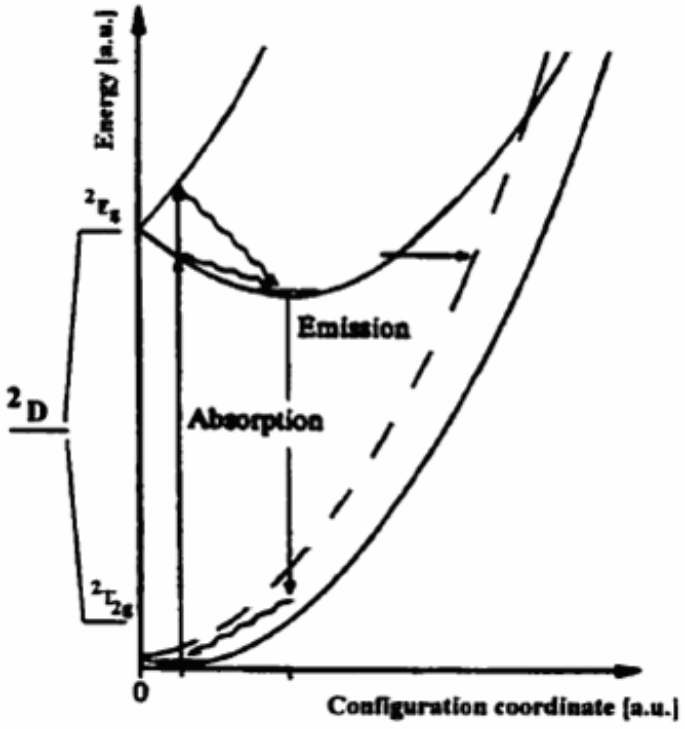

Figure 3.20 Energy level diagram for Ti^{3+} in sapphire (Elsayed, 2002).

In this research the crystal was characterized by determining the refractive index using Brewster method. The Brewster angle is important to investigate because by placing the crystal at the Brewster angle, the loss of energy during pumping process can be minimized. The schematic diagram for Brewster angle measurement is shown in

Figure 3.21. He-Ne laser was used as a source of illumination. The Ti:sapphire crystal was placed on a rotating stage. He-Ne laser was incident on to the crystal at an angle. The reflection of the beam was detected by photodetector and displayed the power on power meter.

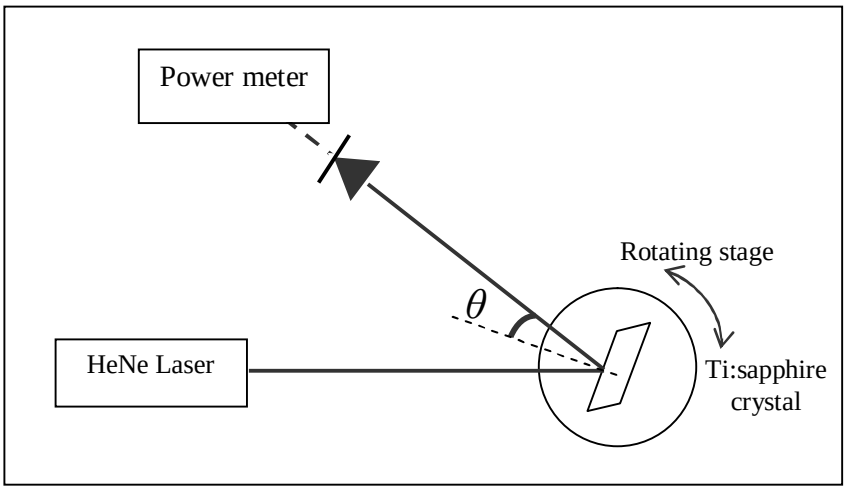

Figure 3.21 Schematic diagram of Brewster angle experiment.

In this experiment the power of the reflected beam from the crystal was measured. The He-Ne laser was placed in two polarization directions. Firstly in the vertical polarization (perpendicular component) and secondly in the horizontal polarization (parallel component). The result obtained from the experiment was shown in Figure 3.22. For the perpendicular component, the power was found gradually increase with the angle. In contrast, the parallel component gradually decreases until reach at 60^{o}. Immediately after the minimum point the reflectance power drastically increases with the increment of the angle. The graph is in the good agreement with the result obtained by Hecht and Zajac (1982). The parallel component of the beam was used to calculate the Brewster angle. The curve showed that Brewster angle of the crystal is equal to 60^{o}. From the result, the refractive index also can be calculated using Equation (3.1) (Ouseph *et al.,* 2001).

$$\tan \theta_B = \frac{n_2}{n_1} \tag{3.1}$$

where θ_B is brewster angle, n_1 is air's refractive index and n_2 is crystal's refractive index. From the calculation, the refractive index of Ti:Sapphire crystal was obtained as 1.73 with a small deviation of 1.70 % from the actual value which is 1.76 which very close to the value given by manufactured as (1.76).

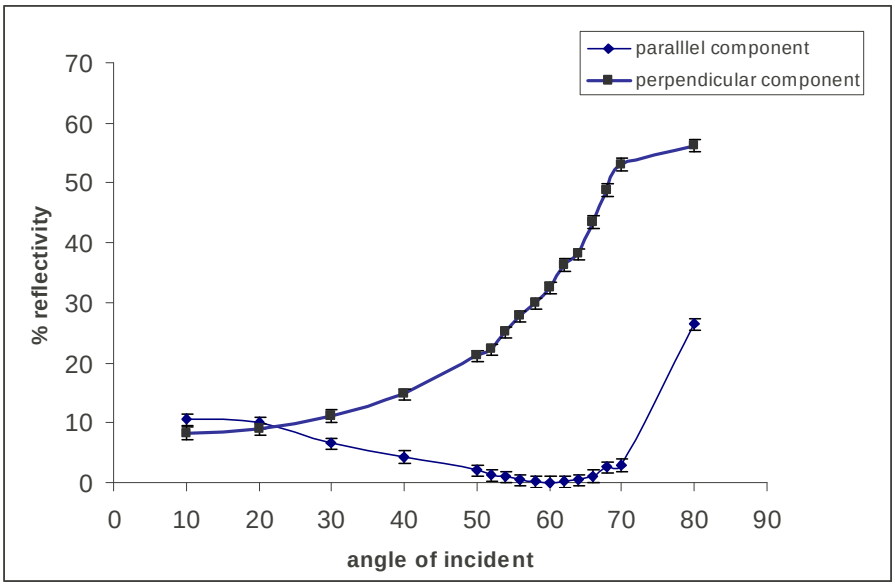

Figure 3.22 Brewster angle determination.

3.7.2 Verdi 5 Diode Pumped Solid State Laser

Basically, Verdi 5 DPSS laser consists of the laser diode as a pumping source, Nd:YVO_4 as a gain medium and LBO as a frequency doubler. Figure 3.23 illustrated the simple schematic of the DPSS laser operation. According to Figure 3.23 the Diode Laser with 808 nm wavelength pumped the Nd:YVO_4 crystal to produce 1064 nm beam. Then LBO crystal is strike by 1064 nm beam. The LBO acts as a frequency doubler to produce 532 nm beam.

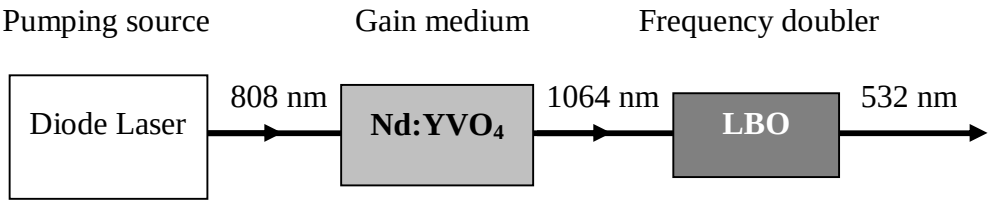

Figure 3.23 The DPSS laser system

In the actual alignment more optical components are provided in the laser cavity. Figure 3.24 shows the entire optical alignment included in the laser cavity of Verdi 5. The major element in the laser cavity is Nd:YVO_4 (Neodymium Vanadate) as the gain medium, LBO (Lithium tribonate) as the frequency doubling crystal, etalon as the single frequency optic, optical diode, astigmatic compensator and three cavity mirrors.

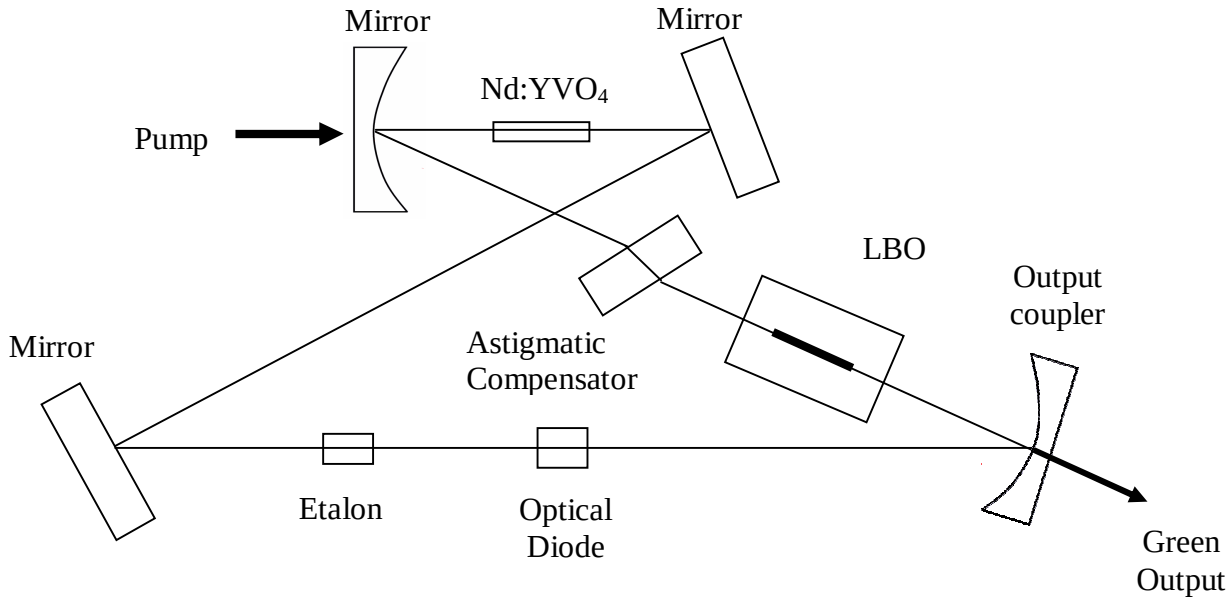

Figure 3.24 The optical components in the laser cavity (Coherent, 2005)

The temperature of the Nd:YVO_4 crystal and etalon are controlled by thermoelectric cooler (TEC), which are capable of heating and cooling the optical

element. The heat from the laser cavity is dissipated by heat sink mounted on the laser head base plate. The nonlinear medium for the system is a Type I, none critically phase matched LBO crystal held at approximately 150 ^{o}C. Optical diode was used to achieve unidirectional operation which is homogeneously broadened system. Therefore it tends to naturally run single frequency, with etalon reinforcing this behavior.

The laser diode was employed as a pumped source. The laser diode bar efficiently converts low voltage high current electrical power into laser light. Electrical to optical conversion efficiencies typically approach 50 %. The coupling efficiency obtained in launching light from the bar through the fiber array and into a single transport fiber is predictably specified to be not less than 80%, with typical value exceeding 90%. When the nominal wavelength is centered on the strong absorption band associated with neodymium ions in a vanadate host, more than 90% of the incident diode laser light can be absorbed by the crystal to generate high optical gain within a small volume. The tuning rate of diode bars as a function of operating temperature is typically 0.3 nm/^{o}C. Mean that, the higher temperature will imply longer wavelength. Optimum efficiency for the laser diode is typically obtained when the temperature within the range of 5 ^{o}C to 35 ^{o}C.

Nd:YVO_4 was used as a gain medium because offers several significant advantages over alternative solid state laser media common to diode pumped lasers. Neodymium ions doped into vanadate host exhibit a comparatively large absorption coefficient centered at a wavelength convenient for pump diode laser. They are also spectrally broad, therefore insensitive to the precise wavelength or bandwidth of an optical pump source. Both of these characteristics contribute to ease-of-operation and the overall efficiency of diode pumping. The characteristic lasing wavelength of Nd:YVO_4 is nominally 1064 nm, in the near-infrared region of the optical spectrum. This infra red light is, in fact the oscillating of fundamental wavelength in the resonator rather than the visible green output associated with the device. The multilayer dielectric coating of the mirrors that define the ring resonator are designed to provide high reflectance centered at 1064 nm to sustain circulating infrared power levels that typically exceed 100W.

Converting a fraction of this circulating power into visible light is accomplished via the process of non resonant, intracavity, second harmonic generation (SHG).

The nonlinear optical medium used for SHG is birefringent crystal LBO. The efficiency of the SHG process is determined by the crystal orientation, as defined by the direction of light propagation, polarization state of the incident light and nominal crystal temperature. The LBO doubler is housed within an oven that is design to maintain the crystal temperature at a typical value of 150 ^{o}C. Given the proper crystal orientation and considering appropriate polarization states, the refractive indices of the birefringent crystal can be arranged to be identical for both fundamental 1064 nm wavelength and its second harmonic at 532 nm. When the phase matching condition between the two different wavelength implied by these consideration are satisfied, substantial power flow from the fundamental to the second harmonic is obtainable during a single pass through the doubler.

The plane of polarization for the fundamental is parallel to the laser base plate, while the green polarization is perpendicular to it. The green light is then extracted from the resonator via a dichroic output coupling mirror, which is coated to be highly reflecting at 1064 nm, but essentially transparent at 532 nm.

3.7.2.1 Verdi 5 operation

Since the Verdi 5 can produce beam up to 5.5 W and have very bright green beam, so it is very dangerous when operating this laser especially for our eye which absorb highest at green wavelength. This laser is classified as Class IV which can harm the end user. Safety goggle must always be used when operated this laser to protect the eye from potentially damaging exposure.

The step by step instruction for operates the laser system is as follows. Firstly make sure key switch is in the STANDBY position (Figure 3.25). Then set power switch on the power supply rear panel to "ON". The AC power and LASER EMISSION indicator will light. After that, allow about 30 minutes for the heater and Thermoelectric cooler (TEC) to achieve operating temperature. The display will show "SYSTEM WARMING UP". Once the process finished, the display will indicate "STANBY" means the system now ready for key on. Then put the key switch in ON position then open the shutter by pressing the SHUTTER OPEN push button on power supply front panel. Then the laser light will emit from the laser head after the current ramp-up. Lastly the desire power can be adjusted using POWER ADJUST KNOB

Figure 3.25 Power supply Front panel control

3.7.2.2 Beam profile of Verdi 5

Figure 3.26 shows the beam profile of the Verdi 5 DPSS laser in 3D and 2D. The beam profile of the Verdi 5 DPSS laser shows the better quality beam. Figure 3.26 (b)

shows the beam spot is in perfect TEM_{00}. Figure 3.27 (a) shows the horizontal cursor profile and Figure 3.27 (b) shows vertical cursor profile of the Verdi 5 DPSS laser. Both vertical and horizontal profile indicated that the beam almost perfectly overlapping with the normal distribution of theoretical Gaussian beam.

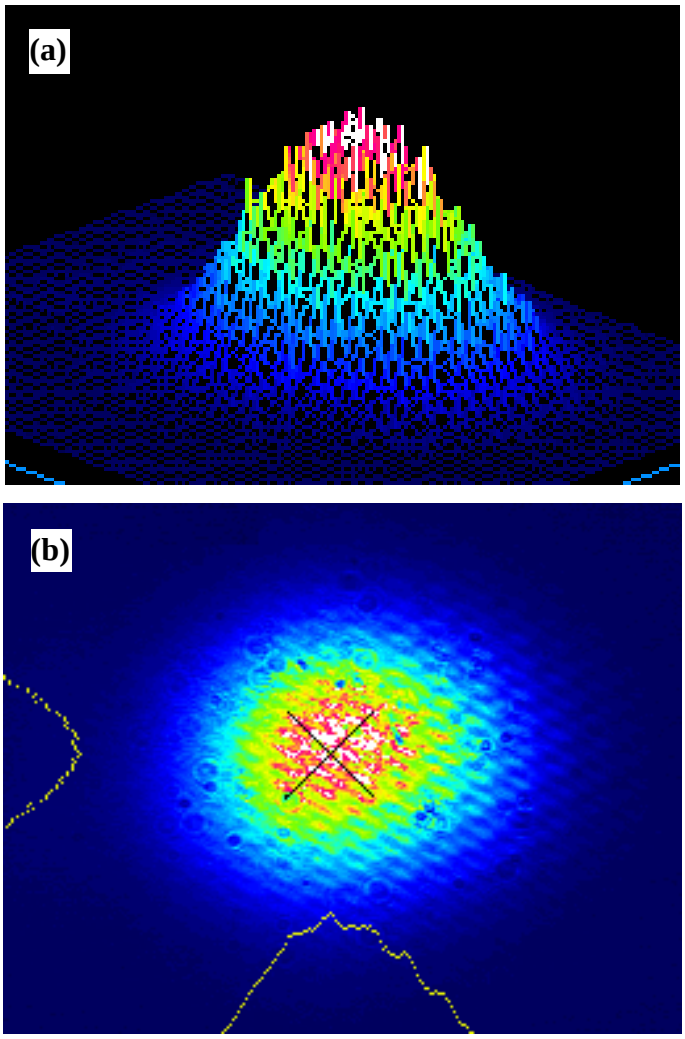

Figure 3.26 3D (a) and 2D (b) beam profile of Verdi 5 DPSS laser

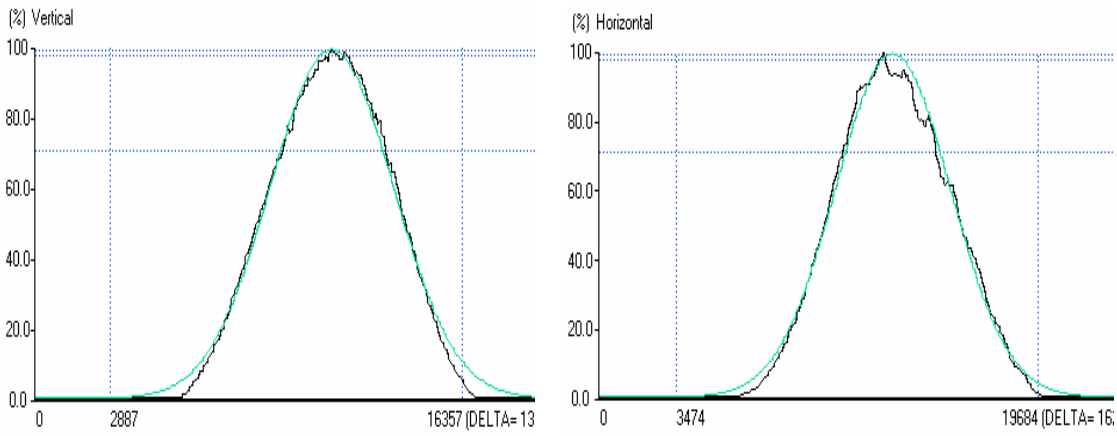

Figure 3.27 a) Horizontal cursor profile b) Vertical cursor profile

3.7.2.3 Laser spectrum of Verdi 5

The typical spectrum produced from Verdi 5 DPSS laser is shown in Figure 3.28. Tremendously, only one line of 532.06 nm is appeared. This indicates Verdi 5 DPSS laser has eliminate the pumping beam. This is showed that Verdi 5 is suitable to be as a pumping source of Ti:sapphire crystal.

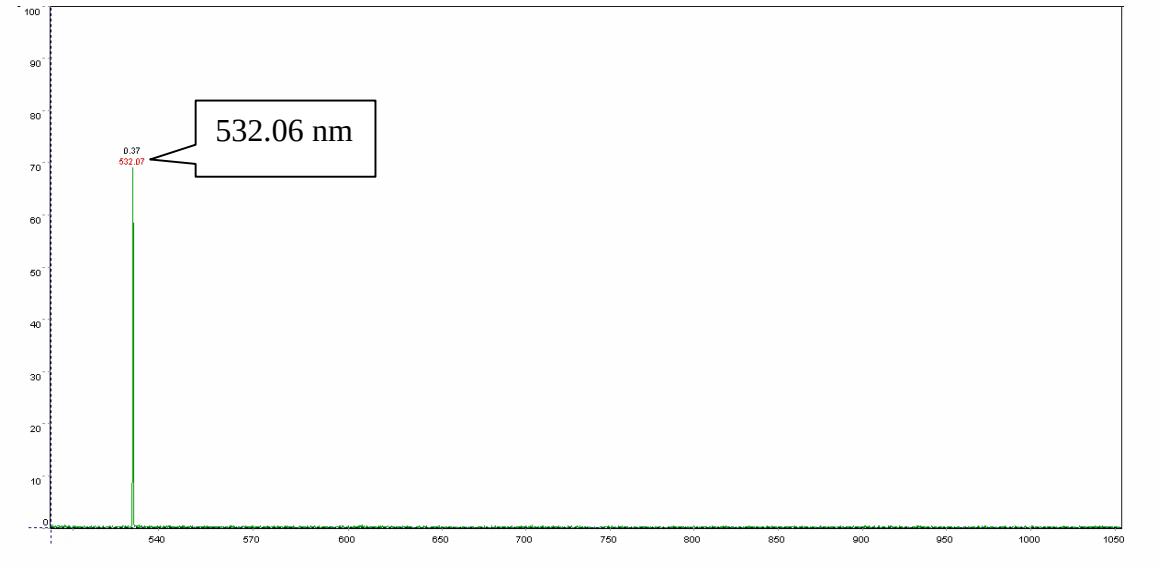

Figure 3.28 The spectrum of Verdi 5 DPSS laser output

3.7.3 Optical component of Ti:sapphire laser

In the development of Ti:sapphire laser, its comprised of many optical components beside active medium and the pumping source. The optical components used in the development are including mirrors, lens, output coupler and prisms.

3.7.3.1 Dielectric mirror

There are 4 dielectric mirrors employed in the development of Ti:sapphire laser, namely M1, M2, M3 and M4. The dimension of the mirror is 20 mm in diameter with the thickness of 6 mm. The reflectivity for the mirror at IR is about 99.8 %. Mirror M1 and M2 are concave mirrors but mirror M3 and M4 are flat mirror. In this work the curve mirrors M1 and M2 with radius of curvature (ROC) of 100 mm and coated with highly transmission at 488 to 540 nm and highly reflection at 672 to 887 nm. However, the flat mirrors M3 and M4 are coated with only highly reflection at 672 to 887 nm.

3.7.3.2 Focusing lens

The DPSS Laser beam needs to focus sharply to ensure high intensity of the beam exposed to the crystal. The intensity need to be highly enough to produce a strong nonlinearity. Therefore the beam needs to focus by using a particular focusing lens. The lens used in this project is made from BK 7 glass and specially coating with highly transmission at 532 nm, in order to maximize the pumping power incident to the crystal. The focal length of the lens is 100 mm.

3.7.3.3 Output coupler

In the laser system, a mirror which is partially reflect is necessary to emit the laser beam. The 95 % reflection mirror was used as an output coupler. In this case only 5 % of the beam will be lased out and the rest will be reflected and amplified in the cavity. The output coupler in this experiment was coated with high transmission at 642 to 830 nm. The percentage of the transmission of the output coupler is depends to the wavelength of the laser output desired to be produced (Figure 3.29). For the wavelength at higher gain for example from 750 nm to 850nm, output coupler with transmission around 10 to 15 % is recommended. At the lower gain in the range of 700 - 850 nm and 850 - 900 nm, low transmission around 3 to 7% is needed to be used. At the range of 750 nm to 850 nm the transmission can be higher because in this range the laser gain is higher therefore with higher transmission the gain already enough to amplify in laser cavity. Because of the output coupler in this work was coating with high transmission of 642 to 830 nm, the transmission percentage suitable to use is about 5 %.

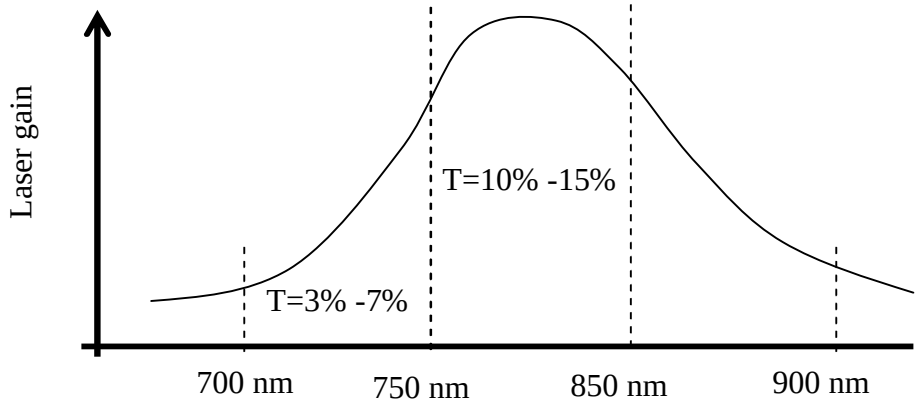

Figure 3.29 Ti:sapphire gain cross section.

3.7.3.4 Prisms

The main problem to produce the ultrashort pulse is the dispersion. Dispersion can cause the different wavelength of light to experience different phase shift (Poutous, 1996). As a result, the shorter wavelength to lag behind the longer wavelength. The main source of dispersion is the laser crystal itself. Prism pair can be used to compensate the dispersion by producing a negative dispersion as explained in Chapter 2.

3.7.4 Detection Devices

There are several devices use to detect and analyze the output of the Ti:sapphire laser. The devices are comprised of Newport power meter, Beamstar CCD beam profiler, Ocean Optics spectrometer, Tektronic oscilloscope and photodiode.

3.7.4.1 Power meter

Newport power meter Model 841-PE is the newest version to Newport's power meter family. This powerful tool is also easy to use and intuitive enough to master in minutes. This meter can also be networked via USB or RS-232.

The built-in features of the 841-PE include a complete statistics package that have line plot and a histogram. The Data sampling parameters depending on whether a power or energy detector is being used can be set by using the same screen. The 841-PE meter is equipped with a DB15 input connector for direct compatibility with Newport's

new 818P and 818E Series High Power and Energy Detectors. In this project 818P-020-12 series of high power detector was used.

This detector is very sensitive and has broadband flat spectral response from 0.19 to 11 μm. Besides that it has high peak power pulse damage resistance. The power can be measured in the range of 1 mW to 20 W. Typical applications of this detector is including the measurements for CW or pulsed Ion, Nd:YAG, Ti:sapphire, CO_2, high-power laser diodes and Excimer laser.

3.7.4.2 Beam Star CCD profiler

The BeamStar CCD Laser Beam Profiler is a beam diagnostic measurement system for real – time measurement of continuous or pulse laser beam. It provides an extensive range of graphical presentations and analysis capabilities of laser beam parameters such as beam width, shape, position, power and intensity profiles. The CCD based laser beam profiler is fully utilized by powerful software that displays any structure larger than one pixel in vivid color, calculates the beam distribution and profile as well as total beam intensity distribution in order to allow full analysis of the laser beam's characteristics.

3.7.4.3 Spectrometer

In this project, two kinds of spectrometer were used. Those spectrometers are USB2000 Spectrometer and Wave Star CCD laser spectrum analyzer. The USB 2000 spectrometer is used to measure the spectrum from Ti:sapphire laser and Wave Star CCD laser spectrum analyzer is used to analyze the spectrum of DPSS laser.

The USB2000 Miniature Fiber Optic Spectrometer is a small footprint, plug-and-play version of spectrometer. The USB2000 couples a low-cost, high-performance 2048-element linear CCD-array detector with an optical bench, make it small enough compared to another spectrometer. The USB2000 accepts light energy transmitted through single-strand optical fiber and disperses it via a fixed grating across the linear CCD array detector, which is responsive from 200-1100 nm. Setting up the USB2000 Spectrometer is easy. The USB2000 is easy to use by simply installs the Spectrometer Operating Software and then connects the USB cable from the spectrometer to the computer.

The Ophir Wave Star spectrum analyzer is a spectrometer which introduces a new level of accuracy and ease in spectral measurements. This device can easily and accurately measure spectra from a wide variety of sources including continuous and pulsed sources from microwatts to watts in intensity. The program automatically tags the peaks with the wavelength so the result is readily available. The WaveStar is available with interchangeable filters which together with the variable shutter speed allow to easily and accurately measure any type of source from fractions of a microwatt to watts in intensity. Fiber adapters are available to connect to fiber sources.

3.7.4.4 Oscilloscope

Tektronix Oscilloscope Model TDS3054B with 500 MHz bandwidths sample rates up to 5GSa/s and having 4 Channels was employed in this work. It contains Full VGA Color LCD, 25 Automatic Measurements, 9-Bit Vertical Resolution, FFT Standard, Multi-language User Interface, QuickMenu Graphical User Interface for Easy Operation and WaveAlert Automatic Waveform Anomaly Detection. The oscilloscope delivers 3,600 wfms/s continuous waveform capture rate to capture glitches and infrequent events three times faster than comparable oscilloscopes. In addition, the oscilloscope's real-time intensity grading highlights the details about the "history" of a

signal's activity, making it easier to understand the characteristics of the waveforms captured. In this research the oscilloscope was used to display the mode locked pulse train captured using fast photodetetor.

3.7.4.5 Photodetector

The photodetector Model PD24K001 was used to detect the fluorescence produced by the excited Ti:sapphire crystal. Initially photodiode is used to observe the fluorescence increment because it more sensitive and have faster respond compared by using power meter. The rise time of the photodetector is 3.5 ns. The photodetector having active area of 10 mm^2 with response wavelength in the range of 350 nm to 1100 nm.

3.7.4.6 Fast photodetector

A fast photodiode Model P1N 800 is possible to monitor the output of Q-switch lasers and mode locked laser. In this work the photodiode was utilized to capture a pulse train produced by the Ti:sapphire laser during mode locked operation which couple to Tektronix oscilloscope. The type of photodiode is a PIN detector. The rise time of the photodetector is 200 ps. It has an active area of 1 mm^2 with response wavelength in the range of 350 nm to 1100 nm.

3.7.5 Software

In this work, Matrox Inspector Version 2.1 and ToptiCalc V25 softwares were utilized for analysis. The Matrox Inspector Version 2.1 was particularly used to measure the bandwidth of the spectrum produced by Ti:sapphire laser. Meanwhile, ToptiCalc V25 software was used to calculate the pulse duration of the mode locked Ti:sapphire laser signal.

3.7.4.1 Matrox Inspector 2.1

Matrox Inspector Version 2.1 software have 32-bits application running under Windows 95, Windows NT or Window XP that allow to load, grab, process, view, analyze, print, organize, and save images. It does not need a frame grabber to run and comes with a number of sample images and scripts. This software is used to analyze the spectrum which measured using spectrometer. The typical spectrum are the result from the fluorescence and mode locked output. Prior to the measurement, the software needs to be calibrated according the spectrum scale. By using this software, the bandwidth of the spectrum can be determined precisely.

3.7.4.2 ToptiCalc V25

ToptiCalc V25 is TOPTICA Photonics AG's scientific calculator especially designed for using in optic laboratories. The special features of ToptiCalc is mathematical expressions which entered in a simple intuitive syntax, dots and commas are accepted as decimal separators, a history list collects all entered expressions and the calculated results. Furthermore it contains important fundamental constants are available

in SI units, spectroscopy constants are available in convenient 'lab units', arbitrary functions and variables can be defined by the user and some optics and spectroscopy calculations are implemented.

CHAPTER 4

CHARACTERIZATION OF TITANIUM SAPPHIRE LASER OUTPUT

4.1 Introduction

In this section, the output Ti:sapphire laser will be discussed. This is started from the fluorescence process of the Ti:sapphire crystal. The characterization is included the continuous wave (CW) and mode-locking operation. The output both cases are measured in term of the spectrum and the power produced from the system. The mode-locked pulse properties will also discuss in detail in this section.

4.2 The fluorescence Ti:sapphire crystal

Titanium sapphire crystal was pumped by DPSS laser. The schematic diagram of the experiment setup for this pumping process is shown in Figure 4.1. DPSS laser was employed as a pumping source. Ti:sapphire crystal was utilized as an active medium. The green light of DPSS laser is used to excite the Ti:sapphire crystal using end

pumping technique. The pumped beam finally dumped into the beam dumper. Immediately after the Ti:sapphire crystal was pumped by green beam of DPSS laser, the fluorescence was emitted. The fluorescence beam is confined in the cavity comprised of two mirrors M1 and M2.The spherical mirrors of M1 and M2 were coated with highly reflective to the infrared (IR) beam and let through the visible light of green beam. The fluorescence beam is incident at an angle of approximately 20^{o} to mirror M1. The reflected the IR beam was detected by using spectrometer which coupled to personal computer. A Matrox Inspector software was conducted to analyze the spectrum of fluorescence beam produced from the excited Ti:sapphire crystal.

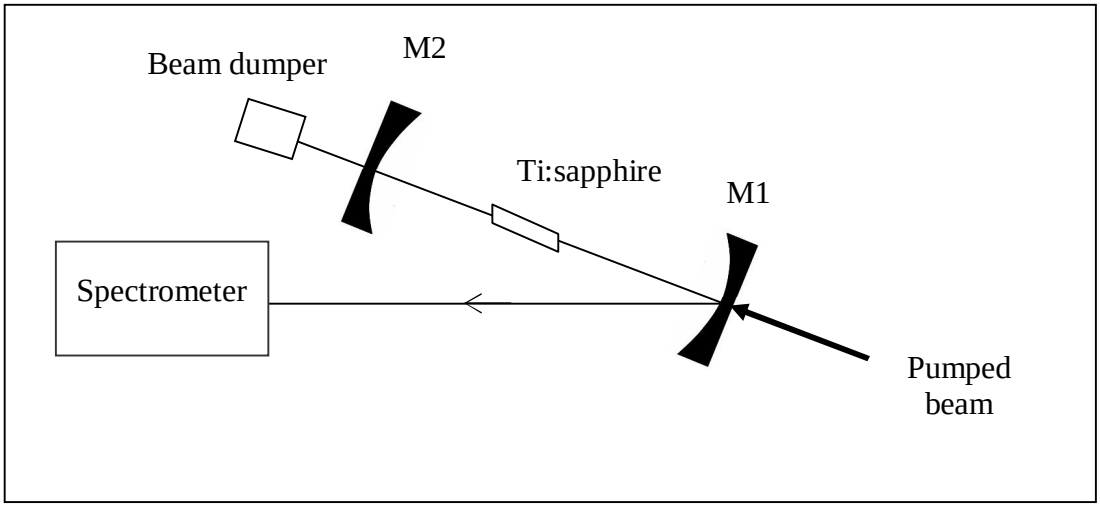

Figure 4.1 The experimental setup for the fluorescence detection

Basically, when green light from DPSS laser hits Ti:sapphire crystal that lead the titanium atoms into excited state. Naturally de-excitation occurs whereby the atoms return to the ground level and released energy spontaneously. The spontaneous emission produces fluorescence or also known as *luminescence*. The typical luminescence spectrum captured by an Ocean Optics spectrometer is depicted in Figure 4.2. The spectrum dispersed in the range between visible regime of 613.61 nm to infrared regime of 855.28 nm with roughly bandwidth of 241.67 nm. The spectrum is particularly produced after the Ti:sapphire crystal pumped by DPSS laser at power of 3.5 W. The

precise measurement of bandwidth could be performed by using Matrox Inspector Version 2.1 Software. The fluorescence supposes to produce broader bandwidth. But with the application of coated mirrors M1 and M2, that limit the broadening bandwidth of the spectrum.

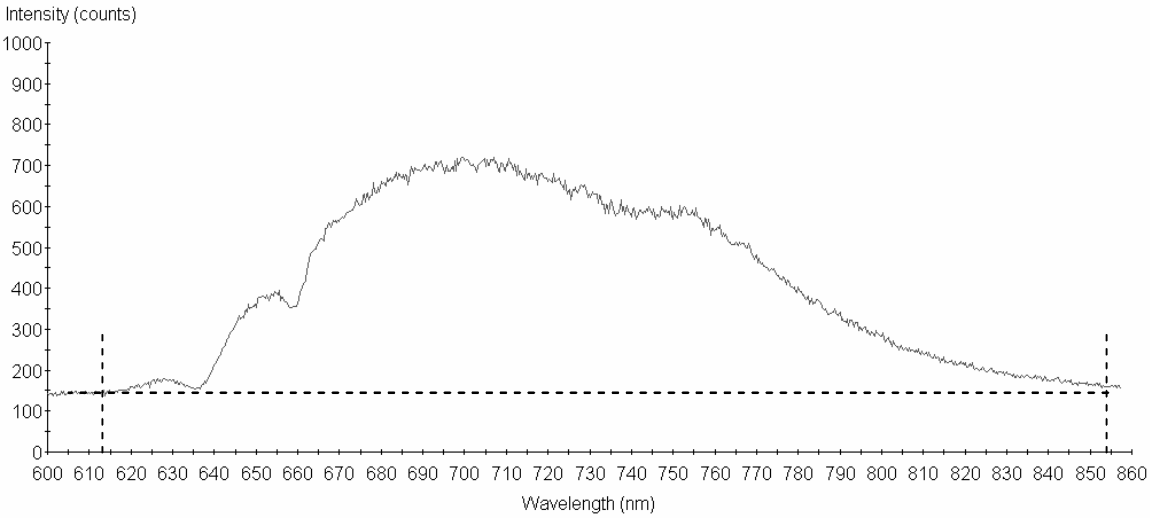

Figure 4.2 The fluorescence intensity as a function of wavelength

The fluorescence phenomenon was investigated by further increasing the power of the DPSS laser as a pumping source. The typical results obtained are shown in Figure 4.3. The spectrograms are arranged in the increasing order of pumped power. No significant spectrum is observed at low pump power. As the pumped power increases, the peak intensity obviously increases too. The maximum intensity obtained is 831.43 in arbitrary corresponding to 5 W pumping powers. The collected data of intensity measurement are used to plot graph as shown in Figure 4.4. The intensity of the fluorescence beam is found to be proportional upon the pumping power. This mean the higher power to pump the crystal the more intense fluorescence is produced. In the fluorescence band, a little drop was occurred at wavelength of 660 nm and 740 nm. This happened because of the impurities and defect of the crystal such as point defect and line defect (Duhr and Brauna, 2005).

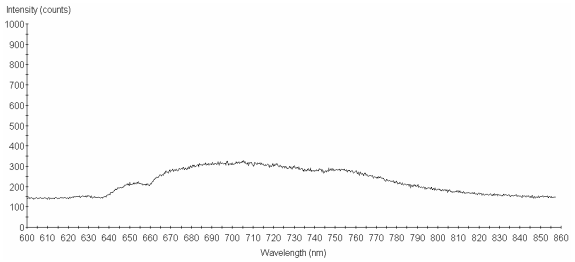

1.5 W

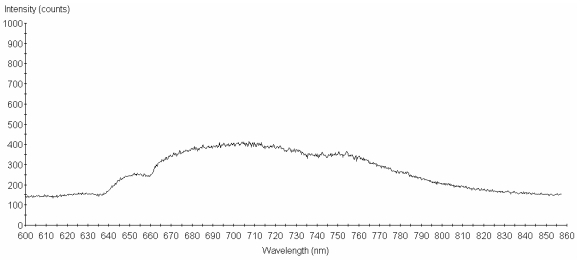

2.0 W

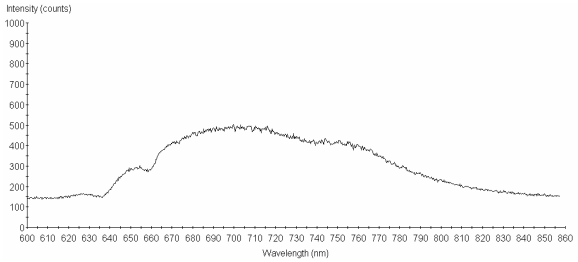

2.5 W

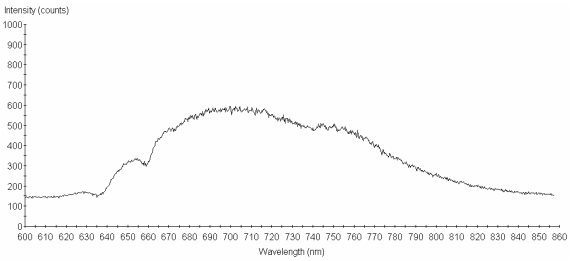

3.0 W

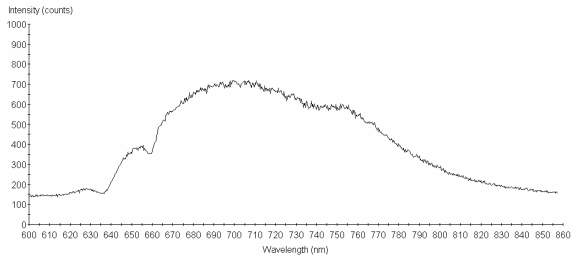

3.5 W

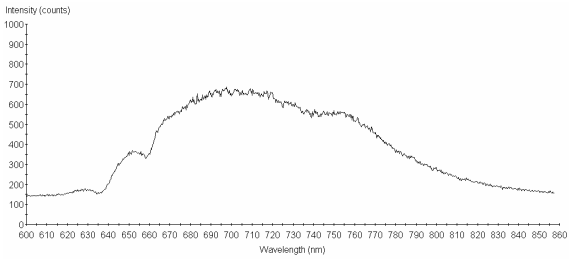

4.0 W

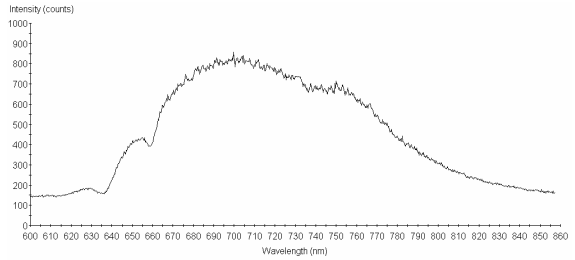

4.5 W

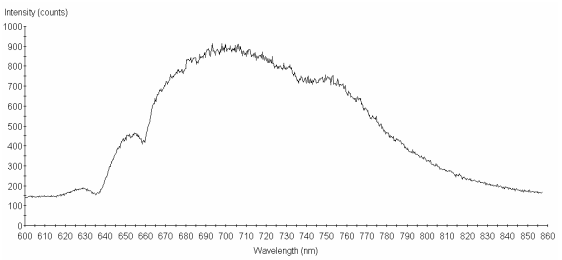

5.0 W

Figure 4.3 The fluorescence intensity at different pumped power

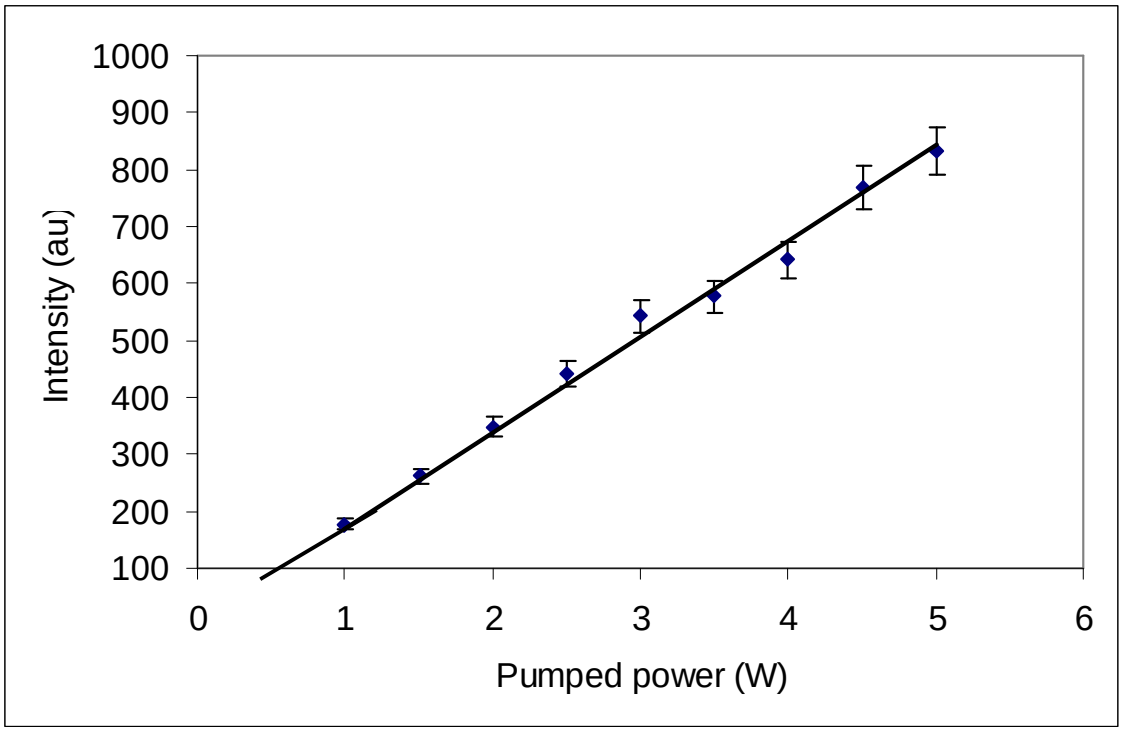

Figure 4.4 The fluorescence intensity as a function of pumping power

4.2.1 Estimation of pulse duration

Since a very narrow pulse required a very wide spectrum (Pearson and Withon, 1993), therefore Ti:sapphire is suitable for producing short pulses lasers. With the bandwidth of 235 nm, the Ti:sapphire crystal was able to support pulses in femtosecond range. An estimation to limit the gain bandwidth of Ti:sapphire impose in pulse duration in a Kerr Lens Mode-Locked (KLM) laser, transform limited Gaussian zero chirp pulse relation can be used.

$$\tau_P = \frac{0.441}{\Delta \nu} \tag{4.1}$$

Where τ_p is the pulse width and $\Delta\nu$ is the gain bandwidth of Ti:sapphire. In this particular case the gain bandwidth can be estimated by knowing the range of the spectrum by

$$\nu = \frac{c}{\lambda} \tag{4.2}$$

$$\Delta\nu = \frac{c}{\lambda_1} - \frac{c}{\lambda_2} \tag{4.3}$$

By solve Equation (4.3) with λ_1 = 613.61 nm and λ_2 = 855.28 nm the $\Delta\nu$ is equal to 138 THz. Therefore the shortest pulse can be determined by solving the Equation (4.1) with calculated $\Delta\nu$. From the calculation, the shortest pulse duration, τ_p is roughly 3.27 fs. However there are many other factors that affect the pulse duration produced such as dispersion, bandwidth limit of the mirror and self focusing in nonlinear medium (Pearson and Withon, 1993).

4.3 Characterization of Continuous Wave (CW) Laser

After the fluorescence was detected, all optical components in laser cavity needs to be aligned properly as discussed in chapter 3 in order to have the laser generation. For these purpose two flat mirrors M3 and Output Coupler (OC) are added in the laser cavity such as shown in Figure 3.9 in chapter 3. "Z" folded cavity configuration is chosen in this experiment.

4.3.1 Spectrum of continuous wave beam

When the fluorescence signals are precisely aligned, the gain in the cavity is higher than the losses. As a result the light amplified and produced lasing from output coupler (OC). The spectrum of the radiation was measured using Ocean Optics

Spectrometer. The result is shown in Figure 4.5. A narrow bandwidth is appeared which center at 784.23 nm. This means the wavelength of the Ti:Sapphire laser in continuous wave (CW) mode is at 784.23 nm.

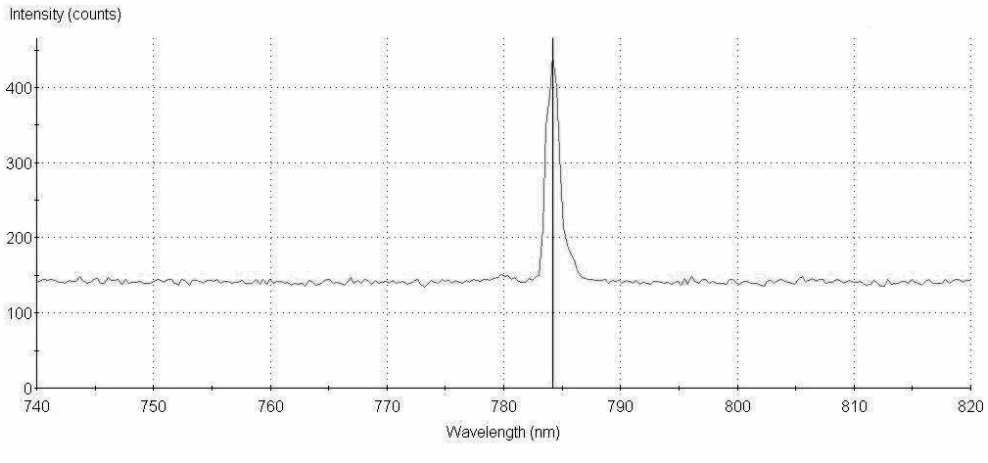

Figure 4.5 The Ti:sapphire laser output spectrum

The output power of the CW operation is verified by increasing the pumping power. The typical results obtained are shown in Figure 4.6. The spectrums are arranged in the increasing order of the input power. In general, all spectrum lines are very narrow, but yet the intensity is obviously increasing from low level power to highest level power tested in this experiment. The intensity of the pulse is measured in arbitrary (au).

The intensity is plotted against the pumping power. The graph is shown in Figure 4.7. Initially no power was detected although the pumping power was increased, meaning no lasing occurs. At this stage, the pumping power was not enough to produce stimulated emission. As a result no emission of coherent beam, consequently no spectrum observed. As the pumping increases further up to 2 W, stimulated emission started to be traced by the spectrometer. The stimulate emission overcome the spontaneous emission. Then the chain reaction took place, which measured by the increasing intensity within 2 W to 5 W. The output was found linearly increases with respect to the pumping after the threshold power of 2 W. The fluctuation in the graph

shows that the CW output of Ti:sapphire laser was unstable. This arises due to the spontaneous emission in the cavity and the sensitivity of the spectrum analyzer detector itself.

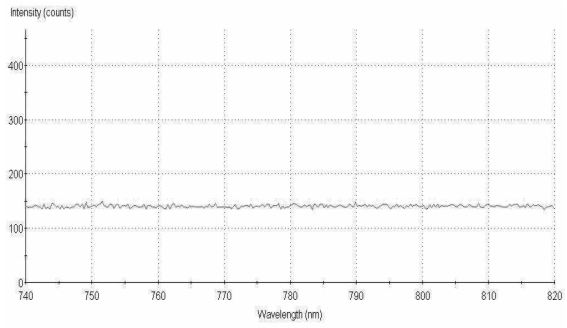

2.0 W

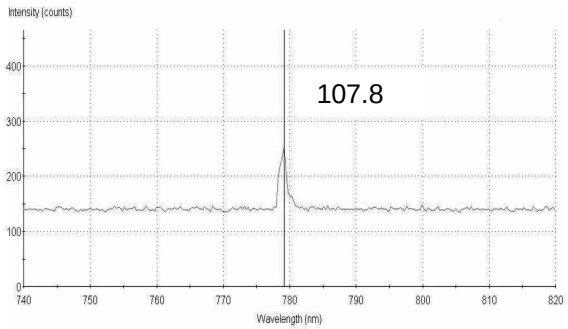

2.5 W

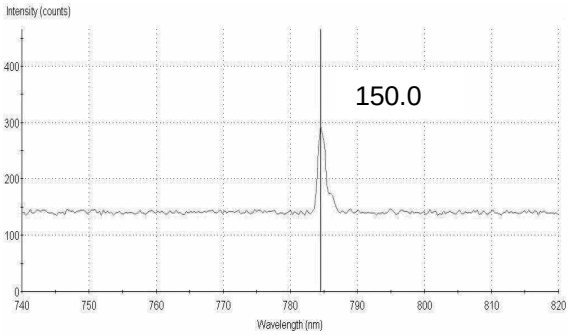

3.0 W

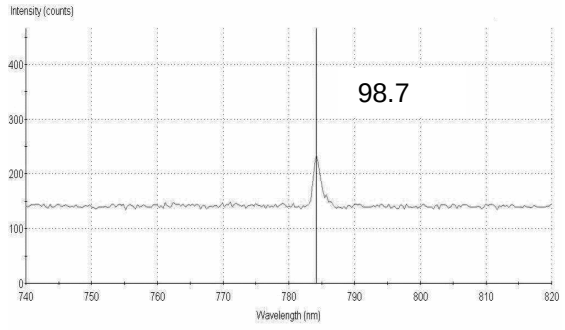

3.5 W

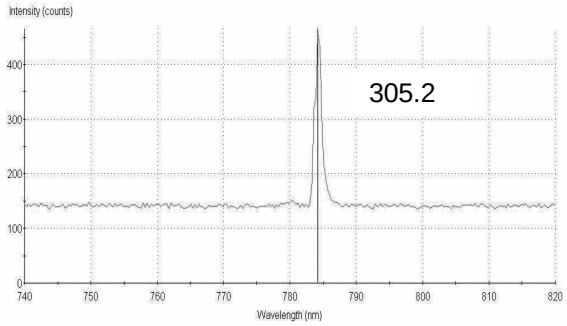

4.0 W

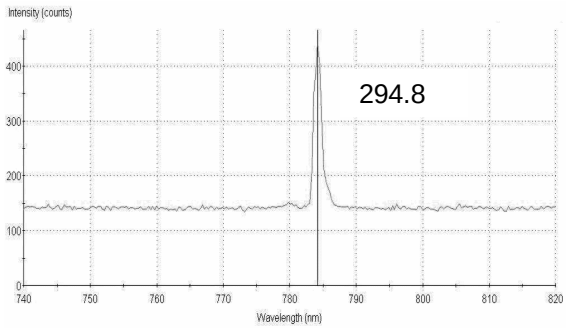

4.5 W

Figure 4.6 The spectrum intensity at different pumped power

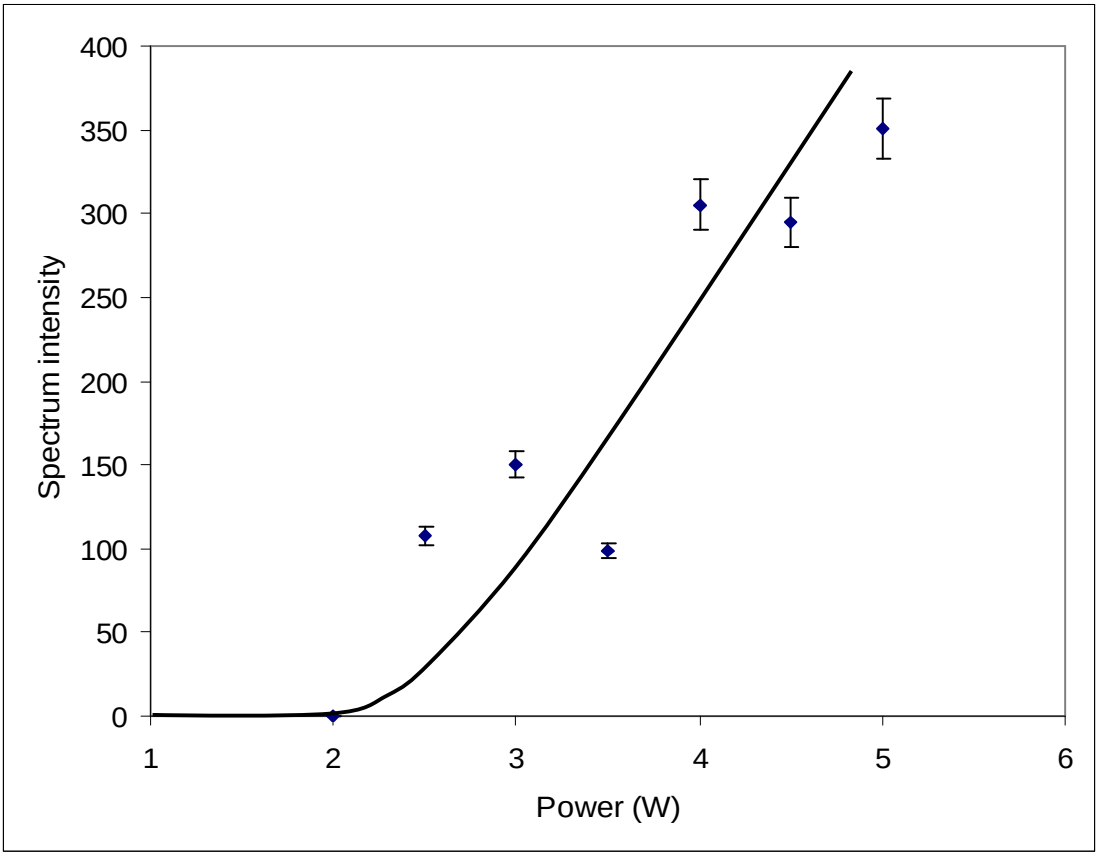

Figure 4.7 The spectrum intensity as a function of power

4.3.2 The power of continuous wave beam

The output power of continuous wave CW Ti:sapphire laser was measured using Newport power meter. The output power for the CW operation was measured as a function of the pumping power. The result is represented in Figure 4.8.

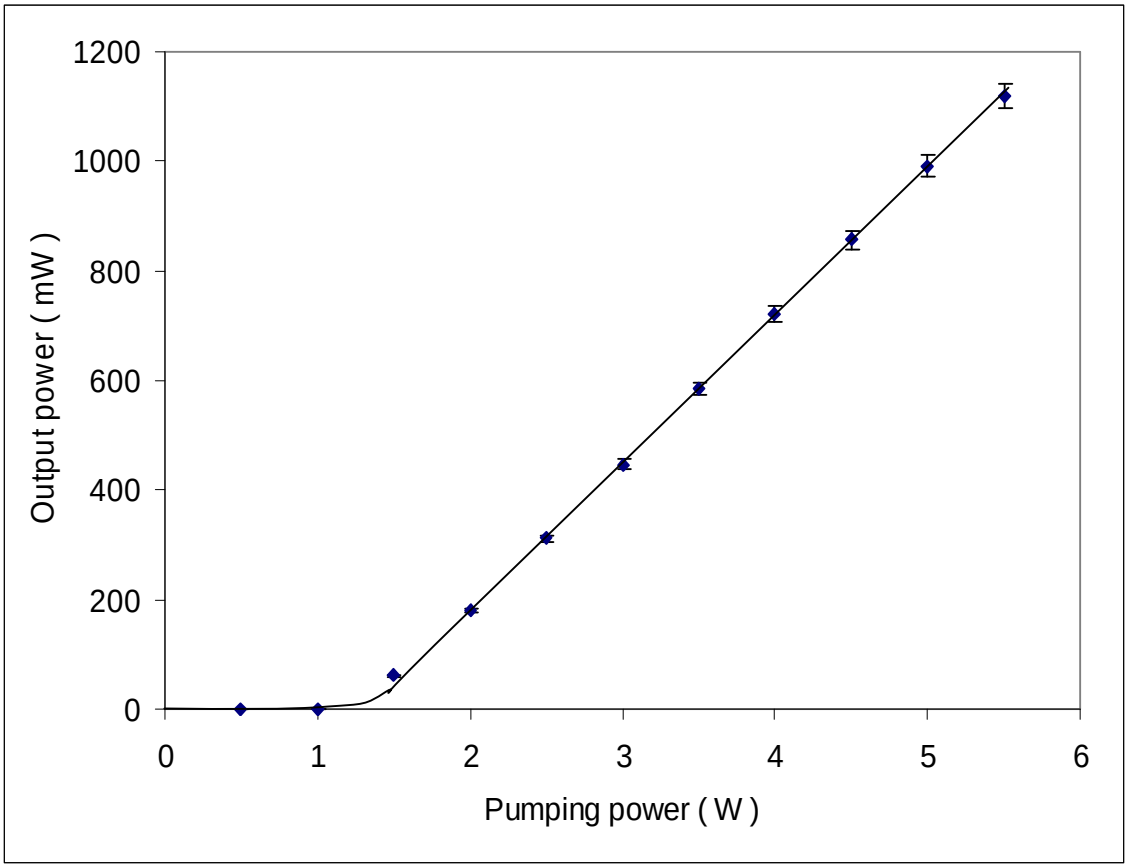

Figure 4.8 Output power as a function of the pumping power

The trend of graph in Figure 4.8 is almost similar to the graph in Figure 4.7. However the distribution of measurement is better than spectrum measurement. The output of laser starts to increase after the input power greater than 1 W. Therefore the threshold power for CW of Ti:sapphire laser is 1.3 W. When the pumping power greater than 1.5 W, the output power is proportionally increases with respect to the pumping power. The maximum output power of the CW Ti:sapphire laser is 1.12 W. This obtained at corresponding pumping power of 5.5 W. The efficiency of the CW Ti:sapphire laser is 26%, which considered as higher compared to other laser system as obtained by Elsayed (2002) which have 22% efficiency.

4.3.3 Beam profile of continuous wave beam

Beamstar CCD beam profiler was employed to measure the profile of CW Ti:sapphire laser. The pumping power was set at 1.7 W. The lower pumping power was conducted to avoid over exposed to the beam profiler detector. The distance between the detector and the beam is 8.0 cm. The beam capture at this distance is referred as *near field* observation. The result of the beam profile in near field for 3D and 2D are represented in Figure 4.9 and 4.10 respectively. Figure 4.10 shows that the beam spot having uniphase mode. This indicates that the Ti:sapphire laser posses a good beam quality.

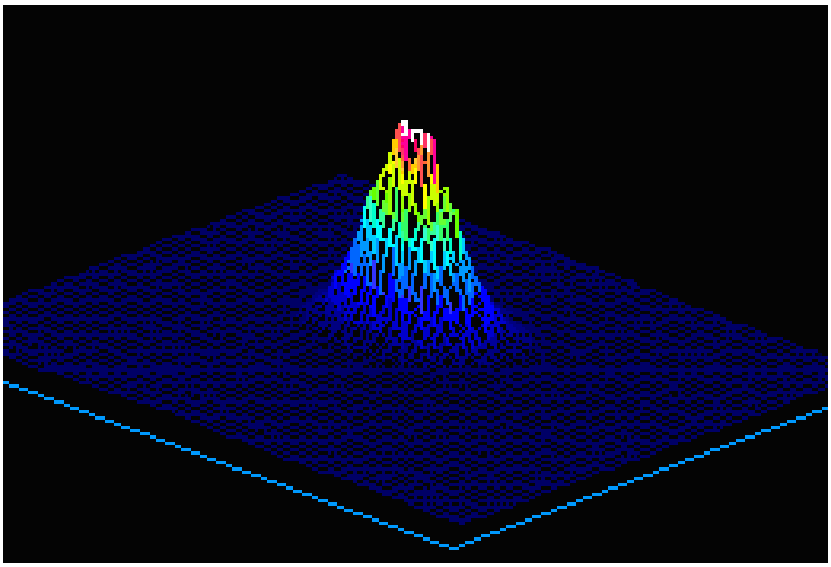

Figure 4.9 3D beam profile in near field

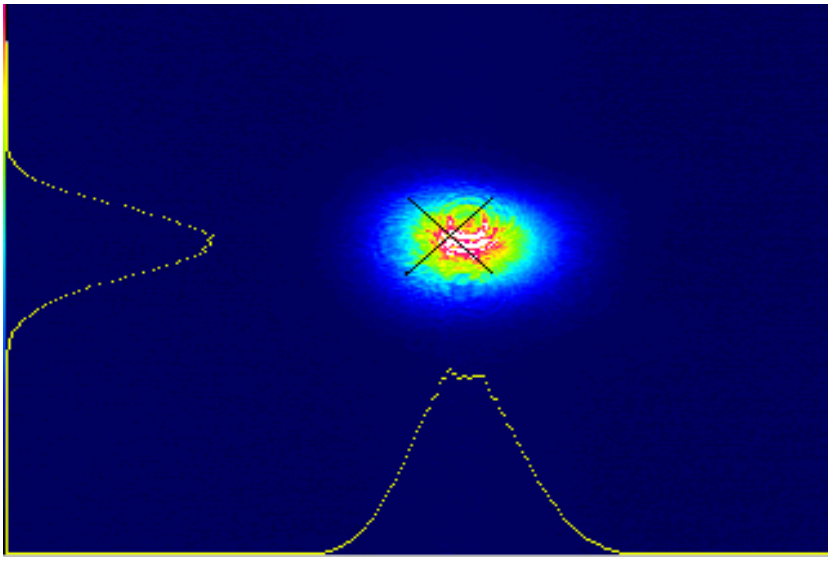

Figure 4.10 2D beam profile in near field

On the other hand, the beam was also observed from the far field at distance between the detector and the beam of 70 cm corresponding to the same pumping power used in the near field. The result of beam profile in far field for 3D and 2D are represented in Figure 4.11 and 4.12 respectively. The beam profile in far field also shows that the laser still operated in TEM_{00}. This result proved that the beam produced is in good quality beam.

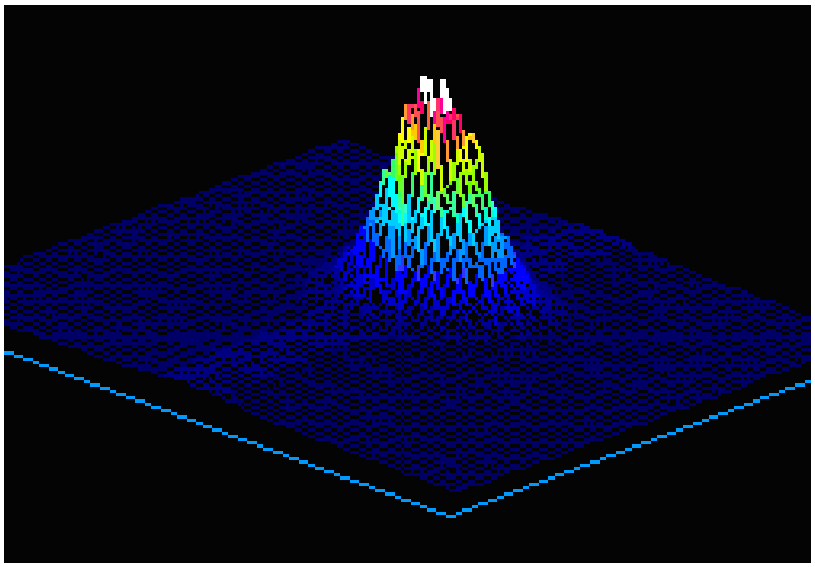

Figure 4.11 3D beam profile in far field

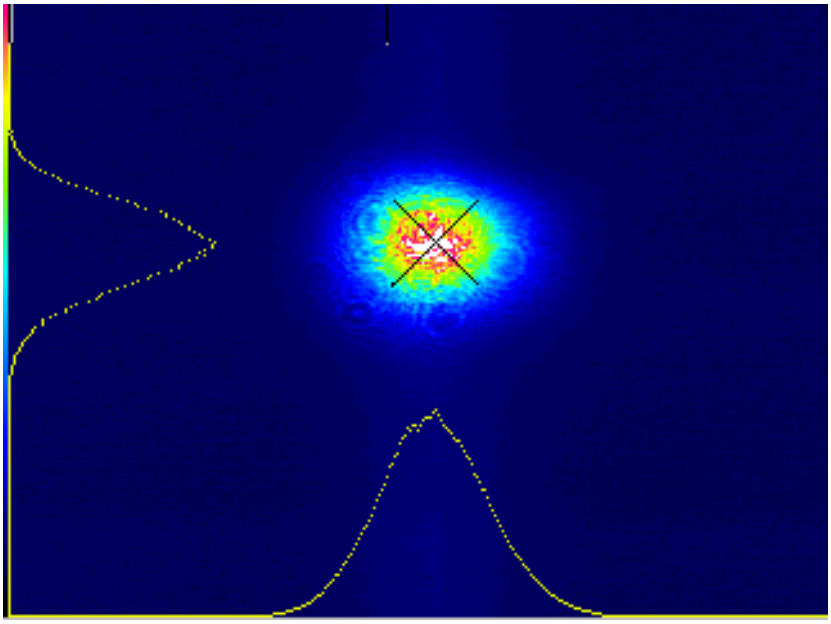

Figure 4.12 2D beam profile in far field

4.4 Characterization of Mode-locked Laser

As explained previously in chapter 3, in order to have the mode-locking operation the cavity such as shown in Figure 3.9 need to have some modification. This is carried out by inserting a prism pair, grating pair or Negative Dispersion Mirror in the cavity. In this particular alignment a prism pair was chosen. The prisms are used to compensate the dispersion in the cavity. Without dispersion compensation a longer wavelength of the pulse propagate faster than shorter wavelength leading to pulse stretching. The uncompensated dispersion will make the femtosecond pulse impossible. The cavity for the mode-locked operation is shown in Figure 3.12 in chapter 3.

4.4.1 Compensating Effect

The laser output from mode-locked cavity was measured using power meter at various pumping power. The collected data of power measurement from mode-locked Ti:sapphire laser are used to plot graph of output against input power. The graph obtained is shown in Figure 4.13.

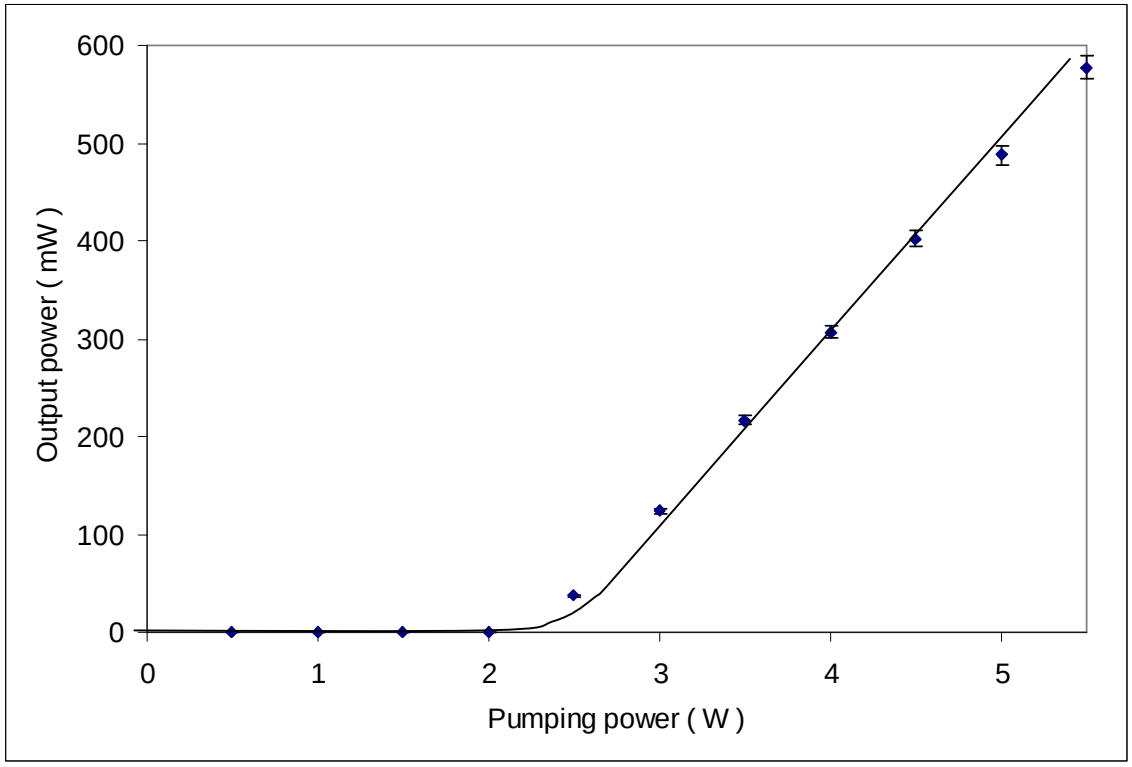

Figure 4.13 Output power as a function of the pumping power

Mode-locked Ti:sapphire laser has produced similar trend of graph as obtained by CW operation. The threshold pumping power for mode-locked cavity is 2.5 W which almost double than CW operation. The insertion of the prism pair in the cavity caused more losses in the pumping power. Beside that more power was dissipated by the reflection on the optical component especially on the prism pair. This factor makes the

gain power in cavity become lower at the same time the loss become higher. Therefore more pumping power is needed in order to make the laser gain higher than losses in the cavity. The output power linearly increases after exceeding threshold power of 2 W. The optimum power produced from this system is 577 mW corresponding to pumping power of 5.5 W. The efficiency of mode-locked Ti:sapphire laser is 18 % which lower compared to the CW operation. Although the efficiency for mode-locked cavity is lower, but this cavity is very important in order to initiate the femtosecond pulse generation.

4.4.2 Cleaning Factors

The cleanness of the optical component play an important role in determining the output power of the Ti:sapphire laser. In order to verify this factor, an experiment was carried out to test the different production of laser output before and after cleaning. In this matter, the optical components in the cavity were exposed in the air. Later without any cleaning, the output power of the Ti:sapphire laser was directly measured with respect to the pumping power. For comparison, another experiment was carried out, but all the optical components were cleaned using alcohol solution like acetone and lens tissue. The other tools employed in the cleaning process are bulb blower and hemostat. Entire tools used in cleaning process are shown in Appendix B.

Firstly the dust needs to be cleaned using bulb blower. The aim for using bulb blower is to remove the particle gently. The surface of optical component is very sensitive because of coating layer available and to maintain the smoothness and the flatness of the surface. Otherwise, rough rapping and washing could cause scratching, incising and removing the coating from the surface. The right technique to clean optical component is by wetting the folded or unfolded lens tissue in the acetone or alcohol solution. In this case acetone was used. The wetting tissue was placed gently on the

surface of optical component. Hemostat was used to hold the lens tissue. The tissue was pulled slowly from the top to the bottom of surface. The same procedure was repeated two or three times. Each time, a different tissue needs to be used, not advisable to use the same one. It's could cause damage to the surface. Alternatively the alcohol solution could be spray on the surface of the component and then wipe it with lens tissue using the same method. Excessive cleaning liquid are dried using bulb blower.

The comparison between the power before and after clean is shown in Figure 4.14. By cleaning the optical component the dust on the optical surface are removed. Without the dust, the light expose on the optical component can enter optimally. This result proves that the cleanness give quite large impact to the output power.

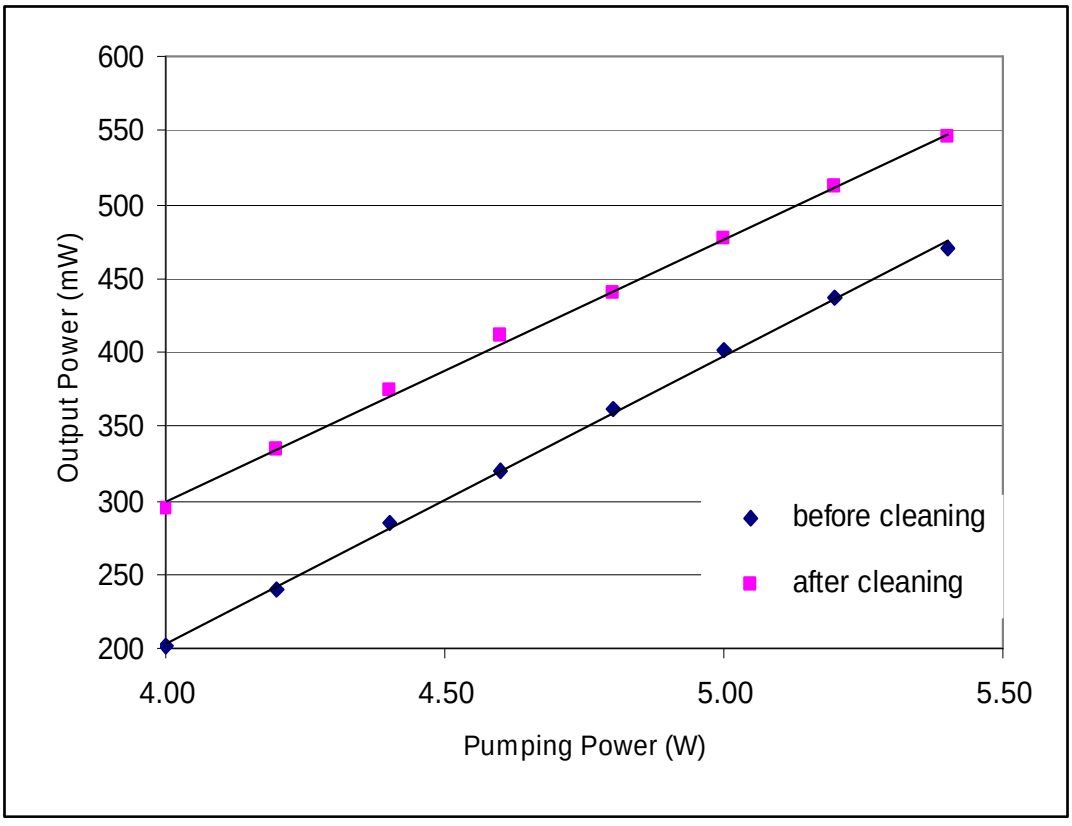

Figure 4.14 Output power before and after cleaning

4.4.3 Stability zone

The stability zone will influence the mode-locked output of the Ti:sapphire laser. In fact the stability of the cavity was depended on the distance of the curve mirror. In order to prove this, one of the mirrors in the cavity that is M2 is provided in micro scale of adjustment to adjust the separation between the curve mirrors. The power produced by adjusting of the mirror M2 or the spacing between two curve mirrors was measured. The graph obtained in Figure 4.15 shows the curve of the second stability zone as explained in Figure 2.15 of the Chapter 2. The graph can be used to identify the occurrence of the mode-locked pulse. According to Xu (1998), the mode-locking pulse is appeared at the closer boundary of stability zone. The near boundary is measured to be in the range of 108.35 mm to 108.75 mm.

Thus, in order to initiate the femtosecond pulse the perturbation need to provide to the prism P1 within 0.4 mm apart. In this case it was in the M1 and M2 spacing range of 108.35 mm to 108.75 mm (Near boundary region). Therefore, if there is no other factor affect the cavity such as the vibration and dust, the femtosecond pulse should be appeared at this range. However to get the femtosecond pulse is very difficult and requires patience. Precise adjustment of the prisms and curve mirror spacing is very important in order to get a better result.

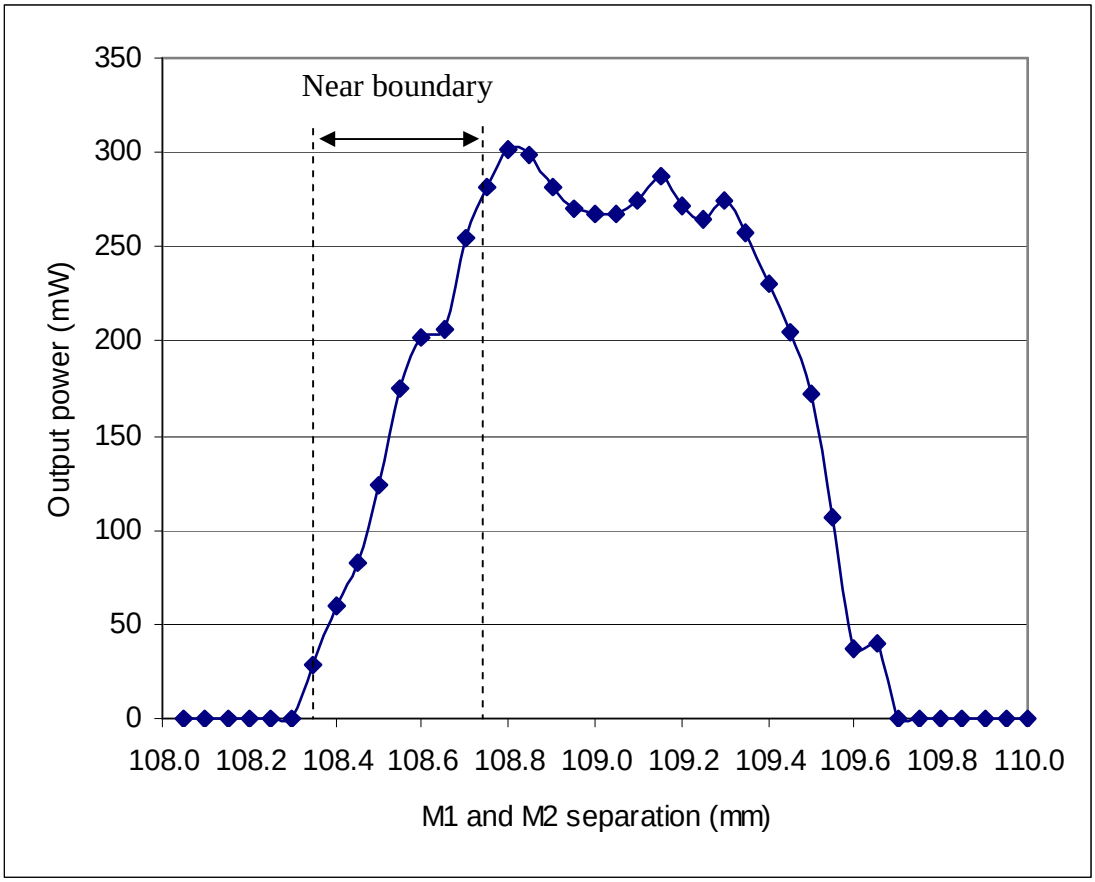

Figure 4.15 Output power by adjustment of the M1 and M2 spacing

4.5 Mode-locked pulse

In order to observe the mode-locked pulse, autocorrelator is appropriate device to be used. Unless such device is not available, fast photodetector can be used (Lin *et al.*, 2002) as replacement to trace the femtosecond pulse formation. However the disadvantage of the fast photodetector it's cannot displayed the pulse in femtosecond scale as compared to autocorrelator. By using fast photodetector only mode-locked pulse train can be traced, therefore the pulse duration cannot be measured. A fast photodiode was coupled to oscilloscope with bandwidth of 500 MHz. The femtosecond pulse

formation during mode-locked operation is shown in Figure 6.16. The result is in good agreement with the result of normal mode-locked pulse obtained by Lin (2002) with the repetition rate of 93.3 MHz. There are many types of the mode-locking pulse including of regular mode locking, period-doubled mode locking, quasi-periodic mode-locking and chaotic mode-locking (Xing *et al.*, 1999). Figure 6.16 is known as the *regular mode locking*. This clarified based on similarity of the amplitude of the signal. The frequency of the pulse is obtained as 96.43 MHz corresponding to pulse spacing of 10.37 ns.

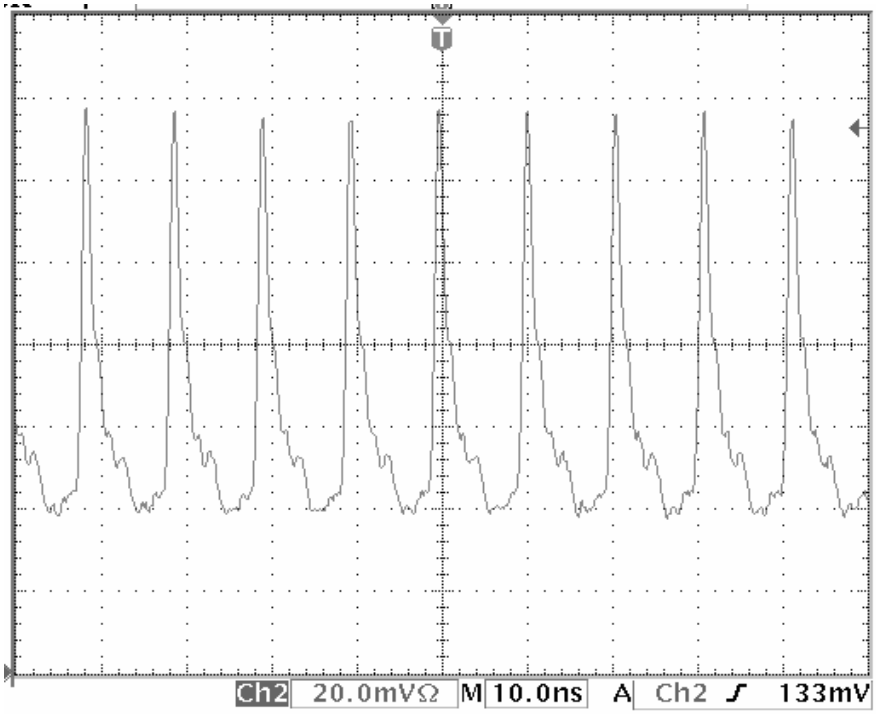

Figure 4.16 Oscillogram of mode-locked pulses

4.6 Femtosecond pulse duration

In stead of using an autocorrelator to measure the pulse duration, the spectrometer also can be used to indirectly measure the pulse duration of femtosecond signal. The spectrum detected by the spectrometer can be used to calculate the pulse duration. The parameters used to calculate the pulse duration is the center wavelength and the bandwidth of the spectrum at full wave half maximum (FWHM). The pulse duration, can be estimated as (Donnelly and Grossman, 1998)

$$\Delta f = \left(\frac{c}{\lambda^2} \right) \Delta\lambda \tag{4.4}$$

Δf is the frequency of the pulse, c is speed of light, λ is the center wavelength and $\Delta\lambda$ is the bandwidth at FWHM of the pulse. By knowing the frequency Δf the pulse duration of Ti:sapphire output can be calculated by using the following equation.

$$\Delta t \approx \frac{1}{\Delta f} \tag{4.5}$$

However the Equation (6.4) is not suitable to calculate the pulse duration for the femtosecond pulse because the femtosecond pulse is in the formation of $Sech^2$ pulse shape (Schneider *et al.*, 2000 and Keller *et al.*, 1991). Therefore the following equation (Rudolf and Wilhelmi, 1989, Vasil'ev, 1995 and, Diels and Rudolph, 1996) needs to be used.

$$\Delta t \approx \frac{0.3148}{\Delta f} \tag{4.6}$$

The typical spectrum of mode-locked signal is shown in Figure 4.17. Such signal is very difficult to obtain. It is required clean environment and vibration free. The mode-locked signal would not be able to grab and display unless the critical condition could be

fulfilled. Matrox Inspector Vesion 2.1 was employed to measure the bandwidth. The signal in Figure 4.17 shows that the center wavelength of the spectrum is obtained as 806.74 nm. The bandwidth for this particular signal is Δf = 24.80 nm measured at Full Wave Half Maximum (FWHM).

The information obtained from this particular signal is used to compute the pulse duration of femto signal. Equation (4.4) and (4.7) are used to estimate the pulse duration. The calculation result showed the pulse duration of the femtosecond pulse is 27.56 fs by assuming this signal having $Sech^2$ shape. The pulse duration can be easily calculated by using ToptiCalc V25 software.

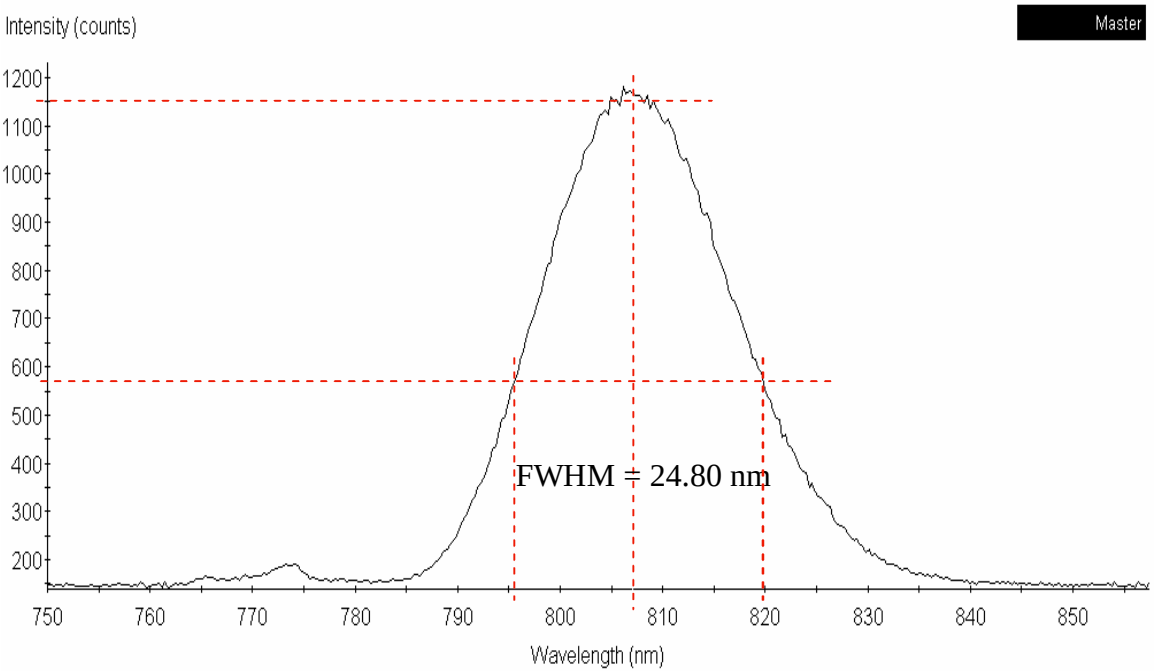

Figure 4.17 Spectrogram of mode-locked pulse

CHAPTER 5

CONCLUSIONS AND SUGGESTIONS

5.1 Conclusions

The femtosecond of Ti:sapphire laser was successfully studied. Two types of Ti:sapphire laser mode which are continuous wave and mode-locked operation have been demonstrated. The laser was pumped using DPSS laser Verdi 5 with wavelength of 532 nm. The Ti:sapphire crystal was used an active medium for the laser to produce output laser at IR region.

For the cavity alignment, a set of mirror with reflection of 99.8 % and coating with broad range of 720 nm to 820 nm was employed. This includes the flat and spherical mirrors. Output coupler with transmission of 5 % was used to transmit the laser. For the mode-locked Ti:sapphire laser, a prism pair was conducted to compensate the dispersion in order to produce the femtosecond pulse. The “Z” folded cavity type was set up in this project. The total length of laser cavity is 150.5 cm. The separation between adjacent mirror M1-M2, M2-M4 and M1-OC was 10.5 cm, 60 cm and 80 cm, respectively.

Both types of laser mode have been successful analyzed. The fluorescence spectrum, output spectrum, output power and beam profile were studied. The maximum power produced by CW laser and mode-locked laser are 1.12 W and 577 mW respectively. The stability zone has been obtained by changing the separation between M1 and M2. The mode-locked operation was detected by observing the pulse train captured using fast photodiode and clearly monitored using 500 MHz oscilloscope. The mode-locked pulses were identified as the regular mode locking. This clarified based on similar of the amplitude of the signal. The frequency of the pulse is 96.43 MHz.

The pulse duration was calculated through the mode-locked spectrum. The mode-locked spectrum was detected using Ocean Optics spectrometer. The spectrum was analyzed precisely by using Matrox Inspector Version 2.1 software. The pulse duration obtained from the calculation according the spectrum is 27.56 fs with bandwidth of 24.80 nm at FWHM and at center wavelength of 806.74 nm.

5.2 Problem

In this work there are a few factors that obstructed the progress of research. The first problem is regarding to the pumping source. It arise when the DPSS laser have not enough pumping power. Therefore the previous system has been replaced with the new one, Verdi 5 DPSS laser. A lot of time was spent waiting for the new laser and involved expensive budget. Another problem is the DPSS laser have very bright and high power beam. Therefore it is very dangerous and we need to follow safety procedure during laser operation. Without safety precaution during handling the DPPSS laser, it will cause bad injury. Figure 5.1 shows the DPSS laser during operation. The DPSS laser beam is in vertical polarization. Therefore the direction of the polarization must be changed to horizontal polarization in order get the Brewster angle condition. This problem is solved

by insert the polarization rotator before strike the Ti:sapphire crystal with the pump beam.

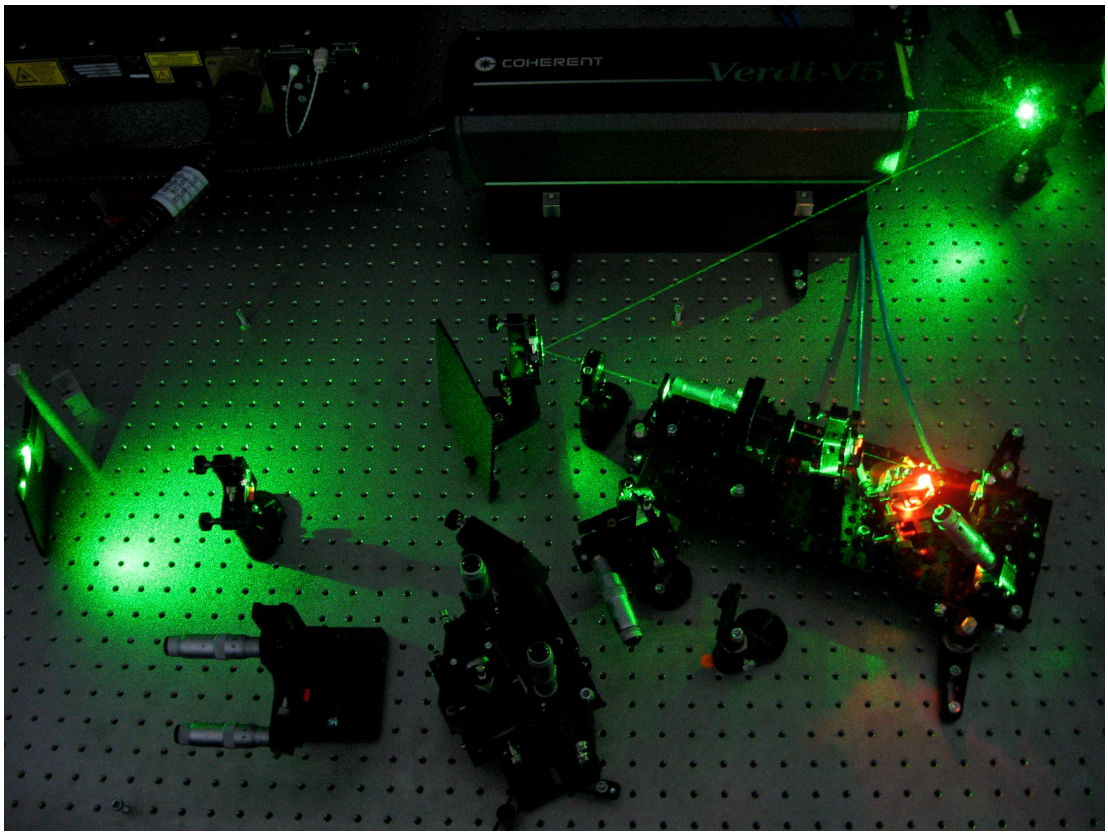

Figure 5.1 DPSS laser during operation.

The second problem was regarding the cavity of the laser. The cavity was "Z" cavity type, therefore it comprised of many optical components and need large space to set up. Besides, the cavity of the laser is very sensitive and need very precise alignment in order to get the laser beam. Moreover, small touch to the component in the laser cavity may cause the laser beam lost and need for other alignments.

The third problem is to generate the laser from the crystal. In order to get lasing from the crystal, firstly the suitable crystal need to be chosen. The crystal characteristics that need to be considered is the doping, dimension and crystal's crystallographic.

Without an appropriate crystal the lasing could not be achieved. Another critical factor is to determine the best position of the crystal. Therefore the crystal's holder that has been used in this cavity can be adjusted in horizontal and vertical. The horizontal adjustment is to adjust the angle of the beam incident to the crystal. While vertical adjustment is to adjust the crystallographic of the crystal.

Lastly about the mode-locked operation. For the mode-locked operation many factors need to be considered. Firstly the environment factor, since the cavity very sensitive to the environment factors such as the vibration and dust therefore a few things need to be done. Initially, any vibration source needs to remove. Then every time modification introduced to the cavity, the optical components need to clean as mention in Chapter 4. Second factor is the dispersion, the dispersion need to be controlled by careful adjustment of the prism pair in cavity. The beam insertion in the prism needs to adjust until stable pulse output produced.

5.3 Suggestions

The main problem that affects the cavity is the dust and vibration. Therefore it is recommended to build proper housing for the laser to avoid the dust expose on the optical components. The cover also can block the green beam reflected by the optical components to the end user. In order to reduce or eliminate the vibration it is suggest that to use using anti vibration table system. This can be done by installing the stabilizer pneumatic isolator to every corner of the table. Another thing can be done is by removing the DPSS laser power supply from the optical table because the fan existed in the power supply will produce the vibration.

Another problem is to make the mode-locked pulse stable and self starting. In this case the laser cavity needs to have some modifications. The first modification is by putting the SESAM mirror in laser cavity as explained by Jung (1997). By using SESAM, no critical alignment is required and the mode-locked operation is self-starting.

The other alternative to make the mode-locked operation self starting is by inserting another nonlinear material in the laser cavity such as ZnS as suggested by Pearson and Whiton (1993). By using this material it is possible to reduce pump requirement, the laser is self starting and improve long stability of the laser.

Ti:sapphire laser is a well known having a very wide tunability. The wavelength can be easily tuned by using birefringent tuning element as reported by Keller *et al.,* (1991). Therefore it is suggested to insert the birefringent plate in the cavity. However the laser tuning range is limited by a mirror reflectivity and birefringent plate itself.

Since femtosecond laser study is still a new field in Malaysia, we hope this research will give benefit to the femtosecond laser studies in our country. Last but not least, hopefully this thesis will be a good reference for future studies.

REFERENCES

Aschom, J. B. (2003). *The role of focusing in the interaction of femtosecond laser pulses with transparent material*. Harvard University: Ph.D. Thesis.

Alaoui, C., and Salameh, Z. M. (2001). Solid State Heater Cooler: Design and Evaluation. Power Engineering. *Proc. Of Large Engineering Systems Conference LESCOPE*.139 – 145.

Bartels, A., Dekorsy, T., and Kurz, H.. (1999) Femtosecond Ti:sapphire ring laser with a 2-GHz repetition rate and its application in time-resolved spectroscopy. *Optics Letters*. 24(14).

Carey J. J. (2002) *Near-field effect of Terahertz pulse*. University of Stratchlyde: Ph.D. Thesis.

Coherent. (2005). Verdi V-2/V-5/V-6 Diode Pumped Laser. Canada: Operator's Manual.

Diels, J. C. and Rudolph, W. (1996). *Ultrashort Laser Pulse Phenomena*. United Kingdom: Optics and photonics.

Donnelly, T. D. and Grossman, C. (1998). Ultrafast phenomena: A laboratory experiment for undergraduates. *Am. J. Phys*. 66 (8): 677-685.

Elsayed, K. A. (2002). *Development of an efficient Ti:sapphire Laser Transmitter for Atmospheric Ozone LIDAR Measurement* . Old Dominion University: Ph.D. Thesis.

Eggleston, J. M., Deshazer, L. G. and Kangas, K. W. (1988) Characteristics and Kinetics of Laser-Pumped Ti:Sapphire Oscillators, *IEEE J. of Quantum Electronics*. 24(6): 1009-1015.

Fermann, M. E., Galvanauskas, A. and Sucha, G. (2001). *Ultrafast Lasers Technology and Applications*. United State: Marcel Dekker.

Gan, F. (1995). *Laser Material*. Singapore: World Scientific.

Haus H. A. (2000). Mode-Locking of Lasers. *IEEE J. of Quantum Electronics*. 6(6): 1173-1185

Huang, C. P. (1995). *Generation, amplification and characterization of ultrashort laser pulses generate by Titanium Doped Sapphire*. Washington State: Ph.D. Thesis.

Hecht, E. and Zajac, A. (1982). *Optics*, Addision-Wesley Publishing Company.

Jung, I.D., Kärtner, F.X., Matusche K. N., Sutter, D. H., Morier-Genoud, F., Shi, Z., Scheuer, V., Tilsch, M., Tschudi, T. and Keller, U. (1997). Semiconductor saturable absorber mirrors supporting sub-10-fs pulses. *Appl. Phys*. B 65: 137–150.

Kalashnikov, V. L., Kalosha, V. P., Poloyko, I. G. and Mikhailov, V. P. (1997). Optimal resonators for self-mode locking of continuous-wave solid-state lasers. *J. Opt. Soc. Am.* B 14(4): 964-969.

Keller, U., ‘tHooft, G. W., Knox, W. H. and Cunningham, J. E. (1991). Femtoseond pulse from continuously self-starting passively mode-locked Ti:sapphire laser. *Optics Letter*. 16(13): 1022-1024.

Keller, U. (2003). Recent developments in compact ultrafast lasers.*Nature* 424: 831-838.

Kuhn, K. (1998). *Laser Engineering*. United State: Prentice Hall Inc.

Koechner, W. and Bass, M. (2003). *Solid-State Lasers A graduate Text*. New York: Springer-Verlag.

Kolgenik, H. W., Ippen, E. P., Dienes, A. and Shank, C. V. (1972). Astigmatically Compensated Cavities for CW Dye Lasers. *IEEE J. of Quantum Electronic*. 8:373-379.

Koumans R. G. M. P. (2001). *Semiconductor Mode-locked laser: Mode locking, Characterization and Application.* California Institude of Technology Pasedena: Ph.D. Thesis.

Kowalevicz, A. M. (2004). *Novel Femtosecond laser development with application in Biomedical Imaging and Photonic Device Fabrication.* Harvard university: Ph.D. Thesis.

Li, M. (1999). *Design of an ultrshort pulse multipass amplifier and investigation of femtosecond breakdown.* University of Connecticut : Ph.D. Thesis.

Lin, J. H., Hsieha, W. F. and Wu, H. H. (2002). Harmonic mode locking and multiple pulsing in a soft-aperture Kerr-lens mode-locked Ti:sapphire laser. *Optics Communications* 212:149–158.

Lingyun Photoelectronic System Co. Ltd. (2005). Diode pumped Solid State Laser System LYDPG-1. China: Operator's Manual.

Lytle, A. L., Gershgoren, E., Tobey, R. I., Murnane, M. M., Kapteyn, H. C. and Müller, D.(2004). Use of a simple cavity geometry for low and high repetition rate modelocked Ti:sapphire lasers. *Optics Express*. 12(7): 1409-1416

Matrox Electronic Sytems Ltd. Matrox Inspector Version 2.1. Canada: User manual.

McKinnie, I. T., Oien, A. L., Warrington, D. M., Tonga, P. N., Gloster, L. A. W., and King, T. A.(1997). Ti Ion Concentration and Ti:sapphire Laser Performance. *IEEE J. Of Quantum Electronics*, 33(7): 1221-1230.

Mukhopadhyay, P.K., Alsous, M.B., Ranganathan, K., Sharma, S.K., Gupta, P.K., Gupta, J., George J. and Nathan, T.P.S. (2003). Simultaneous Q-swithing and mode-locking in an intracavity frequency doubled diode-pumped Nd:YVO4/KTP green laser with Cr4+:YAG. *Optics Communication.* 222: 399-404.

Newport. (2006). The Newport Resource 2006/2007. USA: Catalogue.

Newport. (2004). 818P Series High Power Detector. USA: User's Manual

Newport. (2004). 841-PE Hand-held Optical Power/Energy Meter. USA: User's Manual

Ng, S.P., Tang, D.Y., Kong, J., Xiong, Z. J., Chen, T., Qin, L. J. and Meng, X.L. (2005). Quasi-cw diode-pumped Nd:$GdVO_4$ laser passively Q-switched and mode-locked by Cr^{4+}:YAG Saturable Absorber. *Optics Communications.* 250:168–173.

Ocean Optics Inc. (2005). Fiber Optic Spectrometer USB 2000. USA: Installation and Operation Manual

Ophir Optronic Ltd. (2002). BeamStar, CCD Laser Beam Profiler for Windows. Jerusalem: User Manual.

Pearson and Whiton G. (1993). *Use of ZnS as a self Focusing element in Self Starting Kerr Lens mode locked Ti:Sapphire laser*. Oklahoma State University: Ph.D. Thesis.

Rodriguez, M., Bourayou, R., Mejean, G., Kasparian, J., Yu, J., Salmon, E., Scholz, A., Stecklum, B., Eisloffel, J., Laux, U., Hatzes, A. P., Sauerbrey, R., Woste, L., and Jean, P. Wolf. (2004). Kilometer-range nonlinear propagation of femtosecond laser pulses. *Physical Review E* 69(036607): 1-5.

Rudolf, W. and Wilhelmi, B. (1989). *Light pulse compression*. United Kingdom: Harwood Academic Publishers.

Salin, F. and Brun, A. (1987). Dispersion compensation for femtosecond pulses using high index Prisms. *J. Appl. Phys*. 61(10): 4736-4739.

Sarukura, N. and Ishida, Y. Ultrashort Pulse Generation from a Passively Mode-Locked Ti : Sapphire Laser Based System. *IEEE J. Quantum Electronics*. 28(10): 2134-2141.

Schneider, S., Stockmann, A. and Schulbauer, W. (2000). Self-starting mode-locked cavity-dumped femtosecond Ti:sapphire laser. *Optics Express* 6(11): 220-226.

Shapiro, S. L. (1977) *Ultrashort light pulses Picosecond Technique and Applications*, Germany: Springer Verlag.

Silfvast, W.T. (2004). *Laser Fundamentals*. United State: Cambridge University Press.

Smith, D. L. (1999). Coherent Thinking. *Engineer and Science* 4: 6-17.

Song, C., Hang, Y., Zhang, C., Xu, J. and Zhou, W. (2005) Growth of composite Ti:sapphire by hydrothermal method. *J. of Crystal Growth*. 277: 200-204.

Spence, D. E., Kean, P. N., and Sibbett, W. (1991). 60-fsec pulse generation from a self-mode-locked Ti:sapphire laser. *Optics Letters*. 16(1): 42-44.

Sun, Z., Li, R, Bi, Y., Hu, C., Kong, Y., Wang, G., Zhang, H. and Xu, Z. (2005). Experimental study of high power pulse side pumped Nd:YAG laser. *Optics & Laser Technology* 37: 163-166.

Sutter, D. H., Jung, I. D., Kartner, F. X., Matuschek, N., Genoud, F.M., Scheuer, V., Tilsch, M., Tschudi, T., and Keller, U. (1998). Self-Starting 6.5-fs Pulses from a Ti:Sapphire Laser Using a Semiconductor Saturable Absorber and Double-Chirped Mirrors, *IEEE J. Of Selected Topics In Quantum Electronics*. 4(2): 169-178.

Svelto, O. (1998). *Principles of Lasers Fourth Edition*. United State: Springer.

Tate, J. L. (2004). *Intense Laser Propagation In Sapphire*, Ohio State University: Ph.D. Thesis.

Valdmanis, J. A. and Fork, R. L. (1986). Design considerations for a femtosecond pulse laser balancing self phase modulation, group velocity dispersion, saturable absorption, and saturable gain. *IEEE J. of Quantum Electron*. 22(1): 112–118

Vasil'ev, P. (1995). *Ultrafast Diode Lasers: fundamental and application.* Boston: Artech House Publishers.

Wang, H. W. (1999). *Development and application of high peak ultrafast laser.* University of Michigan: Ph.D. Thesis.

Walker, S. J. (2006). *Development and Characterization of a Regeneratively Amplified Ultrafast Laser System with an All-Glass Stretcher and Compressor*, University of Waterloo:Master Thesis.

Xing, Q., Chai, L., Zhang, W. And Wang, C. (1999). Regular, period-doubling, quasi-period, and chaotic behaviour in a self-mode-locked Ti:Sapphire laser. *Optics Communication.* 162: 71-74.

Xu, L., Tempea, G., Spielmann, C., Krausz, Stingl, F. A. Ferencz, K. and Takano, S. (1998). Continuous-wave mode-locked Ti:sapphire laser focusable to 5 x 10^{13} W/cm^2. *Optics Letters* 23(10): 789-791.

Xu, L., Tempea, G., Poppe, A., Lenzner, M., Spielmann, Ch., Krausz, F., Stingl, A. and Ferencz. (1997) K. High-power sub-10-fs Ti:sapphire oscillators, *J. Appl. Phys.* B 65, 151–159

Ye, J. and Cundiff, S. (2005). *Femtosecond Optical frequency Comb Technology Principle, Operation and Application.* United State: Springer.

Yong, Y. C. (2002). Chartered Electro-Optics, Diode Pumped Solid State Lasers. *Electronic Review.* 16(1):10-11.

Zhang, W., Wang, Y., Chai, L., Xing, Q. and Wang, Q. (1999). Suppression of amplified spontaneous emission in a femtosecond chirped-pulse amplifier. *Optics & Laser Technology* 31: 425-430.

APPENDIX A

Index refraction for sapphire

Wavelength (nm)	Extra-ordinary index (n_e)	Ordinary index (n_o)
488	1.76711	1.77533
515	1.76486	1.77304
694	1.75542	1.76341
755	1.75346	1.76141
780	1.75274	1.76068
800	1.75220	1.76013
820	1.75168	1.75961
860	1.75072	1.75863

Physical constants for sapphire

Physical Constant	Value	Units
Melting point	2,015	C
Density	3.965	gr/cm^3
Thermal expansion coefficient	$8.4\ (10)^{-6}$	m /C
Thermal conductivity	35	W/m C
Heat capacity	79.5	J/mol °K
Thermal Dispersion	$1.4\ (10)^{-5}$	C^{-1}
Hardness	12	Modified mohs

APPENDIX B

Tools for cleaning optical component

Bulb blower

Acetone, alcohol and lens tissue

Hemostat

PRESENTATIONS

1. Wan Aizuddin, W. R., Mohamad Khairi S., Noriah, B. **Diagnostic Of Diode Pumped Solid State Laser**. Annual Fundamental Science Seminar 2005 (AFSS 2005), 4 – 5 July 2005 Ibnu Sina Institute, UTM.

2. Wan Aizuddin, W. R., Mohamad Khairi S., Noriah, B. **Experimental Study Of Thermoelectric Cooler For DPSS Laser**. International Meeting on Frontiers of Physics (IMFP 2005), 25 – 29 July 2005, Kuala Lumpur.

3. Wan Aizuddin, W. R., Mohamad Khairi S., Noriah, B. **Study The Absorption Of Diode Pumped Solid State Laser on Ti:Sapphire Crystal**. 1st National Colloquium on Photonics, 29-30 November 2005, Kajang, Selangor.

4. Wan Aizuddin, W. R., Mohamad Khairi S., Noriah, B. **Indentification Of Ti:Sapphire Laser Oscillator Components.** Seminar Penyelidikan Advanced Optical Crystal for Electro-Optics Application 2006, 21-23 Mei 2006, Melaka.

5. Wan Aizuddin, W. R., Mohamad Khairi S., Noriah, B. **The Configuration of Ti:sapphire Crystal in Cavity.** Laser and Electro-Optic Seminar (LEOS-2006), June 28-29, 2006, Senai, Johor.

6. Wan Aizuddin, W. R., Mohamad Khairi S., Noriah, B. **Study The Absorption And The Emission Of Ti:Sapphire Crystal.** International Conference on Solid State Science and Technology 2006 (ICSSST 2006), September 4-6, 2006, Kuala Terengganu, Terengganu.